OPTIMAL MULTIPLE HYPOTHESIS TESTING WITH AN APPLICATION
IN SIDE LOBE BLANKER DESIGN AND INVARIANCE APPLICATIONS IN
DETECTION AND SYNCHRONIZATION

A THESIS SUBMITTED TO
THE GRADUATE SCHOOL OF NATURAL AND APPLIED SCIENCES
OF
MIDDLE EAST TECHNICAL UNIVERSITY

BY

OSMAN COŞKUN

IN PARTIAL FULFILLMENT OF THE REQUIREMENTS
FOR
THE DEGREE OF DOCTOR OF PHILOSOPHY
IN
ELECTRICAL AND ELECTRONICS ENGINEERING

SEPTEMBER 2017

Approval of the thesis:

OPTIMAL MULTIPLE HYPOTHESIS TESTING WITH AN APPLICATION IN SIDE LOBE BLANKER DESIGN AND INVARIANCE APPLICATIONS IN DETECTION AND SYNCHRONIZATION

submitted by **OSMAN COŞKUN** in partial fulfillment of the requirements for the degree of **Doctor of Philosophy in Electrical and Electronics Engineering Department, Middle East Technical University** by,

Prof. Dr. Gülbin Dural Ünver
Dean, Graduate School of **Natural and Applied Sciences** ⎯⎯⎯⎯⎯⎯⎯

Prof. Dr. Tolga Çiloğlu
Head of Department, **Electrical and Electronics Eng.** ⎯⎯⎯⎯⎯⎯⎯

Prof. Dr. Çağatay Candan
Supervisor, **Electrical and Electronics Dept., METU** ⎯⎯⎯⎯⎯⎯⎯

Examining Committee Members:

Prof. Dr. Orhan Arıkan
Electrical and Electronics Dept., Bilkent University ⎯⎯⎯⎯⎯⎯⎯

Prof. Dr. Çağatay Candan
Electrical and Electronics Dept., METU ⎯⎯⎯⎯⎯⎯⎯

Prof. Dr. Sencer Koç
Electrical and Electronics Dept., METU ⎯⎯⎯⎯⎯⎯⎯

Assoc. Prof. Dr. Sinan Gezici
Electrical and Electronics Dept., Bilkent University ⎯⎯⎯⎯⎯⎯⎯

Assist. Prof. Dr. Gökhan Muzaffer Güvensen
Electrical and Electronics Dept., METU ⎯⎯⎯⎯⎯⎯⎯

Date: ⎯⎯⎯⎯⎯⎯⎯

I hereby declare that all information in this document has been obtained and presented in accordance with academic rules and ethical conduct. I also declare that, as required by these rules and conduct, I have fully cited and referenced all material and results that are not original to this work.

Name, Last Name: OSMAN COŞKUN

Signature   :

ABSTRACT

OPTIMAL MULTIPLE HYPOTHESIS TESTING WITH AN APPLICATION
IN SIDE LOBE BLANKER DESIGN AND INVARIANCE APPLICATIONS IN
DETECTION AND SYNCHRONIZATION

COŞKUN, Osman

Ph.D., Department of Electrical and Electronics Engineering

Supervisor : Prof. Dr. Çağatay Candan

September 2017, 122 pages

This thesis aims to study two problems, namely optimal hypothesis testing in
the sense of Neyman-Pearson in the presence of multiple hypotheses and optimal
hypothesis testing in the presence of non-random unknown parameters (nuisance
parameters). Both problems occur frequently in different applications and their
optimal solution involves some fine details. In the first part of the thesis, the
multiple hypothesis testing problem is examined and the results are applied
on the problem of radar sidelobe blanker system design. The goal of this part
is two folds: To examine and compare the performance of Maisel system (the
conventional sidelobe blanking systems) with the optimal system and determine
the conditions for the Maisel system to approach the optimal blanker performance
so as to assist the design of practical Maisel sidelobe blankers. In the second
part of the thesis, uniformly most powerful invariant (UMPI) tests are examined.
UMPI tests are applicable when there are unknown non-random constants in the
hypothesis testing. UMPI tests retain the optimality properties of uniformly most
powerful tests (UMP) in a restricted setting of transform invariance with respect
to the unknown parameters. Many practical problems do not have UMP tests
and for these problems the general approach is to apply generalized likelihood
ratio test (GLRT) which does not have any optimality properties apart from
asymptotic ones. Similar to the first part of the thesis, our goal is to study the

UMPI tests and examine their performance with respect to well-known GLRT test. After a brief description of UMPI tests, we study two problems namely the problem of low probability of intercept signal detection and the problem of frame synchronization word detection problem. UMPI and GLRT approach based tests are derived for both problems and it is shown that for some operating conditions the invariant detector provides a better performance than GLRT, the performance difference is not significant.

Keywords: Sidelobe Blanking Systems, Neyman-Pearson Hypothesis Testing, Radar Signal Processing, Invariance Detectors

ÖZ

OPTİMUM ÇOKLU HİPOTEZ TESTİNİN YAN LOB KÖRELTME TASARIMINDAKİ BİR UYGULAMASI VE SEZİMLEME VE SENKRONİZASYONDA DEĞİŞMEZLİK UYGULAMALARI

COŞKUN, Osman

Doktora, Elektrik ve Elektronik Mühendisliği Bölümü

Tez Yöneticisi   : Prof. Dr. Çağatay Candan

Eylül 2017, 122 sayfa

Bu tez iki problemin çalışılmasını hedeflemektedir: çoklu hipotez durumunda Neyman-Pearson tipinde optimum hipotez testi ve rasgele olmayan bilinmeyen parametrelerin (parazit parametreler) olması durumunda optimum hipotez testidir. Her iki problem farklı uygulama alanlarında sıklıkla karşılaşılmakta ve söz konusu problemlerin optimum çözümü hassas detaylar içermektedir. Tezin birinci bölümünde çoklu hipotez test problemi incelenmiş ve sonuçları radar yan lob köreltme system tasarımına uygulanmıştr. Bu bölümün amacı iki bölümden oluşmaktadır: Geleneksel yan lob köreltme sistemi olan Maisel sisteminin performansının incelenmesi ve optimum system ile kıyaslanması ile pratik Maisel yan lob köreltme sisteminin tasarımına yardımcı olmak amacıyla Maisel sisteminin performansının optimum köreltici sisteme yaklaştığı durumlar belirlenmeye çalışılmıştır. Tezin ikinci bölümünde değişmez düzgün en güçlü (DDEG) testler incelenmiştir. Hipotez testinde bilinmeyen rasgele olmayan sabitler olması durumunda DDEG uygulanmaktadır. DDEG testler bilinmeyen parametrelere göre dönüşüm değişmezliğinin sınırlı ayarlamasında düzgün en güçlü (DEG) testlerin optimum özelliklerini korur. Bir çok pratik uygulamada DEG testi mevcut değildir ve söz konusu problemler için genel yaklaşım asimptotik optimum özelliği haricinde optimum özelliklerini barındırmayan genelleştirilmiş olabilirlik oran testinin (GOOT) uygulanmasıdır. Tezin birinci bölümüne benzer şekilde,

amacımız DDEG testlerini çalışmak ve performansını GOOT testlerine göre incelemektir. DDEG testlerinin kısa bir özetinden sonra iki probleme çalışılmıştır. Söz konusu problemler düşük olasılıkla yakalanma radar sinyallerinin sezimlenmesi ve çerçeve senkronizasyon kelimelerinin sezimlesi problemleridir. DDEG ve GOOT yaklaşımlı testler her iki problem için çıkartılmış ve belirli bir çalışma koşullarında değişmez sezimleyicinin GOOT'dan daha iyi performans sergilediği ve performans farkının çok büyük olmadığı gösterilmiştir.

Anahtar Kelimeler: Yan Lob Köreltme Sistemleri, Neyman-Pearson Hipotez Testi, Radar Sinyal İşleme, Değişmez Sezimleyiciler

To my wife and son

Gülcan Coşkun, Sedat Coşkun

ACKNOWLEDGMENTS

I would like to express my special appreciation and thanks to my advisor Professor Dr. Çağatay Candan for the continuous support of my Ph.D study, for his patience, motivation, and immense knowledge. It has been a real honor to be his first Ph.D student. His guidance helped me in all the time of research and writing of this thesis. I will miss our conversations and technical discussions.

There are lots of people without their support this thesis would not have taken place. Since it is very challenging to continue PHD program as well as working at a very demanding place, the support of my friends and my colleagues were very valuable.

Last but not the least, I would like to thank my bellowed wife. Without your support, patience, encouragement and love, this work could have not been possible.

TABLE OF CONTENTS

LIST OF TABLES

TABLES

LIST OF FIGURES

FIGURES

CHAPTER 1

INTRODUCTION

This thesis examines topics of interest in hypothesis testing. The first topic is on Neyman-Pearson type tests for non-binary hypothesis testing. The second topic is hypothesis testing in the presence of nuisance parameters.

Optimum hypothesis testing problem is a well known topic of interest in many fields. The main goal is to select the one hypothesis among multiple alternatives in an optimum way. This problem lies at the heart of radar receiver architecture. In radar receivers, the most important decision is whether the target of interest is present or not. In chapter 2, the hypotheses testing problem is reviewed with some several optimality considerations. The main attention is given to the problem of multiple hypotheses testing.

In chapter 3, an application of Neyman-Pearson type optimum detector involving multiple hypothesis testing is given. The application is called as sidelobe blanker in radar signal processing. The optimum sidelobe blankers are derived and compared with the widely used ad-hoc detector, namely Maisel detector. The implementation of optimal detector depends on several factors such as SNR and JNR of target and jammer. Although it can not be implemented in real time, the optimum detectors derived for each Swerling targets can be used to determine the design parameters of the Maisel sidelobe blankers. One of the most important parameters is the gain margin between the auxiliary antenna and sidelobe of main antenna. The optimum detectors help the designer choose this parameter and forecast its effect on probability of falsely blanking the target signal and probability of blanking the jammer. Chapter 3 presents extensive analysis of

Maisel sidelobe blankers for Swerling-0, Swerling-1 and Swerling-3 targets and compares the performance of it with corresponding optimum detectors for several scenarios. Also, design examples are given to illustrate to use the optimum sidelobe blanker results to determine the parameters of Maisel sidelobe blankers and asses the performance quantitatively.

When there are unknown parameters regarding the probability distribution functions for either hypotheses, there exists some cases that it is not possible to find the optimum detectors via the classical Neyman-Pearson detector which is explained in chapter 2. In order to deal with unknown parameters, there are two well-known methods which are Bayesian approach, in which unknown parameter is known to have a priori probability distribution, and Generalized Likelihood Ratio Test (GLRT) approach, in which one can find the likelihood ratio test by maximizing the probability distribution functions with respect to unknown parameters. The Bayesian approach is optimal in the sense that average Bayesian risk is minimized and the probability distribution function is found by integrating the conditional probability distribution function with respect to the unknown parameter. After marginalization, the classical likelihood ratios can be constructed. GLRT is another method when a priori information is not available. There is no guaranteed optimality properties for GLRT except some asymptotic optimality properties.

In the statistics literature, there is a well known concept called the invariance principle in which one can find a most powerful detector subject to some constraints. These constraints are very general and natural at times that a detector designer would like to have a detector with these constraints. More theoretically, there can be a group of transformations, which can be referred to as constraints, leave the hypothesis testing problem invariant. Namely, the parameter space of each probability distribution functions for both hypotheses remain same and the type of probability distributions does not change except the change in parameters. After finding this group, one can uniquely index all data points for all transformations within the group via maximal invariant function. The new domain in which the maximal invariant test is defined is utilized to find the likelihood ratio test. In chapter 4, the basic concept of invariance principle is

given along with some applications. Concrete application examples given are as follows:

- Low Probability of Intercept Radar signal detection problem will be solved by three methods, namely Bayesian, GLRT and Invariance. It is shown that Bayesian and invariance approaches results in the same detector, while GLRT results in a different detector. MATLAB simulations are presented to compare the performances of GLRT and UMPI tests. It is shown that the performance of the invariant test is better than GLRT. Moreover, depending on the length of signal of interest, for high and low SNR regions, the performances of GLRT and the energy detector are in close proximity with the UMPI test, respectively.

- Frame synchronization word detection problem is solved by two methods, namely GLRT and invariance. Bayesian approach is used in order to eliminate the random bits effect. It is shown that invariant and GLRT detectors are different, and in some region of interest, the invariant detector outperforms GLRT. For high SNR region, GLRT and invariant detectors have a very close performances. MATLAB simulations are presented in order to understand the new detector design.

Literature survey of optimum sidelobe blanker and invariance applications is given at the beginning of Chapter 3 and Chapter 4, respectively.

The main contribution of this thesis is summarized as follows:

- Optimum sidelobe blankers for Swerling-0, Swerling-1 and Swerling-3 targets are derived analytically and their performances are presented with a comparison with Maisel sidelobe blankers. The statistical characteristics of optimum sidelobe blanker for Swerling-1 target is obtained, while for Swerling-1 and Swerling-3 detectors Monte Carlo simulations are performed in order to estimate their performances. The Maisel sidelobe blanker design example is also given. This study was published in the following journal and proceeding publications.

    1. Coşkun, O. and Candan, Ç. "Design of Maisel sidelobe blankers with

a guarantee on the gap to optimality". In: *IET Radar, Sonar & Navigation* 10 (9 Dec. 2016), 1619–1626(7)

2. Coşkun, O. and Candan, Ç. "On the optimality of Maisel sidelobe blanking system". In: *2015 23nd Signal Processing and Communications Applications Conference (SIU)*. May 2015, pp. 585–591

3. Coşkun, O. and Candan, Ç. "On the optimality of Maisel sidelobe blanking structure". In: *Radar Conf., 2014 IEEE*. May 2014, pp. 1102–1107

- The invariance concept and it's interaction with sufficiency concept and GLRT is studied. The derivations of general signal detection problem is mostly benefited from [4], but the presented examples does not appear in [4] explicitly. Invariance applications of LPI signal detection and frame synchronization word detection problems are novel.

CHAPTER 2

OPTIMALITY CONSIDERATIONS OF HYPOTHESIS TESTING

2.1 Introduction

Choosing the hypothesis between two or more alternatives is cast as hypothesis testing problem. One of the hypotheses is assumed to be null hypothesis which usually represents the noise only situation for the target detection problems. The problem at hand can be restated as what is the best decision rule to choose the hypothesis given the data. There are two approaches for answering this question. In each alternative solutions to the problem, the optimality definition and the prior assumptions about the hypotheses are the deciding factors.

The first approach is Bayesian in which all uncertainties is put into some form of probability distributions. The distinctive feature of this approach is to assume a known a-priori distribution for each hypotheses. The decision is based on minimizing the cost function of choosing a hypothesis.

The second one is Neyman-Pearson approach in which one of the error probabilities is aimed to be minimized while the other error probabilities are aimed to be kept below some predefined value. Explicitly speaking, the probability of falsely not rejecting null hypothesis (in radar jargon, miss detection probability) is minimized while the probability of falsely rejecting null hypothesis (false alarm probability) is kept below some value. In other words, the probability of detection is maximized while false alarm probability is upper bounded by some value. In the subsequent sections, deeper meanings of Neyman-Pearson approach

is explored.

When more than one alternatives in addition to null hypotheses are available, the Bayesian approach is widely used, specifically in the communication problems. The reader is referred to the classic books for details, [5, pp. 52–63], [6, pp. 46–52]. Neyman-Pearson approach in radar jargon is generally employed for the binary hypotheses testing problem in which there is only one alternative hypothesis that is the presence of target. However, in some applications for instance, when there are three options for the decision, namely, noise only, target and jammer presences, if the final goal is to discriminate among the alternative decisions, then the Neyman-Pearson sense of optimality can be useful in constructing detectors.

2.2 Binary Hypothesis Testing Problem

Let the observation random vector be denoted as $\mathbf{x}$, and our goal is to decide between two alternative hypotheses, H_0 and H_1. The decision function is represented as an indicator function $\delta(\mathbf{x})$ and defined as follows:

$$\delta(\mathbf{x}) = \begin{cases} 1, & \mathbf{x} \in D_1 \\ 0, & \mathbf{x} \in D_0 \end{cases} \tag{2.1}$$

where D_1 and D_0 are decision regions in which the hypotheses H_1 and H_0 are chosen accordingly.

2.2.1 Bayesian Approach

Let assume that π_0 and π_1 represent the prior probabilities of H_0 and H_1 respectively. The Bayes risk for the chosen hypothesis H_j is defined as follows:

$$R(\delta|H_j) = \sum_{i=0}^{i=1} C_{ij} P(H_i|H_j) \tag{2.2}$$

where C_{ij} represents the cost of choosing hypothesis H_i when H_j is actually true. The average cost of decision rule δ is defined as:

$$R(\delta) = \pi_0 R(\delta|H_0) + \pi_1 R(\delta|H_1). \tag{2.3}$$

6

The decision rule minimizing the average Bayes risk over all possible alternatives is given as:

$$
\delta(\mathbf{x}) = \begin{cases} 1, & \dfrac{f(\mathbf{x}; H_1)}{f(\mathbf{x}; H_0)} > T \\[2mm] 0, & \dfrac{f(\mathbf{x}; H_1)}{f(\mathbf{x}; H_0)} < T \end{cases} \tag{2.4}
$$

where T is the threshold

$$
T = \frac{\pi_0(C_{10} - C_{00})}{\pi_1(C_{01} - C_{11})} \tag{2.5}
$$

and $C_{ii} < C_{ij}$ is assumed. The reader is referred to [5] for details.

Minimum Error Probability Detector: If we assume the following cost functions;

$$
C_{ij} = \begin{cases} 1, & i \neq j \\[2mm] 0, & i = j \end{cases} \tag{2.6}
$$

The Bayes risk becomes the average error probability

$$
R(\delta) = P(H_1|H_0)\pi_0 + P(H_0|H_1)\pi_1. \tag{2.7}
$$

Also the threshold becomes as $T = \dfrac{\pi_0}{\pi_1}$. This detector, called as minimum error probability detector also maximizes the posterior probability $P(H_j|\mathbf{x})$, and the decision rule can be written as:

$$
P(H_1|\mathbf{x}) \underset{H_0}{\overset{H_1}{\gtrless}} P(H_0|\mathbf{x}). \tag{2.8}
$$

Maximum Likelihood Based Detector: In addition to assumptions given in (2.6), if one also assumes that the priori probabilities are equal to each other, i.e., $\pi_0 = \pi_1 = 0.5$, then the detector given in (2.8) becomes as follows:

$$
f(\mathbf{x}; H_1) \underset{H_0}{\overset{H_1}{\gtrless}} f(\mathbf{x}; H_0). \tag{2.9}
$$

This detector is widely used in communication receivers when there is no prior information about the message being sent.

2.2.2 Neyman-Pearson Approach

An alternative optimality criteria to the Bayesian approach is the Neyman-Pearson approach. Its motivation lies in the radar target detection problem. In radar applications, the goal is usually to fix the probability of false alarm which is defined as the probability of deciding that target is present when there is no target and only noise is present. Moreover, at the same time radar designer aims to maximize the provability of target detection. In other words, we wish to minimize one error probability subject to other error probability upper bounded by some value. The problem can be stated as;

$$\text{minimize } P_M = P(H_0|H_1), \text{ subject to } P_{FA} = P(H_1|H_0) < \alpha \qquad (2.10)$$

where P_M represents the miss detection probability which is the falsely not rejecting the null hypothesis, H_0 : noise only, and P_{FA} is the probability of false alarm which is falsely rejecting the null hypothesis. α is the level of this hypothesis test and represents maximum allowable false alarm probability or size of the test. This feature is the distinctive feature of Neyman-Pearson approach. In the Bayesian approach, the goal is to minimize total error probability which includes the combination of both error probabilities (P_M, P_{FA}) and true decision probability effects.

Although both approaches give the same test, i.e., the likelihood ratio test, their optimality goals are different. The Neyman-Pearson problem can be solved by various methods. Here, two proofs are given to convey some further depth in the Neyman-Pearson approach.

First Proof: The proof in [5] and [7] uses the Lagrange multipliers method to minimize the miss detection probability (or maximize the target detection probability). We construct the cost function F and seek a decision function $\phi(\mathbf{x})$ to minimize it,

$$\phi^*(\mathbf{x}) = \min_{\phi} F(\phi, \lambda) = P_M(\phi) + \lambda(P_{FA}(\phi) - \lambda) \qquad (2.11)$$

The cost function can be rewritten as:

$$F(\phi, \lambda) \;=\; \int_{\mathcal{D}_0} f(\mathbf{x}; H_1) \mathrm{d}\mathbf{x} + \lambda \left[\int_{D_1} f(\mathbf{x}; H_0) \mathrm{d}\mathbf{x} - \alpha \right], \qquad (2.12)$$

8

$$= \int_{\mathcal{D}_0} f(\mathbf{x}; H_1) \mathrm{d}\mathbf{x} + \lambda \left[1 - \int_{\mathcal{D}_0} f(\mathbf{x}; H_0) \mathrm{d}\mathbf{x} - \alpha \right], \quad (2.13)$$

$$= \lambda(1 - \alpha) + \int_{\mathcal{D}_0} \left[f(\mathbf{x}; H_1) - \lambda f(\mathbf{x}; H_0) \right] \mathrm{d}\mathbf{x}. \quad (2.14)$$

The function $F(\phi, \lambda)$ is minimized when the integrand $f(\mathbf{x}; H_1) - \lambda f(\mathbf{x}; H_0)$ is negative and we choose H_0 consequently.

$$\text{if } L(\mathbf{x}) = \frac{f(\mathbf{x}; H_1)}{f(\mathbf{x}; H_0)} < \lambda \text{ then choose } H_0 \quad (2.15)$$

Neyman-Pearson detector is again likelihood ratio test:

$$\phi^*(\mathbf{x}) = \begin{cases} 1, & L(\mathbf{x}) > \lambda \\ 0, & L(\mathbf{x}) < \lambda \end{cases} \quad (2.16)$$

When $L(\mathbf{x}) = \lambda$, either hypotheses H_0 or H_1 can be chosen and this situation is further examined in [5].

Second Proof: The proof in [8, 9, 10] is based on the definitions of indicator function and the likelihood ratio test. Consider the decision functions (here, we assume non-randomized test, so decision function becomes indicator function) $\phi^*(\mathbf{x})$ and $\phi(\mathbf{x})$ which correspond to likelihood ratio test and any other test. Our aim is to minimize P_M subject to $P_{FA} \leq \alpha$. The Neyman-Pearson lemma states that the test obtained from likelihood ratio test has the minimum P_M* unless P_{FA} is increased beyond the level of the test α. Stated differently, $P_M^* \leq P_M$ when $P_{FA} \leq P_{FA}^* \leq \alpha$ where P_M^*, P_M are the miss detection probabilities of the Neyman-Pearson test and any other test, P_{FA}^*, P_{FA} are the false alarm probabilities of Neyman-Pearson test and any other test, respectively. We begin the proof by stating the definition of Neyman-Pearson test as follows:

$$\phi^*(\mathbf{x}) = \begin{cases} 1, & \frac{f(\mathbf{x}|H_1)}{f(\mathbf{x}; H_0)} > T \\ 0, & \frac{f(\mathbf{x}|H_1)}{f(\mathbf{x}; H_0)} < T. \end{cases} \quad (2.17)$$

If $\mathbf{x} \in \mathcal{D}_1^*$, then $\phi^*(\mathbf{x}) = 1$ and $f(\mathbf{x}; H_1) > T f(\mathbf{x}; H_0)$. Likewise; if $\mathbf{x} \in \mathcal{D}_0^*$, then $\phi^*(\mathbf{x}) = 0$ and $f(\mathbf{x}; H_1) < T f(\mathbf{x}; H_0)$. So the following inequality holds for all decision functions:

$$(\phi^*(\mathbf{x}) - \phi(\mathbf{x}))(f(\mathbf{x}; H_1) - T f(\mathbf{x}; H_0)) \geq 0. \quad (2.18)$$

9

Integrating the above function over all values of $\mathbf{x}$, we obtain the following series of equations:

$$\int_{D_1^*} (f(\mathbf{x}; H_1) - Tf(\mathbf{x}; H_0)) \mathrm{d}\mathbf{x} - \int_{D_1} (f(\mathbf{x}; H_1) - Tf(\mathbf{x}; H_0)) \mathrm{d}\mathbf{x} \geq 0 \qquad (2.19)$$

$$1 - P_M^* - TP_{FA}^* - (1 - P_M) + TP_{FA} \geq 0 \qquad (2.20)$$

$$P_M - P_M^* \geq T(P_{FA}^* - P_{FA}). \qquad (2.21)$$

Thus, as long as $P_{FA} < P_{FA}^*$ and since $T > 0$, then $P_M^* < P_M$ holds for any other decision rule. This means that one can not decrease miss detection probability any further unless false alarm probability is increased.

The above proof can be restated with the detection probabilities $P_D = P(H_1|H_1)$. The final inequality becomes as follows:

$$P_D^* - TP_{FA}^* - P_D + TP_{FA} \geq 0 \qquad (2.22)$$

$$P_D^* - P_D \geq T(P_{FA}^* - P_{FA}). \qquad (2.23)$$

To put it differently, the optimal Neyman-Pearson test increases the probability of a decision when in fact H_1 is true under the constraint of probability of same decision when in fact H_0 be upper bounded by a fixed value. This meaning can be deduced with the definition of decision rule δ. One can further extend this as follows: Let's say that the final goal of decision test is to decide some other hypothesis, let's say H_3. The Neyman-Pearson lemma also states that $P(H_3|H_1)$ is maximized when $P(H_3|H_0)$ is wanted to be upper bounded by some value α. This interpretation will be used when constructing optimum radar sidelobe blanker detectors which will be covered in Chapter 3.

2.3 Multiple Hypothesis Testing Problem

2.3.1 Bayesian Approach

When more than two hypotheses are available, the costs for each hypotheses are computed, and the decision rule is found by minimizing the average cost functions. There are ample resources in the literature, specifically in the communication

literature. The Bayesian approach becomes minimum error probability and maximum posterior probability detectors. It is fully covered in [5, 7, 11].

2.3.2 Neyman-Pearson Approach

Because the goal of Neyman-Pearson approach is to minimize one error probability while keeping the other error probability below some fixed value, in case of multiple hypotheses, there are multiple error probabilities to construct trade-offs. In this subsection, three types of Neyman-Pearson detectors are given with their definitions of optimality.

2.3.2.1 Neyman-Pearson Type-1 Detector

This detector design is based on minimizing multiple error probabilities. It is given in [12]. Its main idea is to construct the null hypothesis decision region first, and assume common threshold for false alarm probabilities, i.e, $P(H_1|H_0)$, $P(H_2|H_0)$. This detector may have more applications in communication systems.

Theorem 2.1. *Assume that there are three hypotheses to choose, namely, H_0, H_1 and H_2. Assume that the test determined by the decision regions $\mathcal{D}_0^*$, $\mathcal{D}_1^*$ and $\mathcal{D}_2^*$ is optimal in the sense that, for each other test defined by the sets $\mathcal{D}_0$, $\mathcal{D}_1$ and $\mathcal{D}_2$ with the corresponding error probabilities $\alpha_{l|m}^*$ and $\alpha_{l|m}$ with $\alpha_{l|m}^* = P^*(H_l|H_m), l, m = 0, 1, 2$ and $l \neq m$ if $\alpha_0 \leq \alpha_0^*$, then $\max(\alpha_{0|1}, \alpha_{0|2}) \geq \max(\alpha_{0|1}^*, \alpha_{0|2}^*)$ and if $\alpha_1 \leq \alpha_1^*$ then $\alpha_{1|2} \geq \alpha_{1|2}^*$ for the following decision regions:*

$$\mathcal{D}_0^* = \left\{ \mathbf{x} : \min\left(\frac{f(\mathbf{x}; H_0)}{f(\mathbf{x}; H_1)}, \frac{f(\mathbf{x}; H_0)}{f(\mathbf{x}; H_2)} \right) > T_0 \right\}, \ 1 - P(H_0|H_0) = \alpha_0^*$$

$$\mathcal{D}_1^* = \overline{\mathcal{D}_0^*} \cap \left\{ \mathbf{x} : \frac{f(\mathbf{x}; H_1)}{f(\mathbf{x}; H_2)} > T_1 \right\}, \ 1 - P(H_1|H_1) = \alpha_1^*$$

$$\mathcal{D}_2^* = \mathcal{X}^N - (\mathcal{D}_0^* \cup \mathcal{D}_1^*) \tag{2.24}$$

Proof. Let $\phi^*(\mathbf{x})$ and $\phi(\mathbf{x})$ be the indicator functions of decision regions $\mathcal{D}_m^*$ and $\mathcal{D}_m$, respectively. For the decision region of $\mathcal{D}_0^*$, the following inequality is correct.

$$(\phi^*(\mathbf{x}) - \phi(\mathbf{x})) (f(\mathbf{x}; H_0) - T_0 \max(f(\mathbf{x}; H_1), f(\mathbf{x}; H_2))) \geq 0 \tag{2.25}$$

The above inequality is verified as follows: When $\phi^*(\mathbf{x}) = 1$, then

$$\min\left(\frac{f(\mathbf{x}; H_0)}{f(\mathbf{x}; H_1)}, \frac{f(\mathbf{x}; H_0)}{f(\mathbf{x}; H_2)}\right) - T_0 \geq 0$$

$$\min\left(\frac{f(\mathbf{x}; H_0)}{T_0 f(\mathbf{x}; H_1)}, \frac{f(\mathbf{x}; H_0)}{T_0 f(\mathbf{x}; H_2)}\right) - 1 \geq 0$$

$$\frac{f(\mathbf{x}; H_0)}{T_0 \max\left(f(\mathbf{x}; H_0), f(\mathbf{x}; H_1)\right)} - 1 \geq 0$$

$$f(\mathbf{x}; H_0) - T_0 \max\left(f(\mathbf{x}; H_0), f(\mathbf{x}; H_1)\right) \geq 0$$

When $\phi^*(\mathbf{x}) = 0$, the above inequality reverses, and since $0 \leq \phi(\mathbf{x}) \leq 1$, above inequality holds. Summing over all possible values of $\mathbf{x}$, i.e., $\mathcal{X}^N$, the following series of equations are obtained:

$$\sum_{\mathcal{X}^N} (\phi^*(\mathbf{x}) - \phi(\mathbf{x})) \left(f(\mathbf{x}; H_0) - T_0 \max(f(\mathbf{x}; H_1), f(\mathbf{x}; H_2))\right) \geq 0$$

$$\sum_{\mathcal{D}_0^*} \left(f(\mathbf{x}; H_0) - T_0 \max(f(\mathbf{x}; H_1), f(\mathbf{x}; H_2))\right) -$$

$$\sum_{\mathcal{D}_0} \left(f(\mathbf{x}; H_0) - T_0 \max(f(\mathbf{x}; H_1), f(\mathbf{x}; H_2))\right) \geq 0$$

$$1 - \alpha_0^* - T_0 \max(\alpha_{0|1}^*, \alpha_{0|2}^*) - \left[1 - \alpha_0 - T_0 \max(\alpha_{0|1}, \alpha_{0|2})\right] \geq 0$$

$$T_0 \left(\max(\alpha_{0|1}, \alpha_{0|2}) - \max(\alpha_{0|1}^*, \alpha_{0|2}^*)\right) \geq \alpha_0^* - \alpha_0$$

It is seen that if $\alpha_0 \leq \alpha_0^*$, then $\max(\alpha_{0|1}, \alpha_{0|2}) \geq \max(\alpha_{0|1}^*, \alpha_{0|2}^*)$.

For the other case, similar methodology applies. The following inequality holds:

$$(\phi^*(\mathbf{x}) - \phi^*(\mathbf{x})) \left(f(\mathbf{x}; H_1) - T_0 f(\mathbf{x}; H_2)\right) \geq 0 \tag{2.26}$$

(2.26) can be validated as follows: Note that if $\phi^*(\mathbf{x}) = 1$, it means $\mathbf{x} \in \overline{\mathcal{D}_0^*}$ and $\frac{f(\mathbf{x}; H_1)}{f(\mathbf{x}; H_2)} > T_1$. So $(f(\mathbf{x}; H_1) - T_0 f(\mathbf{x}; H_2)) \geq 0$. If $\frac{f(\mathbf{x}; H_1)}{f(\mathbf{x}; H_2)} < T_1$, then $\phi^*(\mathbf{x}) = 0$, hence the inequality holds.

Carrying out the summation over entire sample space, one obtains the following equations:

$$\sum_{\mathcal{X}^N} (\phi^*(\mathbf{x}) - \phi(\mathbf{x})) \left(f(\mathbf{x}; H_1) - T_1 f(\mathbf{x}; H_2)\right) \geq 0$$

$$\sum_{\mathcal{D}_1^*} \left(f(\mathbf{x}; H_1) - T_1 f(\mathbf{x}; H_2)\right) - \sum_{\mathcal{D}_1} \left(f(\mathbf{x}; H_1) - T_1 f(\mathbf{x}; H_2)\right) \geq 0$$

$$1 - \alpha_1^* - T_1 \alpha_{1|2}^* - (1 - \alpha_1 - T_1 \alpha_{1|2}) \geq 0$$

$$T_1 \left(\alpha_{1|2} - \alpha_{1|2}^*\right) \geq \alpha_1^* - \alpha_1 \tag{2.27}$$

Thus, if $\alpha_1 \leq \alpha_1^*$, then $\alpha_{1|2} \geq \alpha_{1|2}^*$. $\hfill \square$

Detector given in (2.24) can be restated as follows. For the null hypothesis be chosen, two likelihood ratio tests $\left(\dfrac{f(\mathbf{x}; H_0)}{f(\mathbf{x}; H_1)}, \dfrac{f(\mathbf{x}; H_0)}{f(\mathbf{x}; H_2)} \right)$ must be greater than common threshold T_0 at the same time. If one finds the threshold according to error probability $\alpha_0^* = P(H_2|H_0) + P(H_1|H_0)$, then this threshold is used for both likelihood ratio tests. This situation may not seem realistic for the radar applications when more than two hypotheses are to be detected with the Neyman-Pearson test. On the other hand, this detector's structure is simple and optimal within its assumption.

2.3.2.2 Neyman-Pearson Type-2 Detector

In [13], generalized Neyman-Pearson type detector is used to discriminate target and jammer presences. The optimality criteria is maximizing the sum of true detection probability, i.e, $(P(H_0|H_0) + P(H_1|H_1) + P(H_2|H_2))$, subject to distinct false alarm probabilities $(P(H_1|H_0) \leq \alpha_1, P(H_2|H_0) \leq \alpha_2)$ is less than some preassigned values. Its derivation is given appendix of [13]. The derivation uses the Lagrange multiplier method and is presented as follows:

$$\text{maximize} \sum_{k=0}^{2} P(H_k|H_k) \text{ subject to } P(H_2|H_0) = \alpha_2,\ P(H_1|H_0) = \alpha_1. \quad (2.28)$$

over the decision region of H_k, namely, $\mathcal{D}_k\ k = 0,\ 1,\ 2$. H_k is chosen if the observation space $\mathbf{x}$ falls in D_k. The Lagrange multipliers for this problem is defined as:

$$= \max_{\mathcal{D}_1, \mathcal{D}_2} \sum_{k=0}^{2} P(H_k|H_k) + \sum_{k=1}^{2} \lambda_k \left[P(H_k|H_0) - \alpha_k \right]$$

$$= \max_{\mathcal{D}_1, \mathcal{D}_2} \sum_{k=1}^{2} P(H_k|H_k) + P(H_0|H_0) + \sum_{k=1}^{2} \lambda_k \left[P(H_k|H_0) - \alpha_k \right]$$

$$= \max_{\mathcal{D}_1, \mathcal{D}_2} \sum_{k=1}^{2} P(H_k|H_k) + 1 - \sum_{k=1}^{2} P(H_k|H_0) + \sum_{k=1}^{2} \lambda_k \left[P(H_k|H_0) - \alpha_k \right]$$

$$= \max_{\mathcal{D}_1, \mathcal{D}_2} \sum_{k=1}^{2} \left[P(H_k|H_k) - P(H_k|H_0) - \lambda_k P(H_k|H_0) \right]$$

$$= \max_{\mathcal{D}_1, \mathcal{D}_2} \sum_{k=1}^{2} \int_{D_k} [f(\mathbf{x}; H_k) - f(\mathbf{x}; H_0) - \lambda_k f(\mathbf{x}; H_0)] \, \mathrm{d}\mathbf{x} \qquad (2.29)$$

(2.29) can be written in a compact form as follows:

$$\max_{\mathcal{D}_1, \mathcal{D}_2} \sum_{k=1}^{2} \int_{D_k} [L_k - 1 - \lambda_k] \, \mathrm{d}\mathbf{x} \qquad (2.30)$$

where L_k the likelihood ratio test between H_k and H_0 hypotheses is defined as follows:

$$L_k \triangleq \frac{f(\mathbf{x}; H_k)}{f(\mathbf{x}; H_0)} \qquad k = 1, 2. \qquad (2.31)$$

The hypothesis H_k is chosen if the integrand given in (2.30) is greater than that of the other hypotheses.

$$\text{Choose } H_k \quad \text{if} \quad L_k - 1 - \lambda_k \underset{H_0}{\overset{H_k}{\gtrless}} 0 \quad k = 1, 2 \qquad (2.32)$$

$$\text{and}$$

$$L_k - 1 - \lambda_k \underset{H_j}{\overset{H_k}{\gtrless}} L_j - 1 - \lambda_k \quad k \neq j \quad k, j = 1, 2$$

where $L_0 = 1$ by definition (see Eqn. ((2.31))). In other words,

$$\begin{cases} H_0 : & \text{if } L_1 < 1 + \lambda_1 \text{ or } L_2 < 1 + \lambda_2 \\ H_1 : & \text{if } L_1 > 1 + \lambda_1 \text{ and } L_1 - \lambda_1 > L_2 - \lambda_2 \\ H_2 : & \text{if } L_2 > 1 + \lambda_2 \text{ and } L_1 - \lambda_1 < L_2 - \lambda_2 \end{cases} \qquad (2.33)$$

This detector structure is different from Neyman-Pearson Detector-1. The difference between Detector-1 and Detector-2 is the definition of optimality. Here, the false alarm probabilities are aimed to be kept below from some predefined value, and the likelihood ratios L_1 and L_2 are compared with different thresholds $1 + \lambda_1$ and $1 + \lambda_2$. Also this detector does not present any optimality criteria about the error probability ($P(H_2|H_1)$).

14

2.3.2.3 Neyman-Pearson Type-3 Detector

In [14], the optimum detector is derived for the M possible message transmissions within Neyman-Pearson framework and with corresponding optimality definition. We believe that the work in [14] is substantially important to understand and analyze the problem at hand. It is assumed that there is no prior information about the message that was sent. Weinberbger and Merhav defines the four type of error probabilities which are probability of false alarm (P_{FA}), probability of misdetection (P_{MD}), probability of inclusive error (P_{IE}) and probability of exclusive error (P_{EE}). Decision space is divided into $M+1$ disjoint regions which include D_m, $(m = 1 \cdots M)$ and D_m which D_0 correspond to null hypothesis (transmitter is silent) and mth message is sent. For ease of readability, the notations used so far are used in the following description:

$$P_{FA} = \sum_{m=1}^{M} P(H_m|H_0), \tag{2.34}$$

$$P_{MD} = \frac{1}{M} \sum_{m=1}^{M} P(H_0|H_M), \tag{2.35}$$

$$P_{IE} = \sum_{m=1}^{M} P(\overline{H_m}|H_m), \tag{2.36}$$

$$P_{EE} = P_{IE} - P_{MD} \tag{2.37}$$

where $P(\overline{H_m}|H_m)$ is the probability of choosing any hypothesis except H_m, when H_m is true. In other words,

$$P(\overline{H_m}|H_m) = P(H_0|H_m) + \cdots + P(H_{m-1}|H_m)+$$
$$P(H_{m+1}|H_m) + P(H_M|H_m) \ m = 1 \cdots M.$$

The detector is constructed via the following optimization problem:

$$\begin{aligned} &\text{minimize } P_{IE} \\ &\text{subject to } P_{FA} \leq \alpha \text{ and } P_{MD} \leq \beta \end{aligned} \tag{2.38}$$

where α and β are preassigned upper bounds for false alarm and misdetection probabilities respectively.

In the binary Neyman-Pearson hypothesis testing problem, because of the fact that P_{FA} and P_{MD} can not be minimized at the same time, the usual method

is to minimize P_{MD} subject to P_{FA} can not be greater than some preassigned value. By giving relaxation between these two error probabilities, the authors aim to freely minimize P_{IE}.

The solution to the problem given in (2.38) is given in the following lemma:

Lemma 2.1. Let the decision regions $\mathcal{D}_m^*$ be constructed as follows:

$$\mathcal{D}_0^* = \left\{ \mathbf{x} : a. \sum_{m=1}^{M} f(\mathbf{x}; H_m) + \max_m f(\mathbf{x}; H_m) \leq b. f(\mathbf{x}; H_0) \right\} \tag{2.39}$$

$$\mathcal{D}_m^* = \overline{\mathcal{D}_0^*} \bigcap \left\{ \mathbf{x} : f(\mathbf{x}; H_m) \geq \max_{k \neq m} f(\mathbf{x}; H_k) \right\}, \quad m = 1, 2, \ldots, M \tag{2.40}$$

and $\mathcal{D}_m$ any other decision regions. If

$$P_{FA} \leq P_{FA}^* \text{ and } P_{MD} \leq P_{MD}^*, \text{ then } P_{IE}^* \leq P_{IE}. \tag{2.41}$$

Proof of above lemma is based on the usage of indicator functions of $\mathcal{D}_m^*$ and $\mathcal{D}_m$ as in the proof of previous three detectors [14].

The first term in decision region $\mathcal{D}_0^*$, $a. \sum_{m=1}^{M} f(\mathbf{x}; H_m)$, is similar to Neyman-Pearson Type-1 detector (see 2.3.2.1). This can interpreted as the likelihood ratios $\dfrac{f(\mathbf{x}; H_m)}{f(\mathbf{x}; H_0)}$ being not greater than common threshold a. Weinberbger and Merhav consider the special case, when the this term dominates the left hand side of (2.39). It is stated that the first term is like the probability mass function of the event of sending any message or put it differently, the hypotheses other than null. So, the first expression becomes the binary hypothesis testing between null hypothesis and transmission of a message. This fact is asserted asymptotically when $a \gg b$.

When the purpose is to minimize to probability of exclusive error (P_{EE}), the proposed detector is not always optimal. Since the inclusive error already includes the miss detection probability, separating them could be good approach. In the case of replacing the misdetection error probability constraint $P_{MD} < \beta$ with equality $P_{MD} = \beta$, the detector in (2.39) becomes optimal. In the general sense, it is difficult to solve the problem when the aim is minimizing the exclusive error.

16

2.3.2.4 Discussion

When there are multiple hypotheses, Bayesian approach is widely accepted since it has ample of application areas in communication systems. Maximum a posteriori detectors and maximum likelihood detectors are used and well covered in literature (for example, see [5, 7, 11]).

However, when the goal is to discriminate three hypotheses as in radar applications, there is no prior information in general. With this motivation, the Neyman-Pearson approach is revisited in the previous sections. The different types of optimum detectors share common goal, i.e, to minimize the error probability or maximize true detection probability for the hypotheses in concern.

Type-1 and Type-3 Neyman-Pearson detectors can be applied specifically on the communication problems. The assumption of more than two hypotheses and minimizing the error probabilities with common threshold for likelihood ratio tests are the common feature of these detectors.

In the next chapter, ternary hypotheses testing will be covered for the sidelobe blanking application whose details are to be presented later. The detector structure is divided into two parts. In the first one, the blanking decision is performed with some optimality criteria, i.e., maximizing the blanking probability when jammer is present, subject to the constraint of keeping the probability of blanking when target is present below some preassigned value. In the second stage, when decision in the first stage is not to blank, the usual target presence decision is performed, like binary Neyman-Pearson hypothesis testing. Further details are presented in Chapter 3

2.4 Composite Hypothesis Testing

The hypothesis testing problem that was considered up to this point is based on the assumptions of known probability density functions (pdf) under each hypotheses. The pdf $f(\mathbf{x}; H_m)$ is called conditional pdf for H_m hypothesis. We assumed that the complete knowledge of pdf's are available. In the problems

considered so far, the hypothesis testing problems correspond to dividing the parameter space of pdf's into disjoint tests. For example, assume that hypothesis H_0 corresponds to noise only which has pdf of $\mathcal{N}(0, \sigma^2)$, and hypothesis H_1 represents the target presence and its pdf has the form of $\mathcal{N}(A, \sigma^2)$ where A is the amplitude of target signal. So the parameter space Φ consists of two sets which are mean and variance. Let $\Theta = \Phi_0 \cup \Phi_0$, where Φ_0 and Φ_1 are parameter sets of H_0 and H_1 respectively. For this simple example, $\Phi_0 = \{0, \sigma^2\}$ and $\Phi_1 = \{A, \sigma^2\}$. When A and σ^2 are known, hypothesis testing problem is said to be simple and optimum detectors can be found depending on the application. If these parameters are not known, then the problem is called as composite. There are several approaches to tackle to the composite tests. For each approach, the optimality criteria changes and when optimum solution does not exist, some sub-optimum or asymptotically optimum approaches are used.

For a test to be better than the others, it has to have higher detection probability, i.e. the power, among the alternatives. For example, in the case of unknown mean problem, when the sign of A is assumed to be known, then one can reach the likelihood ratio test as follows:

Example 2.1.

$$f(\mathbf{x}; H_1 | A) = \frac{1}{2\pi\sigma^2} \exp\left(-\frac{(\mathbf{x} - A\mathbf{1})^T (\mathbf{x} - m\mathbf{1})}{\sigma^2}\right)$$

$$f(\mathbf{x}; H_0) = \frac{1}{2\pi\sigma^2} \exp\left(-\frac{\mathbf{x}^T \mathbf{x}}{\sigma^2}\right)$$

After taking the logarithm of likelihood ratio test, one can find the following:

$$L(\mathbf{x}|A) = \frac{f(\mathbf{x}; H_1)}{f(\mathbf{x}; H_0)} = A\frac{\mathbf{1}^T \mathbf{x}}{\sigma^2} - \frac{A^2 N}{2\sigma^2} \tag{2.42}$$

We see that even if we don't known the value of A except its sign one can find the test $\mathbf{1}^T \mathbf{x}$ as realizable and most powerful among any other tests. This type of tests are called one-sided tests. It is seen that the decision test statistics is completely known when H_0 is assumed to be true. This feature enables the designer to find the threshold based on preassigned false alarm rate.

If the likelihood ratio is monotonic with $T(\mathbf{x})$, which means, for any θ_0 and $\theta > \theta_0$, $L(\mathbf{x}) = \frac{f(\mathbf{x}|\theta_1)}{f(\mathbf{x}|\theta_0)}$ is nondecreasing function of $T(\mathbf{x})$ for all values of $\mathbf{x}$,

then the following test is uniformly most powerful (UMP) among for one-sided hypothesis testing problem [15].

$$T(\mathbf{x}) \underset{H_0}{\overset{H_1}{\gtrless}} \mathbf{x}_0 \qquad (2.43)$$

Also, it is shown that for the exponential family of distributions, the likelihood ratio test is monotonic in sufficient statistic [15]. For the unknown mean in Gaussian noise problem in example 2.1, the likelihood ratio test is monotonically increasing function of $T(\mathbf{x}) = \mathbf{1}^T \mathbf{x}$, which is the sufficient statistic for mean of Gaussian densities.

When the sign of A is not known, one can not find a single likelihood ratio test, there is no UMP test for this type of problems. To tackle this problem, one can transform the data ensuring that parameter space is not affected and try to eliminate the effects of unknown parameter. For the above problem, an intuitive test will be $|\mathbf{1}^T \mathbf{x}|$. This method will be further explained in chapter 4.

In this section, without giving the well-known concepts in detail which can be found in many classical books, our focus will be on the radar applications and a method, called as invariance, which is lesser-known but has appealing optimality properties.

2.4.1 Bayesian Approach

In the Bayesian approach, prior distributions are assumed to represent the realizations of unknown parameters. Each parameters in the conditional pdf's employ its own distributions. The marginal conditional pdf of data

$$
\begin{aligned}
f(\mathbf{x}; H_0) &= E_{\theta_0}\left[f(\mathbf{x}|\theta_0; H_0)\right] = \int f(\mathbf{x}|\theta_0; H_0) f(\theta_0) \mathrm{d}\theta_0 \\
f(\mathbf{x}; H_1) &= E_{\theta_1}\left[f(\mathbf{x}|\theta_1; H_1)\right] = \int f(\mathbf{x}|\theta_1; H_1) f(\theta_1) \mathrm{d}\theta_1
\end{aligned}
\qquad (2.44)
$$

where $f(\theta_0)$ and $f(\theta_1)$ are pdfs of parameters of each conditional distributions of H_0 and H_1 respectively. After finding the conditional pdfs of $f(\mathbf{x}; H_0)$ and $f(\mathbf{x}; H_1)$, Neyman-Pearson type detector, i.e., the likelihood ratio test can be constructed.

This approach is widely used in many applications. For example, when the phase of the return signal is not known, it is assumed to have uniform distribution, and such detectors are called as non-coherent detectors. Moreover, in radar terminology, four types of Swerling targets are derived from different distribution assumptions of its magnitude and phase.

2.4.2 Generalized Likelihood Ratio Test

When there is no probabilistic information about the unknown parameter, with the Van Trees terminology, unknown deterministic parameter case, the maximum likelihood estimate is found and inserted into likelihood ratio test. Maximum likelihood (ML) estimate of the parameter maximizes the likelihood function which is indeed pdf of data.

$$L_G(\mathbf{x}) = \frac{f(\mathbf{x}|\widehat{\theta_1}; H_1)}{f(\mathbf{x}|\widehat{\theta_0}; H_0)} \tag{2.45}$$

where $\widehat{\theta_m}$ maximizes $f(\mathbf{x}|\widehat{\theta_m}; H_m)$ for $m = \{0, 1\}$. In particular,

$$\widehat{\theta_m} = \left. \frac{\partial \ln f(\mathbf{x}|\theta; H_m)}{\partial \theta} \right|_{\theta = \widehat{\theta_m}}. \tag{2.46}$$

Without claiming any optimality, ML estimations are preferred in many applications due to following desirable properties:

- The solution of (2.46) converges to the true value of parameter, as the number of data samples goes to infinity. This property, also called as asymptotically unbiasedness is referred as consistency [6].

- The mean square error of ML estimate decreases to the Cramer-Rao lower bound as the number of data samples goes to infinity. It is also asymptotically Gaussian with the mean of true value of parameter and variance of Cramer-Raor lower bound of error [6].

- It is invariant with respect to any one-to-one function of parameter. In other words, if $h(\theta)$ is one-to-one function of θ and $\widehat{\theta}$ is maximum likelihood estimate of θ, then $h(\widehat{\theta})$ is maximum likelihood estimate of $h(\theta)$ [9].

2.4.3 Invariance Approach

When there exists no UMP test for the hypothesis testing considered, for example: two-sided tests, there exists a third option to obtain UMP test. The approach in the statistics literature is called the invariance method. The method is based on finding group of transformations that does not change hypothesis testing problem. For example, when the mean of the Gaussian signal is assumed to be unknown for H_1 hypothesis, i.e., $A \neq 0$ and zero for H_0 hypotheses. Then this problem is invariant under adding unknown constants or location shifting. Thus, for all transformations, there exists a unique one which indexes all possible values of transformation, i.e., the maximal invariant function. The mathematical definition of maximal invariant test is given in Chapter 4. After finding the maximal invariant statistics for the given group of transformation, one can obtain usual likelihood ratio test using maximal invariant function. Finally, for a certain type of problem, even there is no UMP test in general, there can be UMP test within invariant transformation of data, called UMP invariant test (UMPI).

Another important aspect of invariant approach, unlike sufficient statistics about unknown parameter, is that this method decreases the dimension of parameter as well as dimension of data as in sufficient statistics. Note that sufficiency definition mentioned here is the one given for unknown parameter. Definition of sufficient statistic and a well known theorem to find the sufficient statistic, Fisher-Neyman Factorization theorem, can be found in many classical detection and estimation theory books. For example, see [9, pp. 80–81]. For example: if mean and variance of gaussian signal is not known for either hypotheses, the sufficient statistics for both parameters are known to be sample mean and sample variance, respectively. By definition of sufficient statistics, it can not decrease the dimension of data, in this case it is two-dimensional. For the invariant approach, it will be shown that the dimension of parameter space is reduced to one and the decision test becomes scalar.

In chapter 4, the mathematical theory of invariance method will be given and some signal processing applications will be solved by using this approach. Among the applications are the general signal detection problem, Low Probability of Intercept

(LPI) radar signal detection and frame synchronization word detection.

CHAPTER 3

DESIGN OF MAISEL SIDELOBE BLANKERS WITH A GUARANTEE ON THE GAP TO OPTIMALITY

3.1 Introduction

Signals intercepted from the antenna sidelobes can cause false target declarations, reduced tracking accuracy, reduced direction finding accuracy and other undesired effects. To reduce the impact such effects, a sidelobe blanking (SLB) architecture, known as the Maisel structure, has been proposed [16]. The Maisel structure uses two receiving channels. The first one is the main channel whose antenna has high gain in the main beam and low gain in the sidelobes. The second channel is called the auxiliary channel and has an omnidirectional pattern, i.e. a flat gain which is typically slightly greater than the sidelobe gain of the main antenna as illustrated in Figure 3.1.

The Maisel structure generates a blanking signal when the ratio of the auxiliary channel output power (v) to main channel output power (u), that is (v/u), is greater than blanking threshold F as shown in Figure 3.2. A blanking decision disables the main channel. Stated differently, the main channel output is discarded without any further processing upon blanking. It should be clear that an erroneous blanking decision causes a degradation in the detection performance. The main goal of sidelobe blanker design is to reliably detect the presence of a sidelobe jammer with a minor loss in the target detection capabilities.

As shown in Figure 3.1, the gain of the omnidirectional antenna (ω^2) should satisfy the condition $\omega^2/\delta^2 = \beta^2 \geq 1$ for a reliable operation. Stated differently,
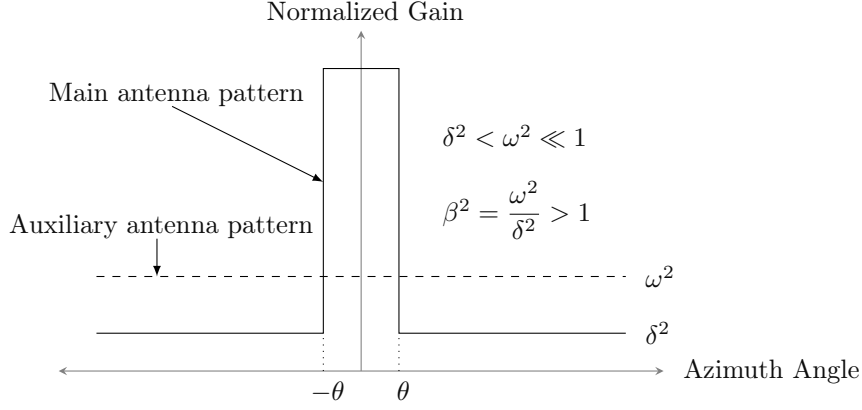
Figure 3.1: Gain patterns of main and auxiliary antennas for a conventional SLB system [17].

the auxiliary antenna acts as a better receiver in comparison to the main antenna for the targets in the sidelobe region. An interfering signal in the sidelobe region with the power α produces main and auxiliary channel output powers of $\delta^2\alpha$ and $\omega^2\alpha$, respectively. The ratio of auxiliary to main channel output, the decision statistics for the Maisel detector, is β^2 and this ratio is to be compared with the threshold F. Therefore, $\beta^2 \geq F$ condition is required to successfully the blank sidelobe interferer [16]. Similarly, in order not to erroneously blank a target in the main lobe region, which produces auxiliary to main channel output ratio of ω^2, the condition of $\omega^2 \leq F$ is also required, [16]. As a summary, the following three conditions are typically required for the design of Maisel sidelobe blankers:
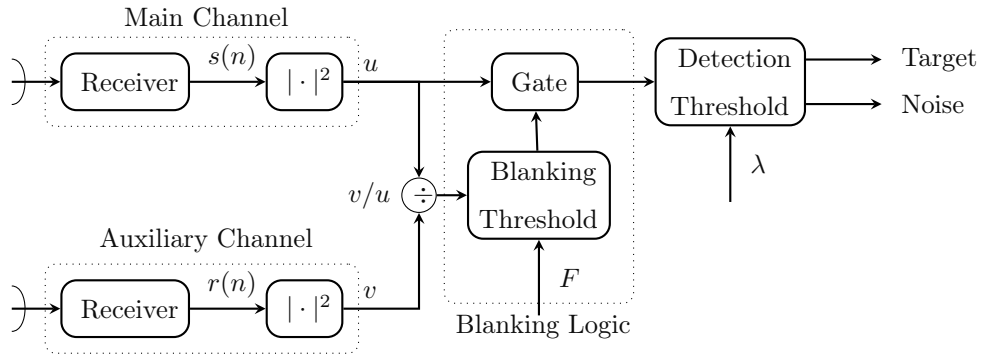
Figure 3.2: Block diagram of Maisel sidelobe blanker [16].

24

1. $\beta^2 = \dfrac{\omega^2}{\delta^2} \geq 1$,

2. $\beta^2 \geq F$,

3. $\omega^2 \leq F$.

It should be noted that these conditions are rather naive, since their derivation is based on noise free operation, that is the statistical variations due to noise, target fluctuations etc. are not taken into account. Typically, these conditions are interpreted as the *necessary conditions* for the design of Maisel SLB systems; but they do not guarantee a satisfactory performance in practical scenarios. In practice, to realize a good performance in the presence of noise and other statistical variations, the parameters β^2, ω^2 and F are chosen such that the conditions are satisfied with a some margin. To the extent of our knowledge, there is no quantitative study on the optimality of Maisel scheme and there is no work on the selection of parameters with the guidance of the optimal Neyman-Pearson test. This study aims to fill this gap in the literature.

The classical SLB systems are well studied in the literature. In [17], Farina examines the classical SLB system in detail and derives the probability of blanking the jammer in sidelobe (P_b), the probability of blanking the target in main beam (P_{tb}), the probability of false target due to jammer in sidelobe (P_{ft}) for Swerling-0 target model. In [18], Farina and Gini extends the aforementioned probability calculation to the Swerling-1 targets. The work is extended to gamma distribution with an arbitrary shape parameter, and shadowed Rice target models [19] and the effects of correlated Gaussian clutter in addition to thermal noise is also accounted in [20]. Shnidman gives the analysis of an arbitrary number of noncoherently integrated pulses for the case of nonfluctuating and gamma fluctuating target in [21]. Shnidman extends the analysis to noncentral gamma (NCG) and noncentral gamma-gamma (NCGG) fluctuations in [22]. In [23], Cui et al. give the performance assessment for arbitrary correlated, possibly nonidentically distributed, fluctuating target and/or jamming returns for a given number of integrated pulses.

To the best of our knowledge, in spite of several important work on the Maisel

structure, its performance gap from the optimal detector is not studied in the literature. In [24], Finn et al. note that the SLB systems derived from the Neyman-Pearson likelihood ratio test (LRT) are hard to implement in real time and the Maisel structure is suggested as a substitute detector with a simple implementation. One of our goals is to justify the good performance of properly designed Maisel SLB systems by conducting a comparison with the optimal Neyman-Pearson detector. It should be mentioned that the optimal Neyman-Pearson test is not possible to implement in practice; since the optimal Neyman-Pearson detector requires several jammer and target parameters which are not typically available to the radar operator. Therefore, our goal is *not* to suggest a practical alternative SLB structure; but to examine the performance gap between the Maisel and optimal system for different scenarios, to identify the conditions that Maisel system operates in the close vicinity of the optimal system and, finally, to present some objective criteria to the designers of Maisel blankers to achieve almost optimal performance.

3.2 Neyman-Pearson Type Optimal Sidelobe Blankers

Let $\tilde{s}$ and $\tilde{r}$ denote the complex valued matched filtered outputs of the main and auxiliary channels at a specific time. We have three hypotheses, namely noise only (H_0), target in main lobe and no jammer in sidelobe (H_1), jammer in sidelobe and no target in main lobe (H_2):

$$H_0 : \begin{cases} \tilde{s} = \tilde{w}_s \\ \tilde{r} = \tilde{w}_r \end{cases}, \tag{3.1}$$

$$H_1 : \begin{cases} \tilde{s} = a_0 \exp\left(j\phi_a\right) + \tilde{w}_s \\ \tilde{r} = \omega a_0 \exp\left(j\phi_a\right) + \tilde{w}_r \end{cases}, \tag{3.2}$$

$$H_2 : \begin{cases} \tilde{s} = c_0 \exp\left(j\phi_c\right) + \tilde{w}_s \\ \tilde{r} = \beta c_0 \exp\left(j\phi_c\right) + \tilde{w}_r \end{cases}. \tag{3.3}$$

Here $\tilde{a} = a_0 \exp\left(j\phi_a\right)$ and $\tilde{c} = c_0 \exp\left(j\phi_c\right)$ indicate target and jammer voltage signal and $\tilde{w}_s \sim \mathcal{CN}(0, \sigma^2)$ and $\tilde{w}_r \sim \mathcal{CN}(0, \sigma^2)$ denote receiver noise in main

and auxiliary channels, respectively. $\mathcal{CN}(0, \sigma^2)$ represents zero mean complex circularly symmetric Gaussian random variables with σ^2 variance. Note that the phrase "jammer" in this work also applies to an interfering target in the sidelobe.

We assume that phases of target and jammer signals are independent of each other. The receiving channels are perfectly matched[1]. Namely, $E\left[\tilde{r}\tilde{s}^*; H_1\right] = \omega E\left[|a_0|^2\right]$ and $E\left[\tilde{r}\tilde{s}^*; H_2\right] = \beta E\left[|c_0|^2\right]$. The LRT to decide blanking the main channel can be formed as follows:

$$\Lambda_m(\tilde{s}, \tilde{r}) = \frac{f_m(\tilde{s}, \tilde{r}; H_2)}{f_m(\tilde{s}, \tilde{r}; H_1)} \underset{\overline{\text{Blank}}}{\overset{\text{Blank}}{\gtrless}} \zeta_m, \quad m = 0, 1, 3. \qquad (3.4)$$

Here, $f_m(\tilde{s}, \tilde{r}; H_2)$ and $f_m(\tilde{s}, \tilde{r}; H_1)$ are the joint probability density functions (pdf) of $\tilde{s}$ and $\tilde{r}$ for Swerling-m $(m = 0, 1, 3)$ target model and the Blank and $\overline{\text{Blank}}$ denote the blanking and not-blanking decisions, respectively. It should be noted that the sidelobe blanker logic given by (3.4) forms the first stage of the detector shown in Figure 3.3.

The sidelobe blanker logic shown in Figure 3.3 generates the decision test which is compared with the threshold ζ_m. If the threshold is exceeded, the main channel is no longer processed and a jammer decision is declared. If the first stage declares the absence of jammer, the main channel output is further processed for the presence or absence of a target.

It can be shown that the sidelobe blanker logic, the first stage of the detector in Figure 3.3, has the optimality properties in the sense that given a fixed probability of (erroneously) blanking the target signal, $Pr(\text{Blank}|H_1)$, the probability of blanking the jammer signal is maximized, $Pr(\text{Blank}|H_2)$, with the shown two-stage test. The proof for this claim is given as follows:

Proof. Let ϕ^* and ϕ denote the indicator functions of blanking decision regions

---

[1] This assumption brings the coherency between receiving channels and only affects the design of optimal detectors which are studied to provide a performance bound for the Maisel blankers.

$\mathcal{B}^*$ and $\mathcal{B}$ which correspond to Neyman-Pearson test and any other test:

$$\phi^*(\mathbf{x}) = \begin{cases} 1 & \mathbf{x} \in \text{Blank}, \quad \text{i.e.} \quad \dfrac{f(\mathbf{x}; H_2)}{f(\mathbf{x}, H_1)} > \zeta \\ 0 & \mathbf{x} \in \overline{\text{Blank}}, \quad \text{i.e.} \quad \dfrac{f(\mathbf{x}; H_2)}{f(\mathbf{x}, H_1)} < \zeta \end{cases}, \tag{3.5}$$

where $\mathbf{x} = \begin{bmatrix} \tilde{s} & \tilde{r} \end{bmatrix}^T$.

The following inequality immediately follows from the above expression.

$$(\phi^*(\mathbf{x}) - \phi(\mathbf{x}))\,(f(\mathbf{x}; H_2) - \zeta f(\mathbf{x}; H_1)) \geq 0. \tag{3.6}$$

Integrating (3.6) over the entire sample space, we get the following equations:

$$\int\limits_{\mathbf{x} \in \mathcal{B}^*} (f(\mathbf{x}; H_2) - \zeta f(\mathbf{x}; H_1))\,\mathrm{d}\mathbf{x} - \int\limits_{\mathbf{x} \in \mathcal{B}} (f(\mathbf{x}; H_2) - \zeta f(\mathbf{x}; H_1))\,\mathrm{d}\mathbf{x} \geq 0$$

$$P(\mathcal{B}^*|H_2) - \zeta P(\mathcal{B}^*|H_1) - P(\mathcal{B}|H_2)) + \zeta P(\mathcal{B}|H_1) \geq 0$$

$$P(\mathcal{B}^*|H_2) - P(\mathcal{B}|H_2) \geq \zeta\,(P(\mathcal{B}^*|H_1) - P(\mathcal{B}|H_1)) \tag{3.7}$$

where $P(\mathcal{B}|H_2)$ and $P(\mathcal{B}|H_1)$ are the probabilities of deciding blanking and not blanking for the any other test except Neyman-Pearson test.

From (3.7), we see that if $P(\mathcal{B}|H_1) \leq P(\mathcal{B}^*|H_1)$ than $P(\mathcal{B}^*|H_2) \geq P(\mathcal{B}|H_2)$ since $\zeta \geq 0$. Thus, any other test whose target blanking probability is desired to be upper bounded by some level will have a smaller jammer blanking probability compared to the Neyman-Pearson test. $\square$

With the adoption of this optimality result, the blanking process and target detection process can be separated.
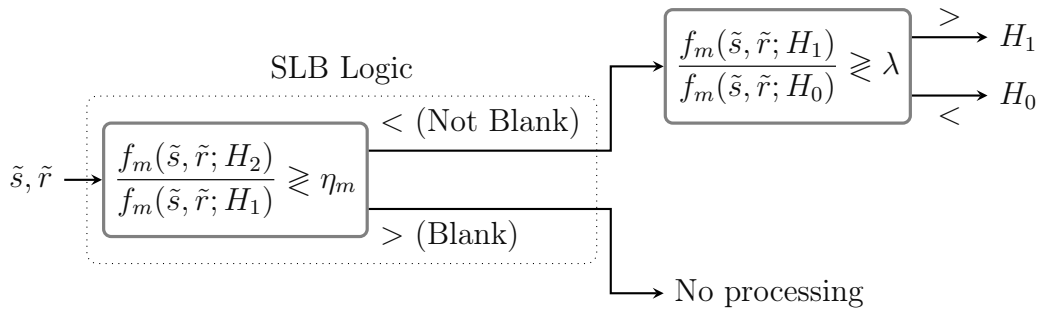
Figure 3.3: Illustration of two-stage radar receiver with a sidelobe blanker logic.

In the rest of this section, the log likelihood ratio tests (LLRT) of hypotheses H_2 and H_1 are calculated for different target fluctuations models. We denote the decision statistics for this purpose as

$$d_m = \log \Lambda_m(\tilde{s}, \tilde{r}) \underset{\overline{\text{Blank}}}{\overset{\text{Blank}}{\gtrless}} \eta_m. \quad m = 0, 1, 3. \tag{3.8}$$

Here, d_m is the decision statistics for the Swerling-m target model. The probability for the undesired event of (erroneous) target blanking probability $P_{tb} = Pr(\text{Blank}|H_1) = \int_{\eta_m}^{\infty} f_{d_m|H_1}(x)\mathrm{d}x$ can be set to a predefined value by adjusting the threshold level. As shown, the threshold value becomes a function of the parameters $\{\text{SNR}, \text{JNR}, \omega^2, \beta^2\}$. After setting the threshold, the probability of the desired event, that is the probability of blanking an active jammer, can be determined as $P_b = Pr(\text{Blank}|H_2) = \int_{\eta_m}^{\infty} f_{d_m|H_2}(x)\mathrm{d}x$. In the following subsections, we present the details of these calculations. Throughout the SLB detector constructions, it is assumed that target and jammer have same Swerling target model except their powers.

3.2.1 Swerling-0 Target Model

Swerling-0 target model assumes that the phase of $\tilde{a}$ (ϕ_a) is uniformly distributed over $(0, 2\pi)$ and the magnitude of $\tilde{a}$ is deterministic.

We first give the conditional pdf's of $\tilde{s}$ and $\tilde{r}$ given that $\tilde{a}$ and $\tilde{c}$ are completely known. The conditional pdf will be Gaussian whose mean is reflected by target and jammer signals and is given as follows:

Under H_1, $f(\tilde{s}|\tilde{a}; H_1) \sim \mathcal{CN}(\tilde{a}, \sigma^2)$ and $f(\tilde{r}|\tilde{a}; H_1) \sim \mathcal{CN}(\omega\tilde{a}, \sigma^2)$. Under H_2, $f(\tilde{s}|\tilde{c}; H_2) \sim \mathcal{CN}(\tilde{c}, \sigma^2)$ and $f(\tilde{r}|\tilde{c}; H_2) \sim \mathcal{CN}(\beta\tilde{c}, \sigma^2)$. Since the conditional pdf's have the same form, we will continue with that under H_1.

$$f(\tilde{s}|\tilde{a}; H_1) = \frac{1}{\pi\sigma^2} \exp\left(-\frac{|\tilde{s} - \tilde{a}|^2}{\sigma^2}\right),$$
$$f(\tilde{r}|\tilde{a}; H_1) = \frac{1}{\pi\sigma^2} \exp\left(-\frac{|\tilde{r} - \omega\tilde{a}|^2}{\sigma^2}\right). \tag{3.9}$$

Since the receiver noise in both channels ($\tilde{w}_s$ and $\tilde{w}_r$) are assumed to be independent, $\tilde{s}$ and $\tilde{r}$ turns to be conditionally independent. Hence,

$$f(\tilde{s}, \tilde{r}|\tilde{a}; H_1) = \frac{1}{\pi^2\sigma^4} \exp\left(-\frac{1}{\sigma^2}\left(|\tilde{s} - \tilde{a}|^2 + |\tilde{r} - \omega\tilde{a}|^2\right)\right). \qquad (3.10)$$

To get rid of the phase dependency of joint pdf's of $\tilde{s}$ and $\tilde{r}$, we use Bayesian approach for random parameters. We carry out the integration of joint pdf's given that phase and magnitude are given over the phase of the target signal. We assume that phases of target in both channels are same. The target signal can be expressed as $\tilde{a} = a_0 \exp(j\phi)$ where ϕ is uniformly distributed over $(0, 2\pi)$, and a_0 is deterministic.

$$f(\tilde{s}, \tilde{r}|a_0; H_1) = \int_0^{2\pi} f(\tilde{s}, \tilde{r}|a_0, \phi; H_1) f_\phi(\phi) d\phi. \qquad (3.11)$$

Expanding (3.11), we obtain the following:

$$f(\tilde{s}, \tilde{r}|a_0; H_1) = \frac{1}{\pi^2\sigma^4} \exp\left(-\frac{1}{\sigma^2}\left(|\tilde{s}|^2 + |\tilde{r}|^2 + a_0^2 + \omega^2 a_0^2\right)\right) I_0\left(\frac{2a_0}{\sigma^2}|\tilde{s} + \omega\tilde{r}|\right)$$

$$\qquad (3.12)$$

where $I_0(\cdot)$ is the modified Bessel function of the first kind. Similarly,

$$f(\tilde{s}, \tilde{r}|c_0; H_2) = \frac{1}{\pi^2\sigma^4} \exp\left(-\frac{1}{\sigma^2}\left(|\tilde{s}|^2 + |\tilde{r}|^2 + c_0^2 + \beta^2 c_0^2\right)\right) I_0\left(\frac{2c_0}{\sigma^2}|\tilde{s} + \beta\tilde{r}|\right)$$

$$\qquad (3.13)$$

where $c_0 = |\tilde{c}|$ is the magnitude of jammer return. Signal to noise ratio and jammer to noise ratio are defined as:

$$\gamma_s \triangleq \text{SNR} = \frac{|\tilde{a}|^2}{E[w_s^2]} = \frac{a_0^2}{\sigma^2}, \qquad (3.14)$$

$$\gamma_j \triangleq \text{JNR} = \frac{|\tilde{c}|^2}{E[w_s^2]} = \frac{c_0^2}{\sigma^2}. \qquad (3.15)$$

Moreover, we assume that phases of target and jammer signals are independent of each other. But across the channels, target and jammer phases do not change. In other words, the two channels are perfectly matched to each other. Also, this assumption brings the coherency between channels. Namely, $E[\tilde{r}\tilde{s}^*; H_1] = \omega a_0^2$ and $E[\tilde{r}\tilde{s}^*; H_2] = \beta c_0^2$.

Likelihood ratio test to decide Blank and Not Blank is

$$\Lambda_0(\tilde{r}, \tilde{s}) = \frac{f(\tilde{s}, \tilde{r}|c_0; H_2)}{f(\tilde{s}, \tilde{r}|a_0; H_1)} \overset{\text{Blank}}{\underset{\overline{\text{Blank}}}{\gtrless}} \zeta_0. \qquad (3.16)$$

Ignoring non-data dependent terms we reach the following test:

$$d_0 = \frac{I_0\left(\dfrac{2c_0}{\sigma^2}|\tilde{s} + \beta\tilde{r}|\right)}{I_0\left(\dfrac{2a_0}{\sigma^2}|\tilde{s} + \omega\tilde{r}|\right)} \begin{array}{c} \text{Blank} \\ \gtrless \\ \overline{\text{Blank}} \end{array} \eta_0. \tag{3.17}$$

Using the test given in (3.17) one can find the optimum SLB detector. The false blanking probability $P_{tb} = Pr(\text{Blank}|H_1) = \int_{\eta_0}^{\infty} f_{d_0|H_1}(x)dx$ is aimed to keep below some predefined value. To this aim, the threshold value is found for each parameters (SNR, JNR, ω^2, β^2). After finding the threshold, we can find the probability of true blanking which is defined as $P_b = Pr(\text{Blank}|H_2) = \int_{\eta_0}^{\infty} f_{d_0|H_1}(x)dx$. With this approach, we can be sure that P_{tb} is kept below some value by changing threshold and the probability of blanking the jammer in the sidelobe is maximized. The decision statistic of (3.17) is analytically formidable to obtain, due to nonlinearities in it. For this reason, Monte Carlo method of simulation is applied in the following sections.

3.2.2   Swerling-1 Target Model

Swerling-1 target model assumes the amplitude of target return, $\tilde{a}$, is Rayleigh distributed and the phase is uniformly distributed as in Swerling-1 case. Also, there is no pulse to pulse to fluctuations in one antenna scan. This model is referred to as scan to scan fluctuation.

To find the joint pdf of $\tilde{s}$ and $\tilde{r}$, we integrate (3.12) over a_0 whose pdf is as follows:

$$f(a_0) = \frac{2a_0}{\sigma_a^2} \exp\left(-\frac{a_0^2}{\sigma_a^2}\right). \tag{3.18}$$

Note that average power of target return signal is σ_a^2 and is complex Gaussian distributed having a variance of σ_a^2, that is, $\tilde{a} \sim \mathcal{CN}(0, \sigma^2)$.

The signal-to-noise-ratio (SNR) and jammer-to-noise-ratio (JNR) are defined as:

$$\gamma_s \triangleq \text{SNR} = \frac{E\left[|\tilde{a}|^2\right]}{E\left[w_s^2\right]} = \frac{\sigma_a^2}{\sigma^2}, \tag{3.19}$$

$$\gamma_j \triangleq \text{JNR} = \frac{E\left[|\tilde{c}|^2\right]}{E\left[w_s^2\right]} = \frac{\sigma_c^2}{\sigma^2}. \tag{3.20}$$

31

Here, two derivations of the optimum SLB detector are provided:

First Derivation:

Proof. By Bayesian approach for random parameters case,

$$f(\tilde{s}, \tilde{r}; H_1) = \int_0^\infty f(\tilde{s}, \tilde{r}|a_0; H_1) f(a_0) da_0. \tag{3.21}$$

Putting (3.12) and (3.18) into (3.21), we have the following equation:

$$
\begin{aligned}
f(\tilde{s}, \tilde{r}; H_1) &= \int_0^\infty \frac{1}{\pi^2 \sigma^4} \exp\left(-\frac{1}{\sigma^2}\left(|\tilde{s}|^2 + |\tilde{r}|^2\right)\right) \exp\left(-\frac{1}{\sigma^2} a_0^2 (1+\omega^2)\right) \\
&\quad \times I_0\left(\frac{2a_0}{\sigma^2}|\tilde{s} + \omega\tilde{r}|\right) \frac{2a_0}{\sigma_a^2} \exp\left(-\frac{a_0^2}{\sigma_a^2}\right) da_0
\end{aligned}
\tag{3.22}
$$

$$
\begin{aligned}
&= \frac{1}{\pi^2 \sigma^4} \exp\left(-\frac{1}{\sigma^2}\left(|\tilde{s}|^2 + |\tilde{r}|^2\right)\right) \\
&\quad \times \underbrace{\int_0^\infty \exp\left(-a_0^2\left(\frac{1+\omega^2}{\sigma^2} + \frac{1}{\sigma_a^2}\right)\right) I_0\left(\frac{2a_0}{\sigma^2}|\tilde{s} + \omega\tilde{r}|\right) \frac{2a_0}{\sigma_a^2} da_0}_{I}.
\end{aligned}
$$

$$\tag{3.23}$$

By making use of the relation [25]

$$\int_0^\infty 2xa \exp\left(-ax^2\right) I_0(bx) dx = \exp\left(\frac{b^2}{4a}\right),$$

The integral (I) in (3.23) can be written as:

$$I = \exp\left(\sigma_a^2 \left(\frac{|\tilde{s}|^2 + \omega^2|\tilde{r}|^2 + 2\omega \mathrm{Re}(sr^*)}{\sigma^2 \left(\sigma_a^2(1+\omega^2) + \sigma^2\right)}\right)\right) \frac{\sigma^2}{\sigma_a^2(1+\omega^2) + \sigma^2}. \tag{3.24}$$

Putting (3.24) into (3.23), we obtain the joint pdf as:

$$
\begin{aligned}
f(\tilde{s}, \tilde{r}; H_1) &= \underbrace{\left(\frac{\sigma^2}{\sigma_a^2(1+\omega^2) + \sigma^2}\right)}_{K_1} \underbrace{\frac{1}{\pi^2 \sigma^4} \exp\left(-\frac{1}{\sigma^2}\left(|\tilde{s}|^2 + |\tilde{r}|^2\right)\right)}_{K} \\
&\quad \times \exp\left(\sigma_a^2 \left(\frac{|\tilde{s}|^2 + \omega^2|\tilde{r}|^2 + 2\omega \mathrm{Re}(sr^*)}{\sigma^2 \left(\sigma_a^2(1+\omega^2) + \sigma^2\right)}\right)\right). \tag{3.25}
\end{aligned}
$$

Rewriting the joint pdf of $\tilde{s}$ and $\tilde{r}$ in terms of SNR and JNR, we obtain the

following simplified expression for H_1 and H_2 hypotheses:

$$f(\tilde{s}, \tilde{r}; H_1) = K_1 \exp\left(-\frac{(-\gamma_s \omega^2 - 1)|\tilde{s}|^2 + (-\gamma_s - 1)|\tilde{r}|^2 + 2\mathrm{Re}(sr^*)\omega\gamma_s}{\sigma^2 \left(\gamma_s(1 + \omega^2) + 1\right)}\right)$$

(3.26)

$$f(\tilde{s}, \tilde{r}; H_2) = K_2 \exp\left(-\frac{(-\gamma_j \beta^2 - 1)|\tilde{s}|^2 + (-\gamma_j - 1)|\tilde{r}|^2 + 2\mathrm{Re}(sr^*)\beta\gamma_j}{\sigma^2 \left(\gamma_j(1 + \beta^2) + 1\right)}\right)$$

(3.27)

where K_1 is defined in (3.25) and K_2 is defined as:

$$K_2 = \frac{\sigma^2}{\sigma_c^2(1 + \beta^2) + \sigma^2}.$$

The likelihood ratio test to decide Blank or $\overline{\text{Blank}}$:

$$\Lambda_1(\tilde{r}, \tilde{s}) = \frac{f(\tilde{s}, \tilde{r}; H_2)}{f(\tilde{s}, \tilde{r}; H_1)} \underset{\overline{\text{Blank}}}{\overset{\text{Blank}}{\gtrless}} \zeta_1.$$

(3.28)

$\Lambda_1(\tilde{r}, \tilde{s})$ in (3.28) can be found as:

$$\Lambda_1(\tilde{r}, \tilde{s}) = K_3 \exp\left[|\tilde{s}|^2 \left(\frac{\gamma_s \omega^2 + 1}{\gamma_s(1 + \omega^2) + 1} - \frac{\gamma_j \beta^2 + 1}{\gamma_j(1 + \beta^2) + 1}\right)\right.$$
$$+ |\tilde{r}|^2 \left(\frac{\gamma_s + 1}{\gamma_s(1 + \omega^2) + 1} - \frac{\gamma_j + 1}{\gamma_j(1 + \beta^2) + 1}\right)$$
$$\left. + 2\mathrm{Re}(sr^*) \left(\frac{-\omega\gamma_s}{\gamma_s(1 + \omega^2) + 1} - \frac{\beta\gamma_j}{\gamma_j(1 + \beta^2) + 1}\right)\right]. \quad (3.29)$$

where $K_3 = \dfrac{K_2}{K_1}$ is non-data dependent factor.

Taking the logarithm of (3.29) and ignoring non-data dependent terms we have the following test:

$$d_1 = A|\tilde{s}|^2 + B|\tilde{r}|^2 + C2\mathrm{Re}(sr^*) \underset{\overline{\text{Blank}}}{\overset{\text{Blank}}{\gtrless}} \eta_1,$$

(3.30)

where

$$A = \frac{\gamma_s \omega^2 + 1}{\gamma_s(1 + \omega^2) + 1} - \frac{\gamma_j \beta^2 + 1}{\gamma_j(1 + \beta^2) + 1}, \tag{3.31a}$$

$$B = \frac{\gamma_s + 1}{\gamma_s(1 + \omega^2) + 1} - \frac{\gamma_j + 1}{\gamma_j(1 + \beta^2) + 1}, \tag{3.31b}$$

$$C = \frac{-\omega\gamma_s}{\gamma_s(1 + \omega^2) + 1} - \frac{\beta\gamma_j}{\gamma_j(1 + \beta^2) + 1}. \tag{3.31c}$$

$\square$

Second Derivation:

Proof. We note that the random variables $\tilde{r}$ and $\tilde{s}$ are correlated. The correlation under different hypotheses is as follows: $E[\tilde{r}\tilde{s}^*; H_1] = \omega\sigma_a^2$ and $E[\tilde{r}\tilde{s}^*; H_2] = \beta\sigma_c^2$. We introduce $\mathbf{x} = \begin{bmatrix} \tilde{s} & \tilde{r} \end{bmatrix}^T$ as a two dimensional Gaussian random vector with the correlation matrix $\mathbf{C}_i$ as follows:

$$\mathbf{C}_i = E[\mathbf{x}\mathbf{x}^H; H_i] = \begin{bmatrix} E[|\tilde{s}|^2; H_i] & E[\tilde{s}\tilde{r}^*; H_i] \\ E[\tilde{s}^*\tilde{r}; H_i] & E[|\tilde{r}|^2; H_i] \end{bmatrix}, \; i = \{1, 2\}$$

The probability density function (pdf) of $\mathbf{x}$ under H_i becomes

$$f(\mathbf{x}; H_i) = \frac{1}{\pi^2 |\mathbf{C}_i|^2} \exp\left(-\mathbf{x}^H \mathbf{C}_i^{-1} \mathbf{x}\right), \; i = \{1, 2\}$$

and the covariance matrices $\mathbf{C}_1$ and $\mathbf{C}_2$ can be given as follows:

$$\mathbf{C}_1 = \sigma^2 \begin{bmatrix} \gamma_s + 1 & \omega\gamma_s \\ \omega\gamma_s & \omega^2\gamma_s + 1 \end{bmatrix}, \tag{3.32a}$$

$$\mathbf{C}_2 = \sigma^2 \begin{bmatrix} \gamma_j + 1 & \beta\gamma_j \\ \beta\gamma_j & \beta^2\gamma_j + 1 \end{bmatrix}. \tag{3.32b}$$

The likelihood ratio test to decide blanking or not blanking can be written as:

$$\Lambda(\tilde{r}, \tilde{s}) = \frac{f_{\mathbf{x}}(\mathbf{x}; H_2)}{f_{\mathbf{x}}(\mathbf{x}; H_1)} \underset{\overline{\text{Blank}}}{\overset{\text{Blank}}{\gtrless}} \zeta. \tag{3.33}$$

Taking the logarithm of $\Lambda(\tilde{r}, \tilde{s})$ and ignoring non-data dependent terms, we reach the following test [6]:

$$d_1 = \mathbf{x}^H (\mathbf{C}_1^{-1} - \mathbf{C}_2^{-1})\mathbf{x} \underset{\overline{\text{Blank}}}{\overset{\text{Blank}}{\gtrless}} \eta. \tag{3.34}$$

$\square$

The test consists of quadratic forms of complex Gaussian random variables. The statistic of $\mathbf{x}^H \mathbf{Q} \mathbf{x}$ is important in several telecommunication applications [26, 27, 28, 29]. Following the notation of [27] and [28], we define the $\mathbf{Q}$ matrix

$$\mathbf{Q} \triangleq \sigma^2 \left(\mathbf{C}_1^{-1} - \mathbf{C}_2^{-1}\right) = \begin{bmatrix} A & C \\ C & B \end{bmatrix}, \tag{3.35}$$

whose entries can be calculated through elementary algebra as

$$A = \frac{\gamma_s\,\omega^2 + 1}{\gamma_s\,\omega^2 + \gamma_s + 1} - \frac{\gamma_j\,\beta^2 + 1}{\gamma_j\,\beta^2 + \gamma_j + 1}, \tag{3.36a}$$

$$B = \frac{\gamma_s + 1}{\gamma_s\,\omega^2 + \gamma_s + 1} - \frac{\gamma_j + 1}{\gamma_j\,\beta^2 + \gamma_j + 1}, \tag{3.36b}$$

$$C = -\frac{\gamma_s\,\omega}{\gamma_s\,\omega^2 + \gamma_s + 1} + \frac{\beta\,\gamma_j}{\gamma_j\,\beta^2 + \gamma_j + 1}. \tag{3.36c}$$

See [3] for additional details.

The decision statistics d_1 in (3.34) can be expressed as follows:

$$d_1 \;\; = \;\; \mathbf{x}^H\mathbf{Q}\mathbf{x} = A|\tilde{s}|^2 + B|\tilde{r}|^2 + 2C\mathrm{Re}(\tilde{r}\tilde{s}^*) \tag{3.37}$$

and its pdf can be written as [26, 27]:

$$f_d(d) = \begin{cases} \dfrac{ab}{a + b}\exp\left(-ad\right) & d \geq 0, \\[2em] \dfrac{ab}{a + b}\exp\left(bd\right) & d < 0. \end{cases} \tag{3.38}$$

The parameters a and b appearing in (3.38) are defined through a rather complicated functions of $\mu_{\tilde{r}\tilde{s}}$ and r, [28]:

$$a = \sqrt{r^2 + \frac{1}{4(\mu_{\tilde{r}\tilde{r}}\mu_{\tilde{s}\tilde{s}} - |\mu_{\tilde{s}\tilde{r}}|^2)(|C|^2 - AB)}} - r, \tag{3.39a}$$

$$b = \sqrt{r^2 + \frac{1}{4(\mu_{\tilde{r}\tilde{r}}\mu_{\tilde{s}\tilde{s}} - |\mu_{\tilde{s}\tilde{r}}|^2)(|C|^2 - AB)}} + r \tag{3.39b}$$

where $\mu_{\tilde{r}\tilde{s}} = \frac{1}{2}E[\tilde{r}\tilde{s}^*]$ and

$$r = \frac{A\mu_{\tilde{r}\tilde{r}} + B\mu_{\tilde{s}\tilde{s}} + C^*\mu_{\tilde{s}\tilde{r}}^* + C\mu_{\tilde{r}\tilde{s}}}{4(\mu_{\tilde{r}\tilde{r}}\mu_{\tilde{s}\tilde{s}} - |\mu_{\tilde{s}\tilde{r}}|^2)(|C|^2 - AB)}.$$

To verify the pdf given in (3.38), Monte Carlo simulation of 10^7 trials is performed and the result is presented in Figure 3.4. The red solid line show the theoretical output while dark blue bar graph shows the histogram of the quadratic output. From Figure 3.4, it can be clearly stated that the theoretical expression (3.38) is within a very close proximity to the simulated result.

Threshold Calculation: The threshold η_1 for the Neyman-Pearson test can be calculated from (3.38). For a given target blanking probability (P_{tb}), the
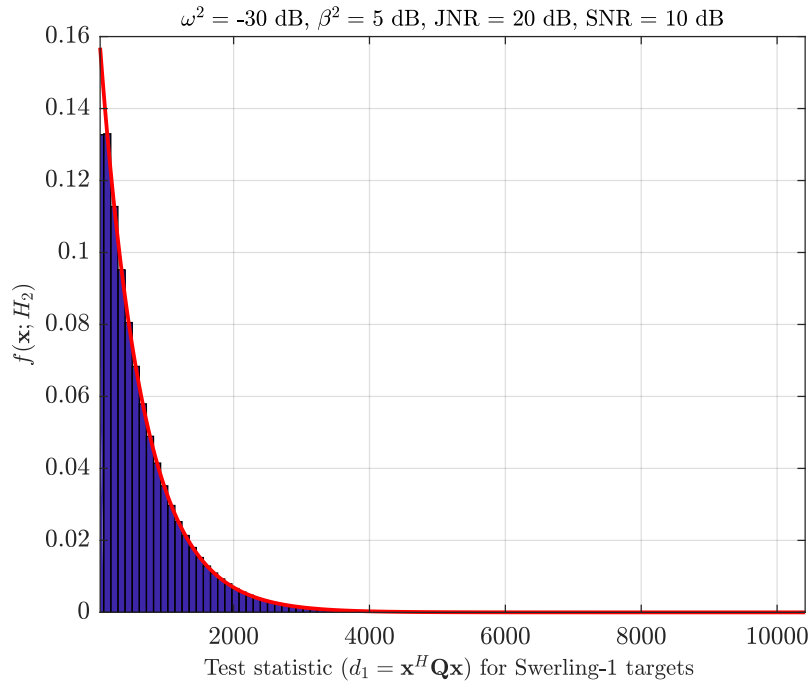
(a) Under H_2
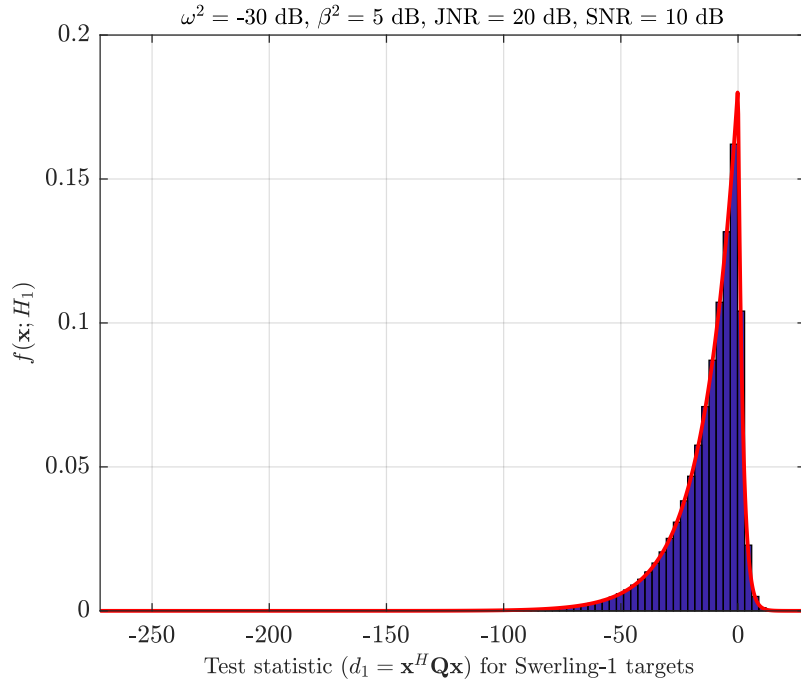
(b) Under H_1

Figure 3.4: The pdf and histogram of the optimum SLB detector. # of Monte Carlo trials $= 10^7$.

threshold η_1 is

$$
\eta_1 = \begin{cases} -\dfrac{1}{a} \ln\left[\left(\dfrac{a+b}{b}\right)P_{tb}\right] & P_{tb} \geq \dfrac{b}{a+b}, \\ \dfrac{1}{b} \ln\left[-\left(\dfrac{a+b}{a}\right)(P_{tb}-1)\right] & P_{tb} \leq \dfrac{b}{a+b}. \end{cases}
\tag{3.40}
$$

Blanking Probability Calculation: Using the threshold η_1, the probability of blanking the jammer in sidelobe is

$$
P_b = \begin{cases} \dfrac{b}{a+b} \exp\left(-a\eta_1\right) & \eta_1 \geq 0, \\ \dfrac{a}{a+b}\left(1 - \exp(b\eta_1)\right) + \dfrac{b}{a+b} & \eta_1 \leq 0. \end{cases}
\tag{3.41}
$$

3.2.3 Swerling-3 Target Model

Swerling-3 target model is similar to Swerling-1 target (scan to scan fluctuation) case except that the magnitude of $\tilde{a}$ is distributed as:

$$
f(a_0) = \frac{8a_0^3}{\sigma_a^4} \exp\left(-\frac{2a_0^2}{\sigma_a^2}\right).
\tag{3.42}
$$

The average power of target signal, $E[a_0^2] = \sigma_a^2$. Here, the inphase and quadrature components are no longer Gaussian distributed. Using the same method in Swerling-1 case, the joint pdf of $\tilde{s}$ and $\tilde{r}$ under H_1 can be written as:

$$
\begin{aligned}
f(\tilde{s}, \tilde{r}; H_1) &= \int_0^\infty \frac{1}{\pi^2 \sigma^4} \exp\left(-\frac{1}{\sigma^2}\left(|\tilde{s}|^2 + |\tilde{r}|^2\right)\right) \exp\left(-\frac{1}{\sigma^2}a_0^2(1+\omega^2)\right) \\
&\quad \times I_0\left(\frac{2|\tilde{a}|}{\sigma^2}|\tilde{s} + \omega\tilde{r}|\right) \frac{8a_0^3}{\sigma_a^4} \exp\left(-\frac{2a_0^2}{\sigma_a^2}\right) da_0,
\end{aligned}
\tag{3.43}
$$

$$
\begin{aligned}
&= \frac{1}{\pi^2 \sigma^4} \exp\left(-\frac{1}{\sigma^2}\left(|\tilde{s}|^2 + |\tilde{r}|^2\right)\right) \\
&\quad \times \underbrace{\int_0^\infty \exp\left(-a_0^2\left(\frac{1+\omega^2}{\sigma^2} + \frac{2}{\sigma_a^2}\right)\right) I_0\left(\frac{2|\tilde{a}|}{\sigma^2}|\tilde{s} + \omega\tilde{r}|\right) \frac{8a_0^3}{\sigma_a^4} da_0}_{I}.
\end{aligned}
\tag{3.44}
$$

By making use of the relation [25]

$$
\int_0^\infty 2x^3 \exp\left(-ax^2\right) I_0(bx) dx = \frac{1}{a^2}\left(1 + \frac{b^2}{4a}\right) \exp\left(\frac{b^2}{4a}\right),
$$

The integral (I) in (3.44) can be written as:

$$I = \frac{\sigma^2}{\sigma_a^2(1+\omega^2)+2\sigma^2} \exp\left(\frac{\sigma_a^2|\tilde{s}+\omega\tilde{r}|^2}{\sigma^2\left(\sigma_a^2(1+\omega^2)+2\sigma^2\right)}\right)\left(1+\frac{\sigma_a^2|\tilde{s}+\omega\tilde{r}|^2}{\sigma^2\left(\sigma_a^2(1+\omega^2)+2\sigma^2\right)}\right).$$

(3.45)

The joint pdf of $\tilde{s}$ and $\tilde{r}$ can be written as:

$$f(\tilde{s},\tilde{r};H_1) = KK_1 \exp\left(\frac{\gamma_s|\tilde{s}+\omega\tilde{r}|^2}{\sigma^2\left(\gamma_s(1+\omega^2)+2\right)}\right)\left(1+\frac{\gamma_s|\tilde{s}+\omega\tilde{r}|^2}{\sigma^2\left(\gamma_s(1+\omega^2)+2\right)}\right),$$

(3.46)

$$f(\tilde{s},\tilde{r};H_2) = KK_1 \exp\left(\frac{\gamma_j|\tilde{s}+\beta\tilde{r}|^2}{\sigma^2\left(\gamma_j(1+\beta^2)+2\right)}\right)\left(1+\frac{\gamma_j|\tilde{s}+\omega\tilde{r}|^2}{\sigma^2\left(\gamma_j(1+\beta^2)+2\right)}\right).$$

(3.47)

In matrix form above expression can be arranged as follows:

$$\mathbf{Q}_1 \triangleq \frac{\gamma_s}{\sigma^2(\gamma_s(1+\omega^2)+2)}\begin{bmatrix} 1 & \omega \\ \omega & \omega^2 \end{bmatrix}, \quad \mathbf{Q}_2 \triangleq \frac{\gamma_j}{\sigma^2(\gamma_j(1+\beta^2)+2)}\begin{bmatrix} 1 & \beta \\ \beta & \beta^2 \end{bmatrix}.$$

(3.48)

$$f(\tilde{s},\tilde{r};H_1) = KK_1 \exp\left(\mathbf{x}^H\mathbf{Q}_1\mathbf{x}\right)\left(1+\mathbf{x}^H\mathbf{Q}_1\mathbf{x}\right),$$

(3.49)

$$f(\tilde{s},\tilde{r};H_2) = KK_1 \exp\left(\mathbf{x}^H\mathbf{Q}_2\mathbf{x}\right)\left(1+\mathbf{x}^H\mathbf{Q}_2\mathbf{x}\right).$$

(3.50)

Likelihood ratio test to blank or not is defined as:

$$\Lambda_3(\tilde{r},\tilde{s}) = \frac{f(\tilde{s},\tilde{r};H_2)}{f(\tilde{s},\tilde{r};H_1)} \overset{\text{Blank}}{\underset{\overline{\text{Blank}}}{\gtrless}} \zeta_3.$$

(3.51)

$\Lambda_3(\tilde{r},\tilde{s})$ can be given as:

$$\Lambda_3(\tilde{r},\tilde{s}) = K_3 \exp\left(\mathbf{x}^H\left(\mathbf{Q}_2-\mathbf{Q}_1\right)\mathbf{x}\right)\left(\frac{1+\mathbf{x}^H\mathbf{Q}_2\mathbf{x}}{1+\mathbf{x}^H\mathbf{Q}_1\mathbf{x}}\right).$$

(3.52)

Then, the log-likelihood ratio test is given as follows:

$$d_3 = \mathbf{x}^H\left(\mathbf{Q}_2-\mathbf{Q}_1\right)\mathbf{x} + \log\left(\frac{1+\mathbf{x}^H\mathbf{Q}_2\mathbf{x}}{1+\mathbf{x}^H\mathbf{Q}_1\mathbf{x}}\right) \overset{\text{Blank}}{\underset{\overline{\text{Blank}}}{\gtrless}} \eta_3.$$

(3.53)

3.3 Maisel SLB Detectors for Swerling-0, Swerling-1 and Swerling -3 Target Models

In this chapter, in order to understand the design of Maisel SLB detectors and comparison it with optimal detectors, the key formulas and facts about Maisel SLB detectors will be given for each Swerling target models which are of interest in this dissertation.

As stated in [17], there are three regions of interest whose probabilities are important for the design of Maisel SLB detectors. Blanking region under different conditions lead us to find the probability of blanking the jammer in sidelobe and probability of blanking the target in the main lobe. Here our concern is limited in finding the best parameters of Maisel SLB detectors which indeed is finding the value of β^2 assuming all the other antenna related parameters are kept fixed in conjunction with the comparison with optimal detectors. The design examples will be given in Section 3.6

As stated in the introduction part, the blanking occurs when the ratio of auxiliary to main channel signal v/u is greater than F. This statement can be formulated as follows:

$$P_b = \int\limits_0^\infty f(v; H_2) \int\limits_0^{v/F} f(u; H_2)\mathrm{d}u\mathrm{d}v. \qquad (3.54)$$

To find the probability of false blanking, one can change pdfs conditioned on H_2 with H_1.

The main requirement of Maisel SLB detector is that the threshold F has to be less than gain margin β^2 as shown in Figure 3.1. For this purpose, probability of blanking curve against F will be provided for a predetermined value of β^2 for each Swerling target models.

Another point to be noted, thanks to the assumption of target in the main lobe, the probability of target blanking decreases as SNR increases. So, for lower P_{tb} values, higher SNR values are required to obtain them. The comparative figures will be provided for different Swerling target models.

3.3.1 Swerling-0 Target Model

The outputs of square law detector from the main and auxiliary channels can be calculated easily via the elementary probability knowledge using (3.18) and given as follows:

$$f(u|a_0; H_2) = \frac{1}{2\sigma^2} \exp\left(-\frac{u + a_0^2}{2\sigma^2}\right) I_0\left(\frac{a_0\sqrt{u}}{\sigma^2}\right), \tag{3.55}$$

$$f(v|c_0; H_2) = \frac{1}{2\sigma^2} \exp\left(-\frac{v + \beta^2 c_0^2}{2\sigma^2}\right) I_0\left(\frac{\beta c_0\sqrt{v}}{\sigma^2}\right). \tag{3.56}$$

After putting above equations into (3.54), one can obtain the following expression of P_b

$$P_b = \frac{F}{1+F} + \frac{1}{1+F}Q\left(\beta\sqrt{\frac{2\gamma_j}{1+F}}, \sqrt{\frac{2\gamma_j F}{1+F}}\right)$$

$$-\frac{F}{1+F}Q\left(\sqrt{\frac{2\gamma_j F}{1+F}}, \beta\sqrt{\frac{2\gamma_j}{1+F}}\right) \tag{3.57}$$

where

$$Q(a,b) = \int_b^\infty y \exp\left(-\frac{y^2 + a^2}{2}\right) dy$$

is the Marcum function and $\gamma_j = \frac{c_0^2}{\sigma^2}$.

The probability of blanking target in the main lobe can be obtained by replacing the parameters β^2 with ω^2 and $JNR = \gamma_j$ with $SNR = \gamma_s$ and given as follows:

$$P_{tb} = \frac{F}{1+F} + \frac{1}{1+F}Q\left(\omega\sqrt{\frac{2\gamma_s}{1+F}}, \sqrt{\frac{2\gamma_s F}{1+F}}\right)$$

$$-\frac{F}{1+F}Q\left(\sqrt{\frac{2\gamma_s F}{1+F}}, \omega\sqrt{\frac{2\gamma_s}{1+F}}\right). \tag{3.58}$$

Figure 3.5(a) shows the dependency of P_b against the threshold F. P_b increases as F decreases as the usual behaviour of hypothesis testing. Also, it shows that the performance of Maisel SLB is not satisfactory if F is comparable with β^2. Another point to be noted from the figure, the required JNR to achieve some P_b value depends on the chosen F value. For example to achieve the value of 0.9 probability of blanking, the possible (F, JNR) pair would be (-3 dB, 0 dB), (0

40

dB, 5 dB) and (2 dB, 10 dB). This topic will be examined in depth in the design of Maisel SLB detector in later sections.

Figure 3.5(b) shows the required SNR values to achieve certain P_{tb} values for different values of gain margin when ω^2 is set to -30 dB. From this figure, it is seen that required SNR increases if the desired probability of target blanking is lowered. Also, the probability decreases if the chosen threshold F increases.

3.3.2 Swerling-1 Target Model

As stated in [18], the probability of blanking for fluctuating targets can be calculated by averaging the probability of blanking formula for Swerling-0 targets with respect to amplitude fluctuation. Namely,

$$P_b = \int_{a_0} P_b^* f(c_0; H_2) \mathrm{d}a_0 \tag{3.59}$$

where P_b^* is the probability of blanking for Swerling-0 targets, that is the probability of blanking conditioned on the amplitude of the target. Depending on the assumed target fluctuation model $f(c_0; H_2)$ can vary accordingly.

The probability of blanking the jammer in the sidelobe is calculated in using the equations (3.18) and (3.59) and given as below:

$$P_b = \frac{1}{2} \left[1 - \frac{1}{1+F} \cdot \frac{\gamma_j(F - \beta^2) - F - 1}{\sqrt{[\gamma_j(F - \beta^2) + F + 1]^2 + 4\gamma_j(F + 1)\beta^2}} \right.$$
$$\left. - \frac{F}{1+F} \cdot \frac{\gamma_j(F - \beta^2) + F + 1}{\sqrt{[\gamma_j(F - \beta^2) - (F + 1)]^2 + 4\gamma_j(F + 1)F}} \right]. \tag{3.60}$$

Similarly, P_{tb} is calculated as

$$P_{tb} = \frac{1}{2} \left[1 - \frac{1}{1+F} \cdot \frac{\gamma_s(F - \omega^2) - F - 1}{\sqrt{[\gamma_s(F - \omega^2) + F + 1]^2 + 4\gamma_s(F + 1)\omega^2}} \right.$$
$$\left. - \frac{F}{1+F} \cdot \frac{\gamma_s(F - \omega^2) + F + 1}{\sqrt{[\gamma_s(F - \omega^2) - (F + 1)]^2 + 4\gamma_s(F + 1)F}} \right]. \tag{3.61}$$
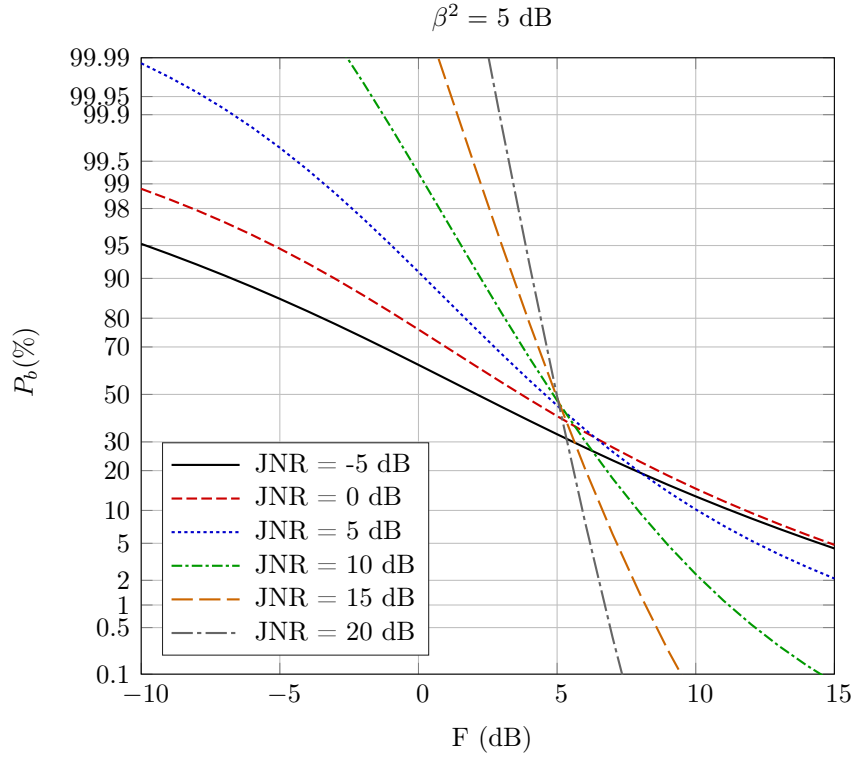
(a) P_b vs F
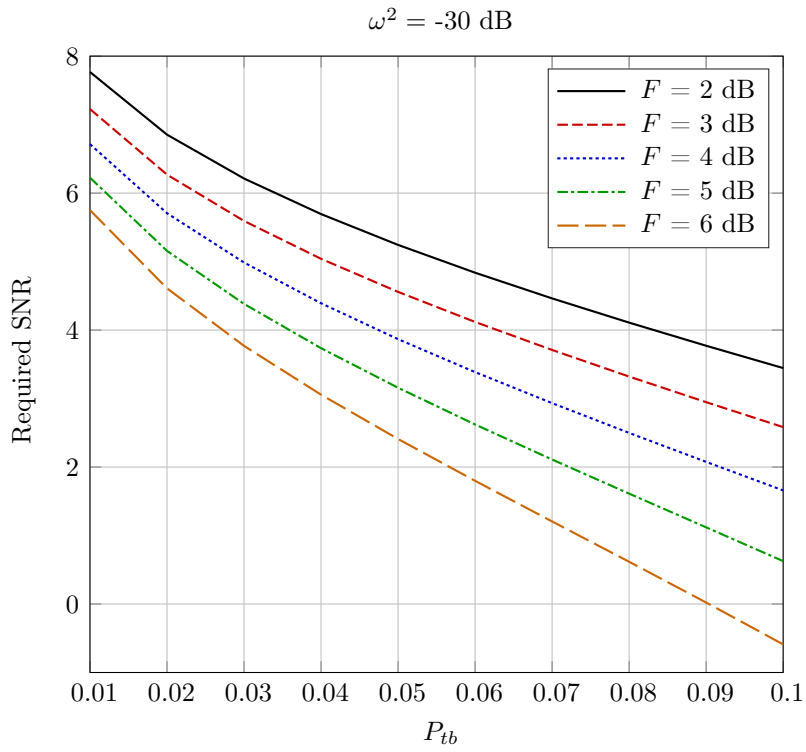
(b) SNR vs P_{tb}

Figure 3.5: Performance plots of Maisel SLB detector for Swerling-0 targets.

where γ_s and γ_j are SNR and JNR, respectively.

Figure 3.6(a) shows the probability of blanking as a function of F when β^2 is set to 5 dB. As seen from the figure, if the main requirement of the Maisel system is not satisfied, i.e., if F is not less than β^2, the performance of the detector deteriorates seriously. Also, decreasing F improves the threshold. But decreasing F also increases P_{tb}, since there is no controlled way of determining F in Maisel SLB detectors. This point is the core feature of optimum SLB detector. To put it differently, the threshold is adjusted to meet the desired P_{tb} value.

Figure 3.6(b) shows the required SNR values for obtaining P_{tb} when ω^2 is set to -30 dB. It is seen that in order to maintain low P_{tb} values, one needs to increase the SNR values. Also, it is seen that for the same SNR and P_{tb} values, increasing F has an effect of decreasing P_{tb} as expected.

Comparing Figure 3.5(a) and Figure 3.6(a), one can see that the probability of blanking is relatively lower for Swerling-1 targets than Swerling-0 targets for the same JNR and F value. This is expected due to the assumption of nonfluctuating amplitude of Swerling-0 and highly fluctuating nature of Swerling-1 targets. This can be validated also for the required SNR values for the same P_{tb} values when Figure 3.5(b) and Figure 3.6(b) are compared. For example, the required SNR for the threshold value of $F = 4$ dB to achieve $P_{tb} = 0.05$ is around 4 dB, while for Swerling-1 target case it is around 8 dB. As can be predicted, the required SNR value for the same scenario for the Swerling-3 target would be somewhere between 4 and 8 dB, thanks to the medium fluctuation assumption of target amplitude. Swerling-3 target case will be explored in the next section.
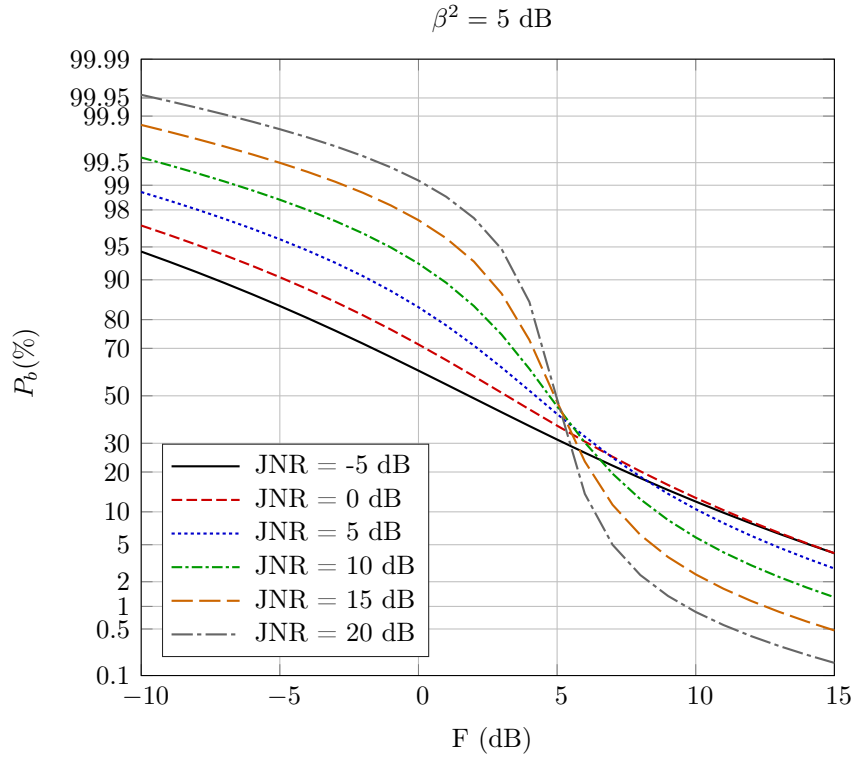
(a) P_b vs F
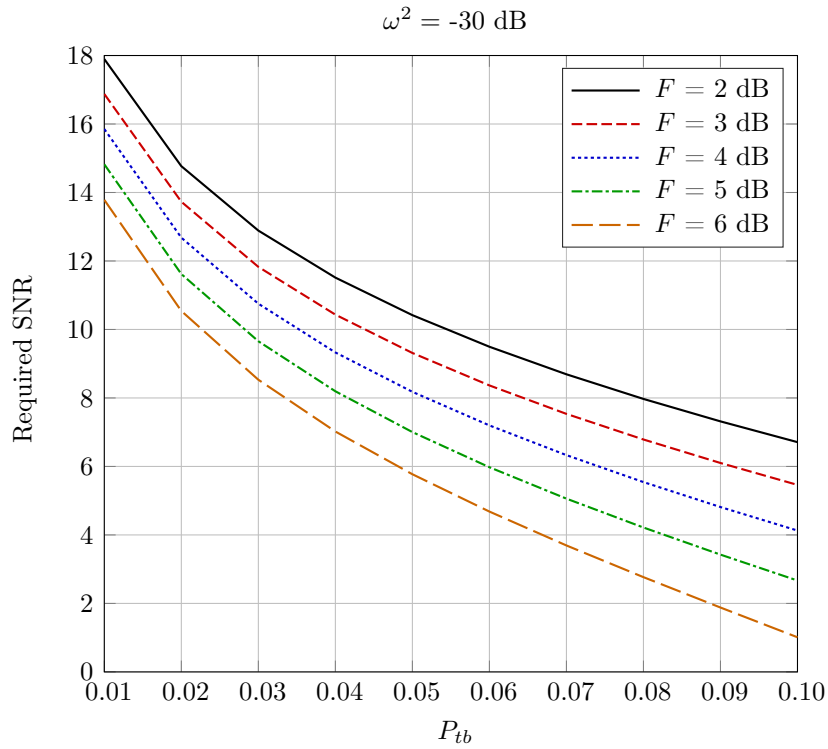
(b) SNR vs P_{tb}

Figure 3.6: Performance plots of Maisel SLB detector for Swerling-1 targets.

3.3.3 Swerling-3 Target Model

De Maio et al. [30] derives the probability of blanking formula for jammer whose distribution is Swerling-Chi model [30]:

$$f(x) = \frac{2m^m x^{2*m-1}}{\Omega^m \Gamma(m)} \exp\left(-\frac{mx^2}{\Omega}\right) \tag{3.62}$$

where m is the shape parameter of fluctuation, Ω is the average power of the jammer and $\Gamma(m) = \int_0^\infty x^{m-1} \exp(-x)\mathrm{d}x$ is the gamma function. $\Gamma(m) = (m-1)!$ for integer values of m. In (3.62), $m = 1$ corresponds to the Rayleigh amplitude model (Swerling-1 target) and $m = 2$ corresponds to the Swerling-3 target model.

The probability of blanking can be calculated using the equations (3.62) and (3.59) and given as below [30]:

$$P_b = \frac{F}{1+F} + \frac{1}{1+F} I_x(a, b, \Omega, m) - \frac{F}{1+F} I_x(b, a, \Omega, m) \tag{3.63}$$

where the function $I_x(a, b, \Omega, m)$ is given in terms of another function $H_x(a, b, \Omega, m)$ as follows:

$$I_x(a, b, \Omega, m) = \begin{cases} H_x(a, b, \Omega, m) & a < b \\ H_x(a, b, \Omega, m) + 0.5 & a = b \\ H_x(a, b, \Omega, m) + 1 & a > b \end{cases} \tag{3.64}$$

where a and b are defined as:

$$a = \frac{2}{\sigma^2}\sqrt{\frac{\beta^2}{1+F}}, \qquad\qquad b = \frac{2}{\sigma^2}\sqrt{\frac{F}{1+F}}. \tag{3.65}$$

$H_x(a, b, \Omega, m)$ is defined for integer values of m as follows:

$$H_x(a, b, \Omega, m) = \frac{\xi_1(\rho - \xi_1^2)}{1 - \xi_1^2} - \sum_{n=1}^{m}\left(\frac{2}{\mu}\right)^{n-1}\frac{\xi_2^{3n-2}}{(1-\xi_2^2)^{2n-1}}$$
$$\times \sum_{j=0}^{n-1}\binom{2n-j-2}{n-1}\left(\frac{1-\xi_2^2}{\xi_2^2}\right)^j\left[\rho\binom{n-1}{j} - \xi_2\binom{n}{j}\right] \tag{3.66}$$

with

$$c = \sqrt{\frac{2\beta^2\gamma_j}{(1+F)m}}, \qquad\qquad d = \sqrt{\frac{2F\gamma_j}{(1+F)m}}, \qquad (3.67)$$

$$u_1 = \frac{c^2 + d^2}{2cd}, \qquad\qquad u_2 = \frac{c^2 + d^2 + 2}{2cd} \qquad (3.68)$$

and

$$\rho = \frac{d}{c}, \quad \mu = cd, \quad \xi_1 = u_1 - \sqrt{u_1^2 - 1}, \quad \xi_2 = u_2 - \sqrt{u_2^2 - 1}. \qquad (3.69)$$

Figure 3.7(a) presents the dependency of P_b as a function of F. Same comments for Swerling-0 and Swerling-1 target cases are applicable here. It is seen that P_b value for the same JNR and F values are between the values of Swerling-0 and Swerling-1 targets.

Figure 3.7(b) shows the required SNR values for obtaining desired P_{tb} value for different F values. Again, the same comments are applicable as before. For the example given for Swerling-0 and Swerling-1 case, the required SNR for achieving $P_{tb} = 0.05$ when JNR $= 4$ dB is 6 dB as expected. This value was 8 dB for Swerling-1 targets and 4 dB for Swerling-0 targets.

In the next sections, Maisel SLB detector will be compared with the optimum one and some design examples will be given.

3.4 Performance Comparison of Maisel Structure and Optimal Detectors

We present a quantitative critique of the Maisel detector by conducting a comparison with the optimal detector for different target models. The optimal tests for Swerling targets given in (3.30), (3.17) and (3.53) depend on several parameters including operating SNR and JNR. Hence, the optimality, in the sense of Neyman-Pearson, is achieved through the knowledge of target and jammer specific parameters which are not utilized in the classical Maisel SLB system. The performance superiority of the Neyman-Pearson detectors can be attributed to this additional knowledge. In practice, it may not be possible to reliably estimate SNR and JNR values on-the-fly and resorting to classical Maisel
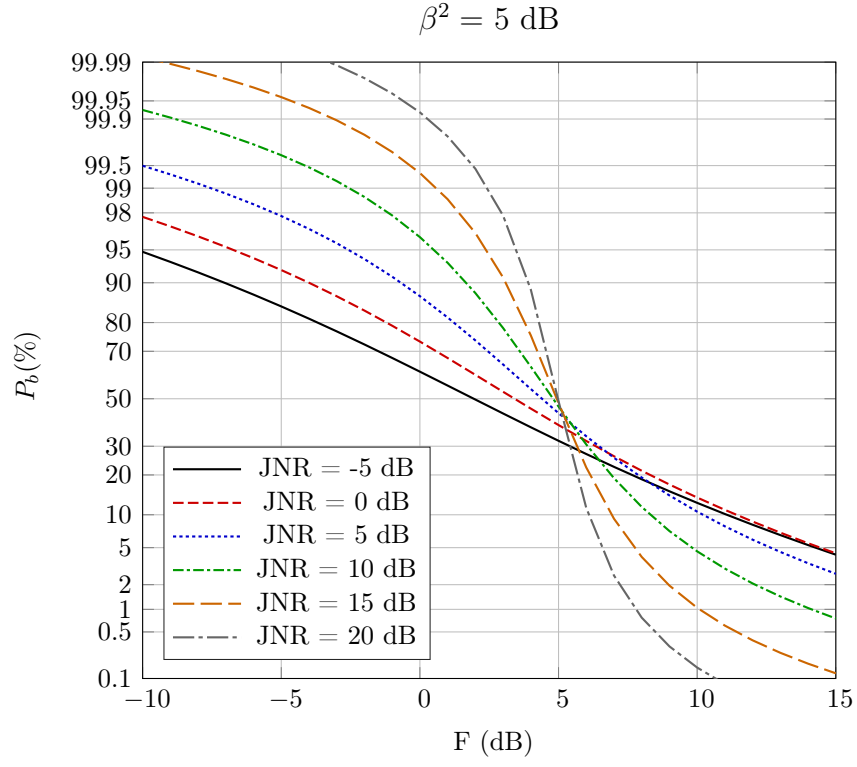
(a) P_b vs F
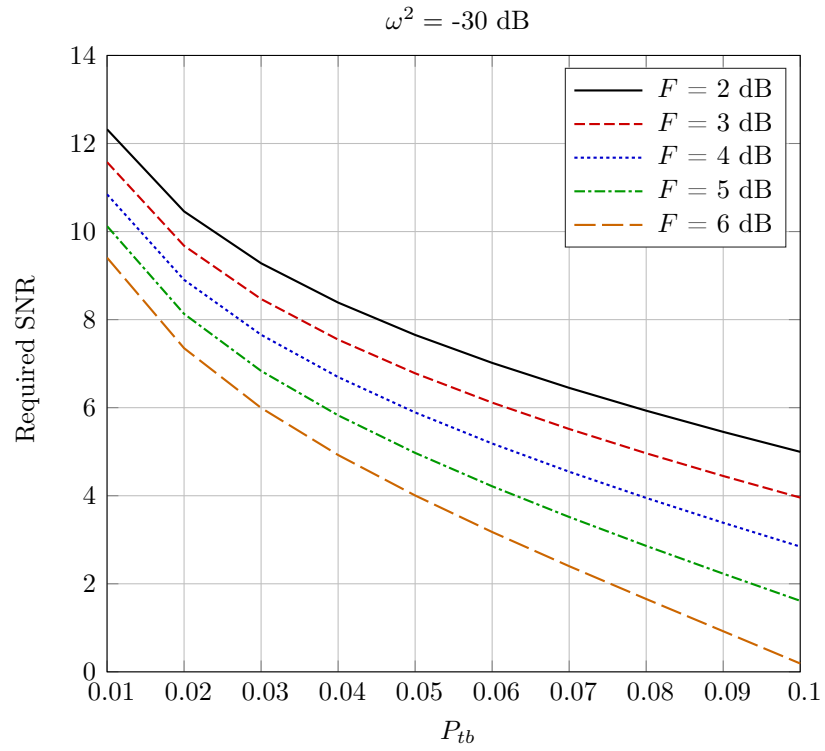
(b) SNR vs P_{tb}

Figure 3.7: Performance plots of Maisel SLB detector for Swerling-3 targets.

structure is unavoidable. Yet, the performance gap between the optimal and Maisel structures, in spite of the unavailable information for the conventional structure, is the main interest of this section.

In the following subsections, we present a numerical comparison of Maisel structure and the optimal detector for three different Swerling models. It is assumed that both systems are equipped with an antenna having identical ω^2 and β^2 values. Both detectors are adjusted to meet a given target blanking (false blanking) probability.

3.4.1 Swerling-1 Target Model

Figure 3.8(a) compares the performance of two systems at a fixed probability of target blanking. The target blanking probability is set to 0.01 and β^2 is chosen as 5 dB. The threshold values for Maisel detector at different SNR values are noted in the figure legend. (The statistics of Maisel SLB are given in [18].) We note that threshold values for the optimum SLB detector depends on JNR; hence the threshold varies for each point given in Figure 3.8(a) for the optimal test. It can be noted from Figure 3.8(a) that the performance gap between Maisel structure and optimum detector is large at SNR = 15.9 dB. For this case, the threshold F for the Maisel structure is comparable with β^2 value. The other cases have much smaller performance gap between optimal test and Maisel structure. It can be noted that the performance gap diminishes as the threshold F of the Maisel structure gets smaller in comparison to β^2.

Figure 3.8(b) presents the result of an identical comparison for a higher target blanking of $P_{tb} = 0.1$. For the given P_{tb} value, the case of $F \approx \beta^2$ occurs at much smaller SNR values, i.e. SNR ≈ 4 dB. It can be noted that the cases for which the condition $F \ll \beta^2$ is satisfied, the performances of Maisel structure and the optimal detector are very similar. This general conclusion is indeed expected; but results given here quantitatively illustrates the performance gap from the optimal detector for different F and β^2 values. In the following section, we present a design guideline on how to make use of the presented results for the design of almost optimal Maisel sidelobe blankers.
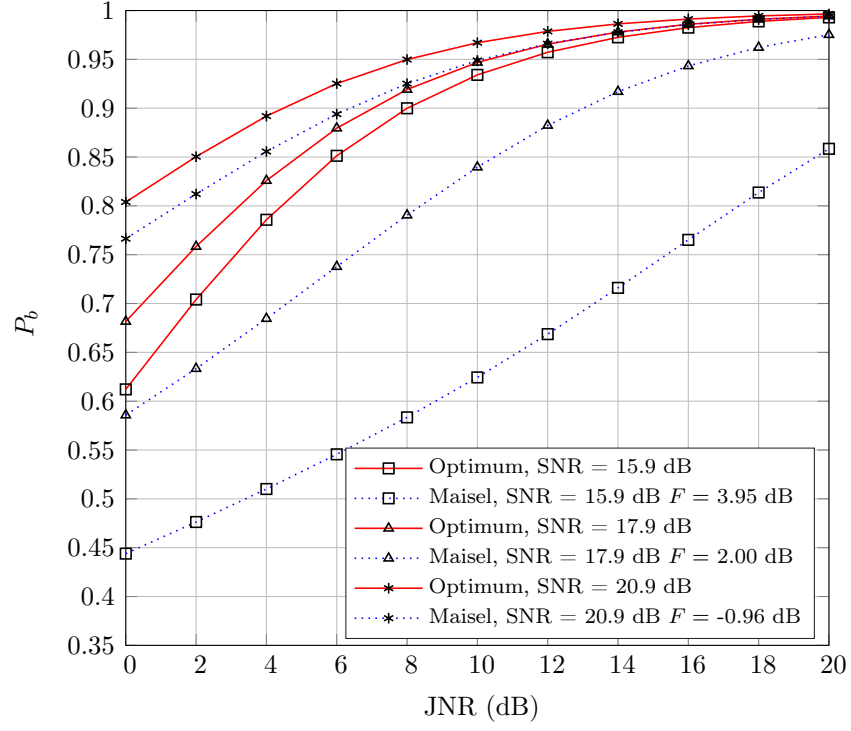
(a) $P_{tb} = 0.01$
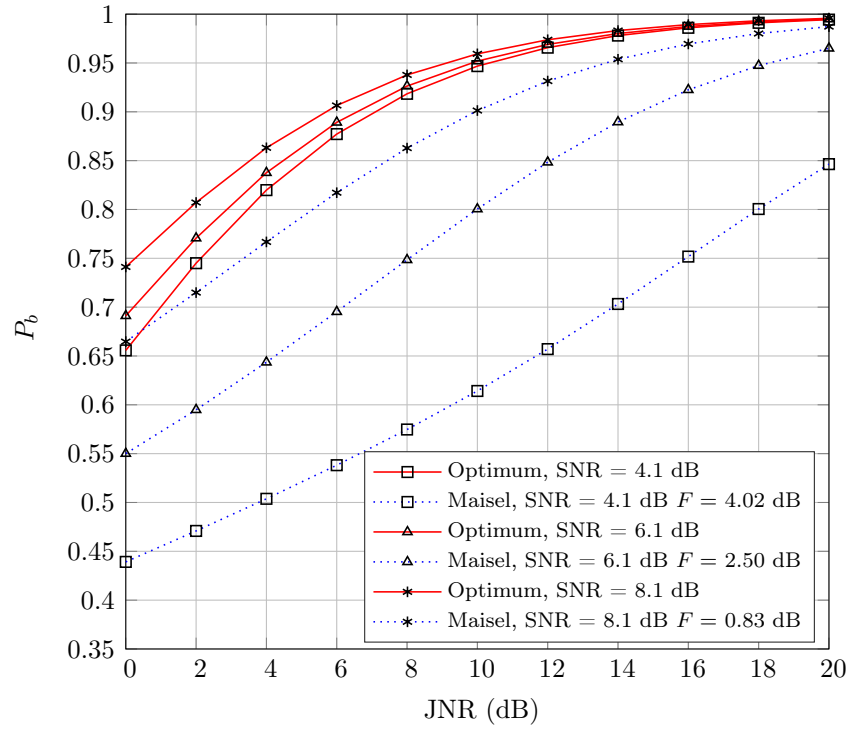
(b) $P_{tb} = 0.1$

Figure 3.8: Comparison of P_b on JNR for Swerling-1 targets. Parameters: $\beta^2 = 5$ dB, $\omega^2 = -30$ dB.

3.4.2 Swerling-3 Target Model

The test given in (3.53) is the optimum Neyman-Pearson test for Swerling-3 targets. As in Swerling-1 case, the threshold η_3 in (3.53) depends on several parameters, including SNR, JNR, ω^2 and β^2. Swerling-3 target model corresponds to medium fluctuation between Swerling-1 and Swerling-0 target model. Since the fluctuation is less than Swerling-1 case, we can achieve the same probability of false blanking (P_{tb}) at lower SNR values.

Figure 3.9 compares the two systems when β^2 is set to 5 dB. The results are similar to the Swerling-1 case. Due to less fluctuation compared to Swerling-1 target, the threshold values (F) and η_3 are smaller in comparison with Swerling-1 case. This results in a higher probability of blanking at the same JNR values than the one of Swerling-1 targets. It can be noted that when the main requirement of Maisel structure $F \ll \beta^2$ is satisfied, the performance of Maisel structure converges to the optimum SLB detector at even low JNR values. When this requirement is not satisfied, the performance of Maisel structure has a large gap from from the optimal test, as in the Swerling-1 case.

3.4.3 Swerling-0 Target Model

The test given in (3.17) is the optimal Neyman-Pearson test for Swerling-0 targets. Figure 3.10(a) compares the two systems for the false blanking probability (P_{tb}) of 0.01. The corresponding threshold values are shown in the figure legend. As in the Swerling-1 case, the Maisel structure behaves poorly when F is not sufficiently smaller than β^2. It can be noted that, the performance gap gets smaller when JNR increases. Figure 3.10(b) shows the identical comparison when the false blanking probability is increased to 0.05.

It can be noted that the optimum SLB structure achieves higher blanking probability at a relatively smaller JNR values when compared with Swerling-1 and Swerling-3 cases. This is, indeed, expected due to the assumption of non-fluctuating target model.
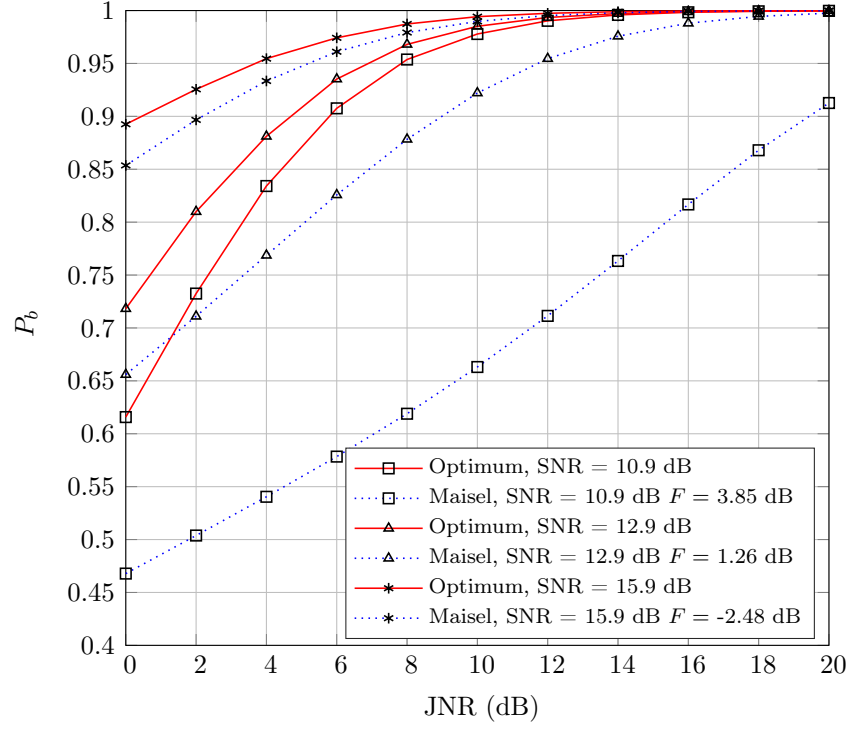
(a) $P_{tb} = 0.01$
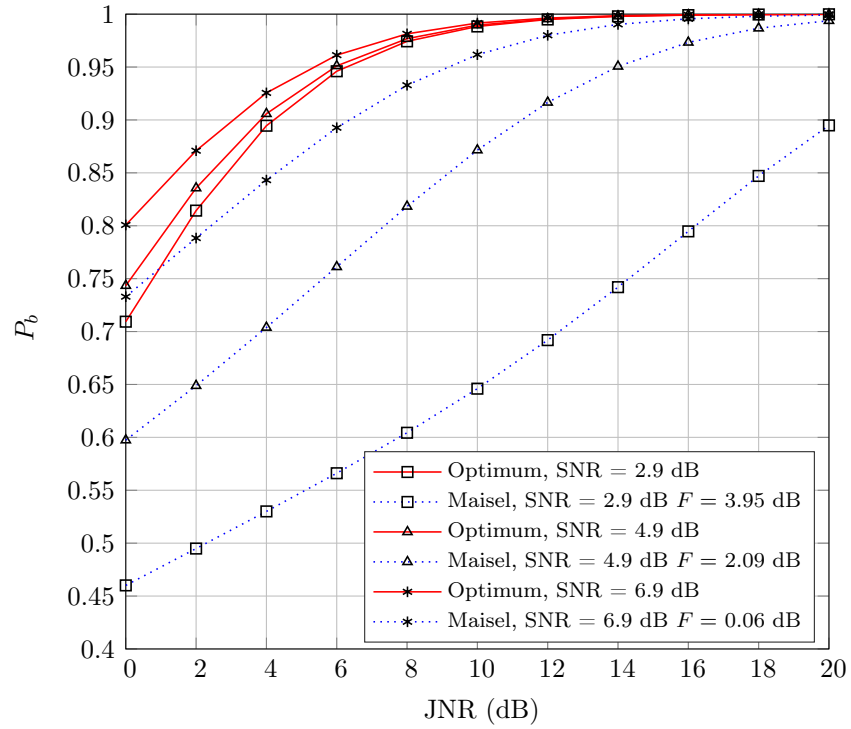
(b) $P_{tb} = 0.1$

Figure 3.9: Comparison of P_b on JNR for Swerling-3 targets. Parameters: $\beta^2 = 5$ dB, $\omega^2 = -30$ dB, # of Monte Carlo trials $= 10^6$.
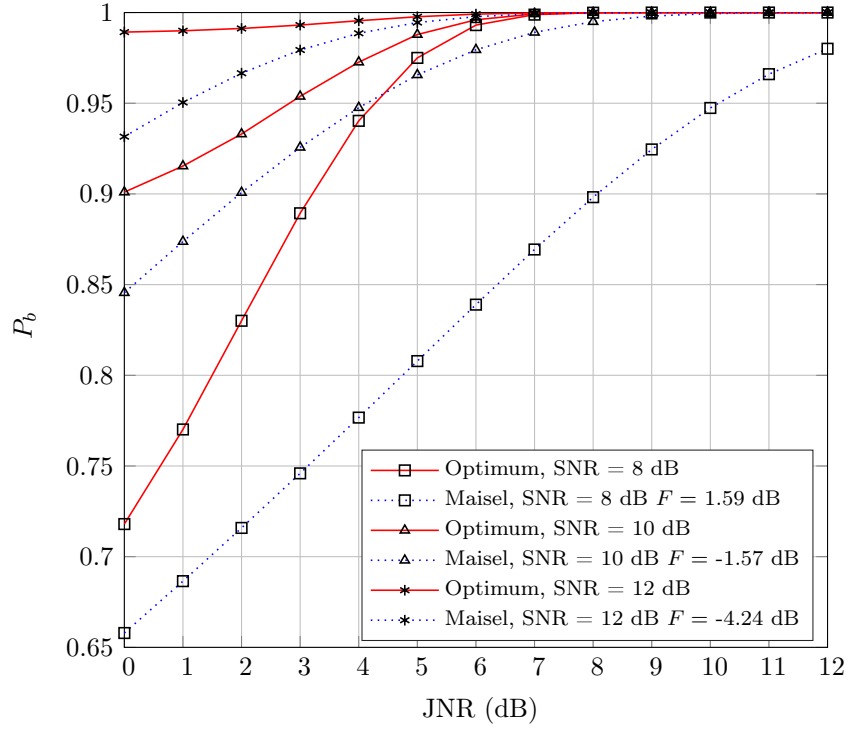
(a) $P_{tb} = 0.01$
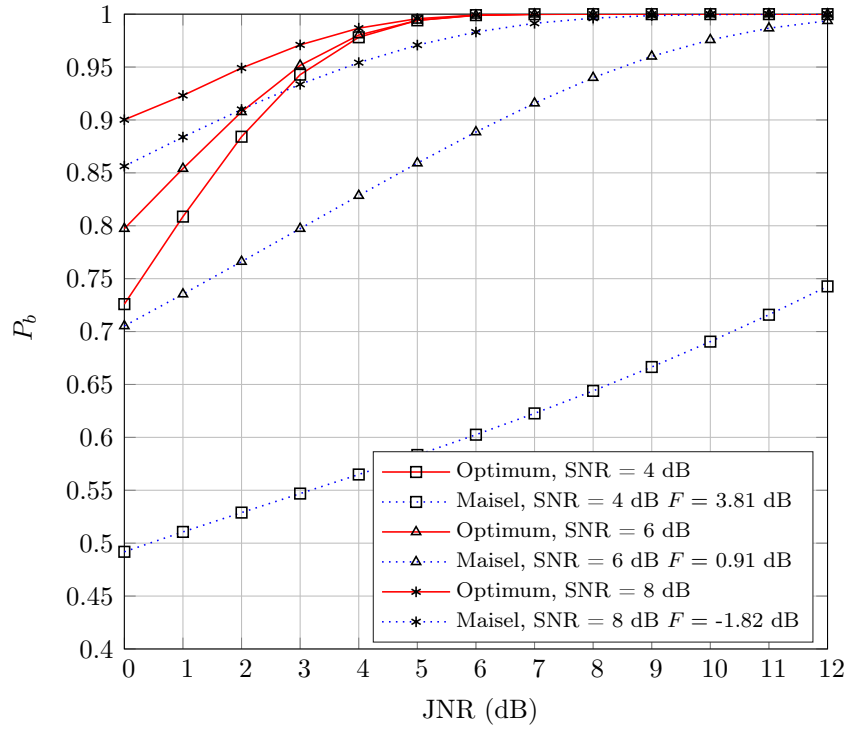
(b) $P_{tb} = 0.05$

Figure 3.10: Comparison of P_b on JNR for Swerling-0 targets. Parameters: $\beta^2 = 5$ dB, $\omega^2 = -30$ dB, # of Monte Carlo trials $= 10^6$.

3.5 Discussion On Typical Target SNR Parameters In Connection With Maisel SLB Detectors

In the previous sections, the performance figures of Maisel SLB and the optimum SLB detectors for chosen scenarios are given. Here, some typical parameters of SNR for radar target detection will be discussed in connection with Maisel SLB detectors.

Probability of target detection depends on the several parameters which are given as follows:

1. The assumed fluctuation model of target. For example, scan to scan or pulse to pulse fluctuation as in Swerling target models.

2. Signal to noise ratio which also depends on the fluctuation model.

3. The presence of Constant False Alarm Rate (CFAR) detector in the radar receiver. If CFAR processor is used to detect the target, it also causes detection loss.

4. The number of pulses integrated either coherently or non coherently.

5. The presence of diversity techniques: For example, frequency agility techniques either pulse to pulse or batch to bach.

The general formula for determining the required SNR for the single pulse to be detected is referred to as detectability factor [31, pp. 121].

If pulse integration is assumed, it also improves the detection performance and required SNR per pulse decreases. The gain is referred to as integration gain. The integration can be either coherent meaning the phases of pulses to be integrated is preserved and noncoherent in which squared magnitudes of signals are summed before comparing it with the chosen threshold.

For Maisel SLB detector, the probability of target blanking depends on the gain margin (ω^2) and SNR of the target. For example, as given in Figure 3.5(b), if the probability of target blanking is to be upper bounded by the value of

0.01, required minimum SNR to achieve this goal is in the range of 5.8 dB and 7.8 dB for the values of the threshold F between 2 dB and 6 dB. If the design goal of $P_{tb} = 0.05$ is chosen, then required SNR range becomes between 2.5 dB and 5.2 dB. Additionally, with the assumption of absence of CFAR receiver, the typical values of SNR to achieve probability of detection of 0.9 and false alarm probability of 10^{-6} is 13.2 dB for Swerling-0 targets (see page 318 in [32], Lecture 6 in [33] and the implementation of Schnidman formula in [34]). If 10 pulses are non-coherently integrated, then required single pulse SNR reduces to 5.3 dB. Thus, depending on design values of P_{tb}, P_{fa} and the number of pulses integrated, one can find the weakest target SNR to be detected. Note that integration of pulses is assumed to be performed after the blanking logic. If we assume that there is no pulse integration at all, required SNR to be detected with 90 percent increases and achievable P_{tb} decreases as well. For the case of pulse integration performed before the blanking logic, Maisel SLB performance needs to be reevaluated and the corresponding optimum detector needs to be found due to change in the pdf for the assumed target model (see also [17, pp. 91–92] for a similar example).

For the case of Swerling-1 targets, due to fluctuating loss, required single pulse SNR to achieve the same design goals as in Swerling-0 targets increases. For the same example ($P_d = 0.9$ and $P_{fa} = 10^{-6}$), the required SNR value is 21.3 dB. If 10 pulses are integrated non-coherently, then required SNR per pulse reduces to 13.5 dB. As can be seen in Figure 3.6(b), one can achieve P_{tb} values between 0.015 and 0.03 for SNR = 13.5 dB and F between 2 and 6 dB. If the number of pulses integrated is increased, then the weakest target's SNR to be detected reduces. In that case, for example if 100 pulses are integrated, then the targets with SNR of 7.2 dB can be detected with $P_d = 0.9$ and $P_{fa} = 10^{-6}$. Then, the achievable P_{tb} values increases to the range of 0.035 and 0.08 (see Figure 3.6(b)). If we want to further reduce the P_{tb} values for low SNR values, the sidelobe of main antenna needs to be decreased.

3.6 Design of Maisel Type SLB Systems With An Optimality Guarantee

In the design of the Maisel sidelobe blankers, there are mainly two parameters, namely (F) and (β^2) to be determined to achieve the desired blanking probability P_b at the expense of a fixed (erroneous) target blanking probability (P_{tb}). In this section, we aim to illustrate the process of designing Maisel type blankers with an optimality guarantee.

We illustrate the design process through a numerical example. In this example, a jammer with a JNR of 5 dB is assumed to be located in the sidelobe region. (It should be noted that the mentioned JNR values are the receiver JNR values, that is after the suppression of the jammer by the main antenna.) Our design goal is to blank the jammer with a probability of larger than 90% and the tolerable erroneous target blanking probability should be at most to 5% for Swerling-1 targets.

Figure 3.11 shows the performance comparison of Maisel type and optimal sidelobe blanker systems for different values of antenna gain margin (β^2) under the conditions of $P_{tb} = 0.05$, JNR $= 5$ dB. From this figure, we can see that when $\beta^2 = 10$ dB, the Maisel SLB provides a blanking probability (P_b) of 0.9, 0.95, 0.97 when the threshold F is adjusted for the erroneous blanking of targets having SNR values 9, 12 and 15 dB, respectively. Hence, if the weakest target (target of lowest SNR) to be detected has an SNR of 9 dB, then it is necessary to have $\beta^2 = 10$ dB. If the weakest target SNR is around 12 dB, $\beta^2 = 7$ dB suffices to achieve the design goals.

It should be noted that a reduction in β^2 is equivalent to a relaxation in the main antenna sidelobe specifications. Hence, the utilization of a smaller β^2 values is desirable from the viewpoint of antenna design. If the weakest target has an SNR value of 9 dB and $\beta^2 = 7$ dB, there exists a large gap between the performance of Maisel detector and optimal detector as illustrated by the vertical double sided arrows in Figure 3.11. It can be noted that even a single dB in increase of β^2 from 7 dB to 8 dB, results in a significant reduction of this gap. Hence, a SLB
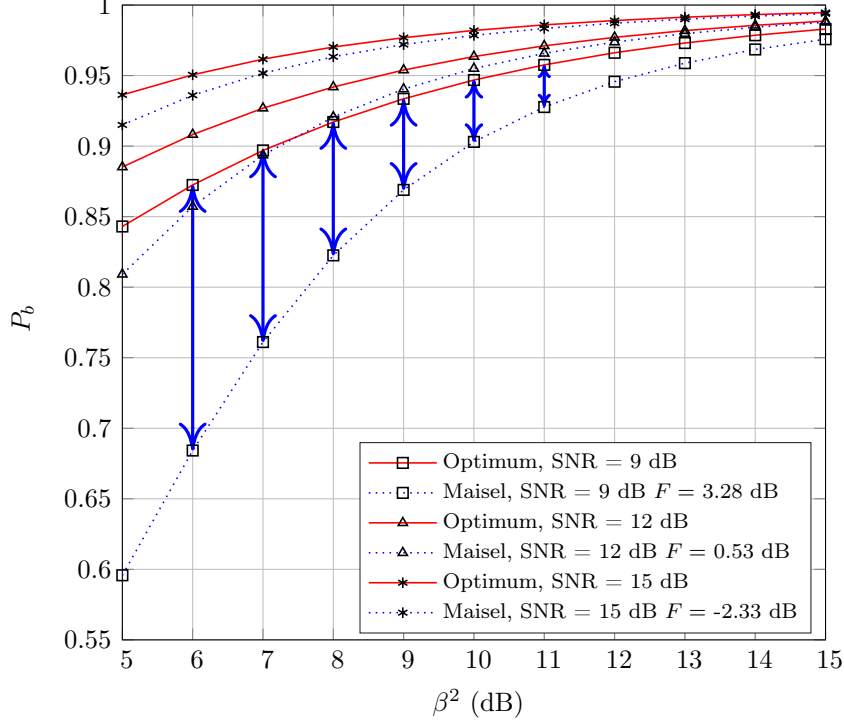
Figure 3.11: Comparison of P_b on β^2 for Swerling-1 targets. Parameters: $P_{tb} = 0.05$, JNR $= 5$ dB, $\omega^2 = -30$ dB.

designer, whose operational scenario includes target SNR values of 9 dB, can rightfully request an effort in the reduction of main antenna sidelobes. If the lowest target SNR values are around 12 dB, the gap between Maisel and optimal detector curves (shown with the triangle marker) is rather small and having a reduction in the main antenna sidelobe levels has a much smaller pay off in terms of the blanking probability.

To further assist the design process, we present the relation between minimum JNR and β^2 in Figure 3.12. The JNR values shown in this figure is the smallest JNR value for which the design criteria are satisfied. Hence, this figure can be interpreted as the blanking effectiveness of the system as a function of β^2. The desired probability of blanking (P_b) is set to 0.90, the erroneous target blanking probability is limited to 0.05, $P_{tb} \leq 0.05$ also in this figure. The curves given in Figure 3.12 show the required JNR value for a fixed β^2 so that the probability gap between Maisel detector and optimal detector is smaller than 0.05. (The mentioned probability gap is illustrated with the double sided arrows in Figure

3.11.) Hence, these points on the curves shown in Figure 3.12 refer to the Maisel systems whose performance has a fixed gap from the optimal detectors.

The curve with the solid black line shows the case of weakest target SNR values of 9 dB. For this case, as noted earlier, $\beta^2 = 10$ dB is required to blank the jammers with receiver JNR of 5 dB with the desired blanking probability of 90%. For the same case, if β^2 happens to be 7 dB, the jammers with 13 dB JNR or higher can be blanked with the desired probability. As can be noted from Figure 3.12, an increase in β^2 from 7 dB to 8 dB, results in the blanking of the jammers with JNR greater than 10 dB with the desired probability. Another dB increment further reduces this JNR value to 7 dB. It can be said that from that figure, the improvement in blanking effectiveness resulting for a single dB increment in β^2 can be read for the Maisel detectors with a fixed case worst case gap from the optimal detectors. Using these curves, a sidelobe blanker designer can asses the return for the reduction of main antenna sidelobe levels in terms of blanking effectiveness.

To further assist the designer, we provide a set of ready-to-use, general purpose MATLAB programs to generate similar figures for different values of parameters such as P_{tb}, P_b, ω^2 etc. in Appendix B

3.7   Conclusion

The main goals of this study are to compare the performance of the Maisel sidelobe blanking structure with the optimal detectors and to provide design guidance for the Maisel systems. To this aim, optimal Neyman-Pearson detectors are studied for Swerling-0, Swerling-1 and Swerling-3 target models. Unfortunately, the optimal detectors are not feasible to implement, since they require SNR and JNR values which are typically not available to the radar operator. Yet, the performance of the optimal detectors can be interpreted as a performance upper bound for the Maisel systems. One of the main goals of this study is to derive the mentioned performance bounds and examine the performance gap between the optimal detector and Maisel structure. A second goal is to develop design
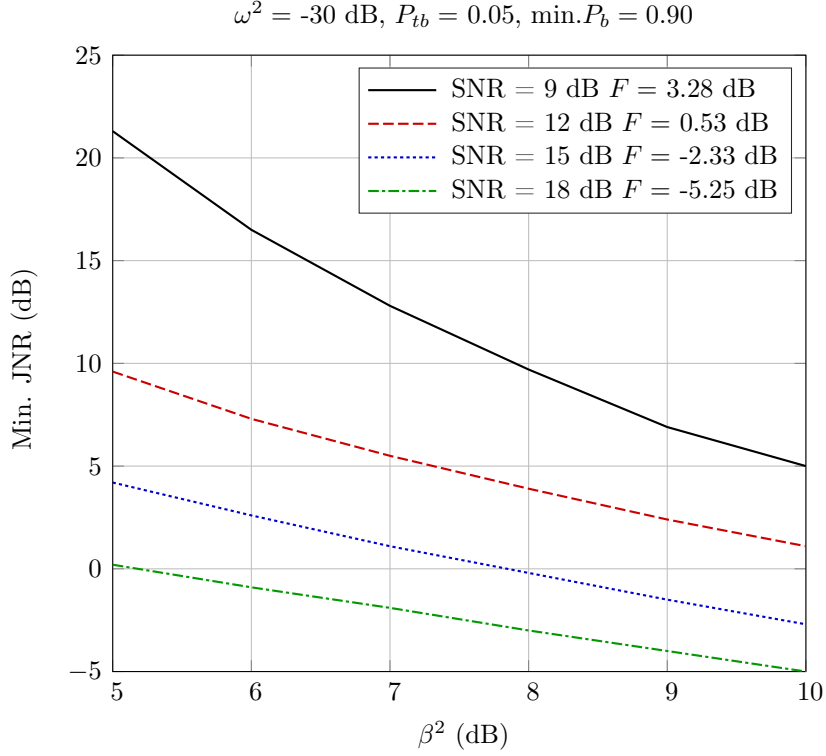
Figure 3.12: Maisel minimum required JNR for different β^2 values (Swerling-1 target). Parameters: $P_{tb} = 0.05$, $\omega^2 = -30$ dB, min.$P_b = 0.90$.

criteria and tools for the Maisel systems that guarantee a final design with a fixed performance gap from the optimal detectors. To this aim, the return in terms of jamming effectiveness as a function of β^2 is studied. More specifically, the return of a single dB increase in β^2 in terms of an increase in the blanking probability or a reduction in the minimum successfully blanked JNR level is examined. A general purpose MATLAB code to assist the design process is provided. Through the utilization of the presented criteria and provided software, a sidelobe blanker designer can easily asses the value of an increase in β^2 for different operational scenarios and design Maisel systems with a provable optimality guarantee.

CHAPTER 4

INVARIANCE PRINCIPLES

When there are unknown parameters in the hypothesis testing problem, The Neyman-Pearson hypothesis test cannot be obtained because of unknown parameters in LRT. As introduced in 2.4.3, one can find optimum detector within the class of invariance receivers. The main idea of invariance principle can be stated as follows: Firstly, finding a group of transformations under which the hypothesis testing problem is invariant is determined. With problem invariance we mean that the decision regions should not change and the transformed data must have same type of distributions as the original data. For each data point, each possible transformations in the group is applied, the orbits are found accordingly. Then, the maximal invariant test is found. The maximal invariant decision rule uniquely indexes these orbits, thus eliminates the nuisance parameters. The interesting feature of the maximal invariant tests is that the parameter space of the maximal invariant test is reduced along with the dimension of data space. Final step is to construct LRT which is the ratio of probability density functions (pdf) of maximal invariant test under both hypotheses.

The application of invariance principle on signal detection problem appears in [9]. Scharf et al. [9] considers four detection problems and derives the UMPI detectors for each of them. The detection problems corresponds to the unknown power and the unknown variance for rank-one and subspace signals. In [9], the fundamental principles are given and a geometric approach is used to reach maximal invariant statistics. The derivations used in the book does not give the details and lacks the classic approach of invariance principles.

Levy [5] explores the same problems in much more detail. Levy [5] combines the sufficient statistic approach with the invariance data reduction method.

In [35], the maximal invariant test is constructed for adaptive radar detection problem. This paper is a highly cited paper and can be considered as a benchmark for the adaptive detection problem. Bose and Steinhardt [35] show that the maximal invariant test consists of two elements which are Adaptive Matched Filter (AMF) and Kelly's GLRT test. Bose and Steinhardt [35] also derive that the statistics of maximal invariant tests under which null hypothesis do not depend on unknown parameter, making the test a CFAR test. This desirable result is the main motivation behind the interest for the invariance principle in adaptive detection problem. In [35] and [36], it is shown that no UMPI test exists and the test statistics depend solely on target SNR.

In [37], Kraut et al. show that even if no UMPI test exists for the general adaptive detection problem, the problem of unknown data scale between test data and training data has a UMPI test which is called as Adaptive Coherent Estimator (ACE). It was shown that ACE statistics is the ratio of elements of the maximal invariant statistics.

In [4], Gabriel studies the application of Wijsman's theorem to reach the maximal invariant test in his dissertation. He also gives the relation between GLRT and UMPI tests by the help of Wijsman's theorem. In his dissertation, the maximal invariant principles are explained well and the practical examples are solved by two methods. The first one is classic approach in which after finding the group of transformations, the hypothesis test is constructed by the ratio of pdf's of maximal invariant functions under two hypotheses. In Wijsman's theorem, the hypothesis test is constructed by the integration of pdf's over all group elements, and no need to find the pdf's of the maximal invariant functions or itself.

In section 4.1, the theoretical framework of invariance is given starting from the definition of a group. Gabriel [4] dissertation [4] is an excellent reference for understanding the basics of the concept. Here, the fundamental definitions and theorems of the concept follow the one in [4]. The examples of groups and maximal invariant functions will be more elobarated with the references of [38]

and [39].

In section 4.2, the invariance concept is applied to the basic signal detection problem in which the amplitude of the known signal can be either completely unknown or its sign may be known along with the variance of noise can be known or unknown. These problems are also studied in [5] and [9]. In this report, we will try to derive the UMPI tests in two ways: first one is the classic approach (pure invariant reduction), second one is the combined approach of sufficient statistic and invariance reduction.

In section 4.3, the invariance concept is applied to Low Probability of Intercept (LPI) signal detection problem. In this section, only the synchronous coherent detection problem is examined. It is derived that the invariant and Bayesian detectors coincide, while the GLRT detector is different. The performance of the invariant detector is compared with the GLRT and the energy detector, called as radiometer in the literature. It is shown that the invariant test is the most powerful test with a slight performance improvement against GLRT. When SNR increases, the power of the GLRT test gets closer to the power of UMPI test.

In section 4.3, the invariance idea is applied to the detection of frame synchronization words. In this section, GLRT and Bayesian combined detector are compared with invariant detector which is derived with the help of Wijsman theorem. It is shown that the invariant detector has slightly better performance than the GLRT test. When SNR increases, both tests converge.

4.1 Theoretical Framework of Invariance Concept

We first define the group and give its axioms, then give the definition of problem invariance under certain group of transformations.

Definition 4.1. *A group is a set G together with a binary operation $\circ$ satisfying following axioms:*

    1. G is closed, that is, for any $g_1, g_2 \in G$, then $g_1 \circ g_2 \in G$.

2. *The operation is associative, that is,* $(g_1 \circ g_2) \circ g_3 = g_1 \circ (g_2 \circ g_3)$

3. *There exists an identity element* $e \in G$ *such that* $e \circ g = g \circ e = g$ *for all* $g \in G.$

4. *There exists an inverse, that is,* $g^{-1} \in G$ *such that* $g \circ g^{-1} = g^{-1} \circ g = e.$

Definition 4.2. *The problem of testing* $H_0 : \Theta \in \Theta_0$ *vs* $H_1 : \Theta \in \Theta_1$ *remains invariant with respect to a group of transformations if*

- *distribution remains in the same family with a possible change of parameter,*

- *parameter spaces of* Θ_0 *and* Θ_1 *are preserved.*

Figure 4.1 shows the problem invariance and maximal invariant approach which will be given in the following sections.

Let X be distributed according to a probability distribution denoted by P_θ, $\theta \in \Theta$ and let $g \in G$ be a transformation acting over the sample space X. The distribution of $g(X)$ belongs to the same family of distributions with perhaps a different value of parameter $\bar{g}(\theta)$, which is an element of original parameter space Θ. Lehmann and Romano [39] denotes this relationship as

$$P_\theta\left(g(X) \in A\right) = P_{\bar{g}(\theta)}\left(X \in A\right) \quad \text{for all Borel sets } A. \tag{4.1}$$

When the above condition is satisfied, we say that the family of distributions P_θ is invariant to G [39].

If $\Theta_0 = \bar{g}(\Theta_0)$ and $\Theta_1 = \bar{g}(\Theta_1)$ also holds, it is seen that parameter space are preserved. If these two conditions are satisfied, then hypothesis testing problem is said to be invariant under G.

4.1.1 Maximal Invariant Statistic

A function $T(x)$ is said to be invariant under group G if $T(g(x)) = T(x)$ for all $x \in X$ and $g \in G$.

Example 4.1. Sign Group: $G = \{g : g(\mathbf{x}) = c\mathbf{x}, c \in \{-1, 1\}\}$ which has two elements (finite order group).
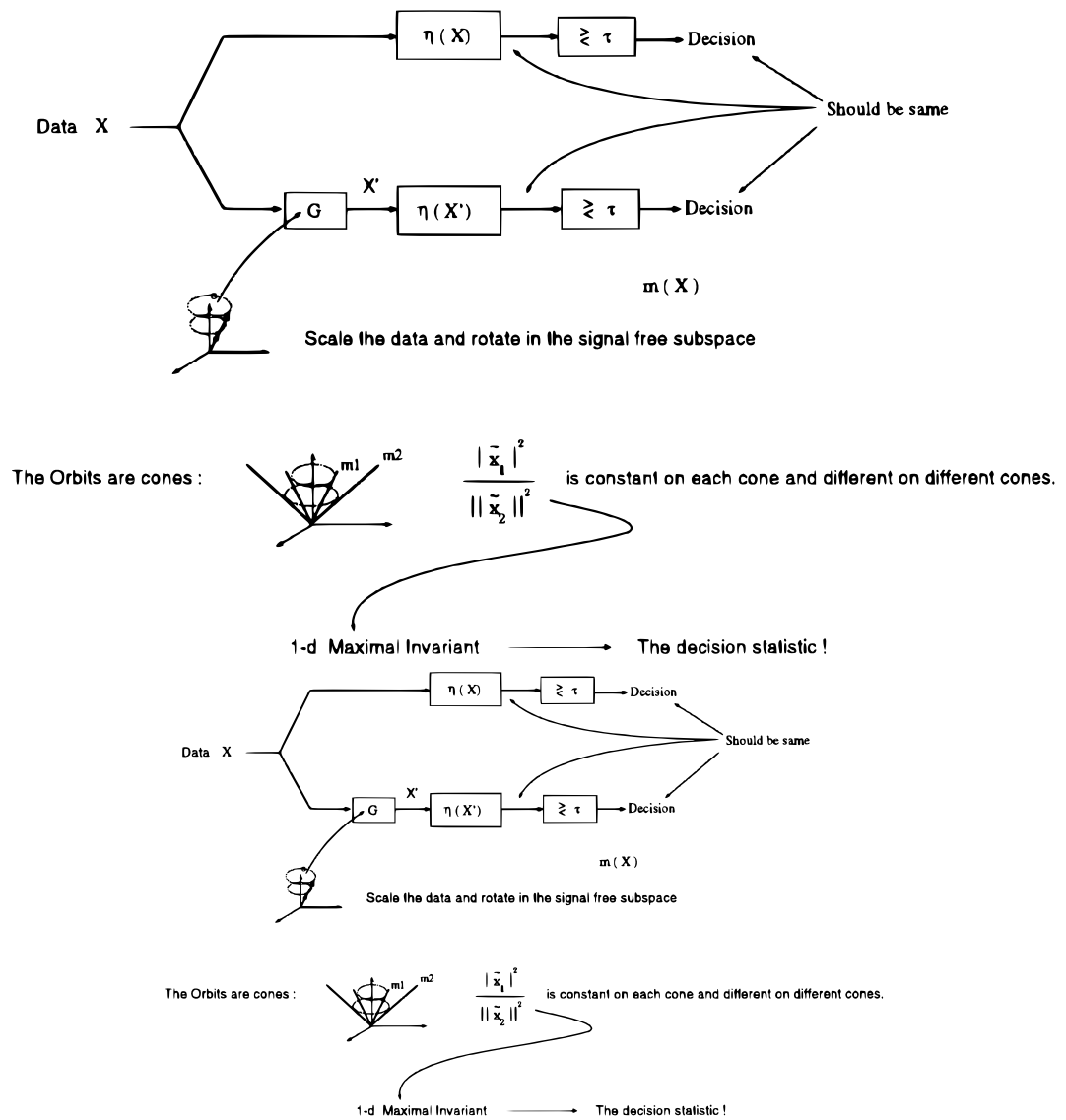
Figure 4.1: Problem invariance and maximal invariant (from [35]).

The statistic $T(\mathbf{x}) = \dfrac{x[1]}{x[0]}$, where $\mathbf{x} = \begin{bmatrix} x[0] & x[1] \end{bmatrix}^T$ is invariant under sign group. Because $T(g(\mathbf{x})) = T(c\mathbf{x}) = \dfrac{cx_1}{cx_0} = \dfrac{x[1]}{x[0]} = T(\mathbf{x})$. Suppose that $\mathbf{x} = \begin{bmatrix} 3 & -2 \end{bmatrix}^T$, Then for $c = 1, c\mathbf{x} = \begin{bmatrix} 3 & -2 \end{bmatrix}^T \Rightarrow T(\mathbf{x}) = -\dfrac{2}{3}$. For $c = -1, c\mathbf{x} = \begin{bmatrix} -3 & 2 \end{bmatrix}^T \Rightarrow T(\mathbf{x}) = -\dfrac{2}{3}$. The two points are obtained by taking a given point x and applying all group elements of transformations to that point. Here, two group of transformations give the same value of the statistic $T(\mathbf{x})$ [4, p. 38].

Definition 4.3. *An orbit is the set of points that are traced out as all group element $g \in G$ are applied to a given sample point. For the sign group: orbit of point $(3, -2)$ are the points $(3, -2)$ and $(-3, 2)$.*

We state the following important remarks:

- All points of an orbit give the same value for an invariant statistic.

- Invariant statistic is constant on each orbit.

Definition 4.4. *A statistic $m(x)$ is maximal invariant if it is invariant and if $m(x_1) = m(x_2)$ implies that $x_2 = g(x_1)$ for some $g \in G$. A maximal invariant statistic is constant on each orbit (invariance), but also it takes different values on each orbit (maximality).*

Example 4.2. Sign invariant statistic $T(\mathbf{x}) = \dfrac{x[1]}{x[0]}$. For point $\mathbf{x}_1 = (3, -2)$, orbit of $\mathbf{x}_1 : (3, -2), (-3, 2), T(\mathbf{x}_1) = \dfrac{-2}{3} = \dfrac{2}{-3}$ (invariant). For point $\mathbf{x}_2 = (9, -6)$, orbit of $\mathbf{x}_2 : (9, -6), (-9, 6), T(\mathbf{x}_2) = \dfrac{-6}{9} = \dfrac{6}{-9}$. Since $T(\mathbf{x}_1) = T(\mathbf{x}_2) = -\dfrac{2}{3}$ and $\mathbf{x}_1, \mathbf{x}_2$ are not on the same orbit, $T(\mathbf{x})$ is not maximal [4, p. 38].

Theorem 4.1. *Let $m(\mathbf{x})$ be maximal invariant with respect to G. Then a necessary and sufficient condition for a function T to be invariant is that it depends only through $m(\mathbf{x})$, that is there exists a function h for which $T(\mathbf{x}) = h(m(\mathbf{x}))$ for all $\mathbf{x}$ [39].*

This theorem means that every invariant test is a function of maximal invariant test. If one wants to find an optimal test within the class of invariant tests, they all will be a function of maximal invariant test. Hence, we focus our attention to find the maximal invariant test.

Remark 4.1. The maximal invariant test is solely based on transformations of

a group. More than one maximal invariant can be found for the specific group. In general, the one which reduce the data is chosen as the maximal invariant tests.

4.1.2 Examples of Maximal Invariant Statistics

In this section common examples of transformations of group and maximal invariant statistics will be given for the following real data vector

$$\mathbf{x} = \begin{bmatrix} x[0] & x[1] & \cdots x[N-1]. \end{bmatrix}^T$$

Example 4.3. Sign Group:

$$G = \{g : g(\mathbf{x}) = c\mathbf{x}, c \in -1, 1\} \tag{4.2}$$

The maximal invariant test is given as follows:

$$m(\mathbf{x}) = \begin{bmatrix} \dfrac{x[0]}{x[N-1]} & \dfrac{x[1]}{x[N-1]} & \cdots & \dfrac{x[N-2]}{x[N-1]} & |x[N-1]| \end{bmatrix} \tag{4.3}$$

To prove that (4.10) is maximal invariant, consider two-dimensional data. It is invariant since $T(\mathbf{x}) = T(-\mathbf{x})$. If $m(\mathbf{x}_1) = m(\mathbf{x}_2)$, then

$$\begin{bmatrix} \dfrac{x_1[1]}{x_1[0]} & |x_1[0]| \end{bmatrix} = \begin{bmatrix} \dfrac{x_2[1]}{x_2[0]} & |x_2[0]| \end{bmatrix} \tag{4.4}$$

$|x_2[0]| = |x_1[0]|$, then $\dfrac{x_2[0]}{x_1[0]} = g$, for some $g \in G$.

$$\frac{x_2[1]}{x_2[0]} = \frac{x_1[1]}{x_1[0]} \Rightarrow x_2[1] = \frac{x_2[0]}{x_1[0]} x_1[1] \Rightarrow x_2[1] = x_1[1]g_s$$

for the same g found above.

Example 4.4. Location Group:

$$G = \{g : g(\mathbf{x}) = \mathbf{x} + c, -\infty < c < \infty\}. \tag{4.5}$$

The following functions are all maximal invariant statistics under G.

$$m_1(\mathbf{x}) = \begin{bmatrix} x[0] - x[N-1], & \cdots, & x[N-2] - x[N-1] \end{bmatrix}^T \tag{4.6}$$

$$m_2(\mathbf{x}) = \begin{bmatrix} x[0] - x[1] & x[1] - x[2] & \cdots & x[N-2] - x[N-1] \end{bmatrix}^T \tag{4.7}$$

$$m_3(\mathbf{x}) = \begin{bmatrix} x[0] - \bar{x} & \cdots & x[N-1] - \bar{x} \end{bmatrix}^T, \text{ where } \bar{x} = \frac{1}{N} \sum_{i=1}^{N-1} x[i]. \tag{4.8}$$

65

Example 4.5. Scale Group:

$$G = \{g : g(\mathbf{x}) = c\mathbf{x}, -\infty < c < \infty\}. \tag{4.9}$$

$$m(\mathbf{x}) = \left[\frac{x[0]}{x[N-1]} \quad \cdots \quad \frac{x[N-2]}{x[N-1]}\right]^T \tag{4.10}$$

Example 4.6. Positive Scale Group:

$$G = \{g : g(\mathbf{x}) = c\mathbf{x}, c > 0\}. \tag{4.11}$$

$$m(\mathbf{x}) = \begin{cases} 0 & z = 0 \\ \left[\dfrac{x[0]}{z} \quad \cdots \quad \dfrac{x[N-1]}{z}\right]^T & z \neq 0 \end{cases} \tag{4.12}$$

where $z^2 = \sum_{i=1}^{N-1} x_i^2$.

Example 4.7. Orthogonal Scale Group: Let G be the group of all orthogonal transformations such that

$$G = \{g(\mathbf{x}) = \mathbf{\Gamma}\mathbf{x}\} \tag{4.13}$$

where $\mathbf{\Gamma\Gamma}^H = \mathbf{I}$. Then

$$m(\mathbf{x}) = \mathbf{x}^T\mathbf{x} = \sum_{i=1}^{N-1} x_i^2 \tag{4.14}$$

is the maximal invariant.

4.1.3 Induced Maximal Invariant Statistic

Theorem 4.2. *If $m(\mathbf{x})$ is invariant under G, and if $v(\theta)$ is maximal invariant under the induced group $\overline{G}$, then the distribution of $m(\mathbf{x})$ depends only on $v(\theta)$.*

The above theorem says that the statistics of maximal invariant test depends only on the maximal invariant of induced group acting on parameter space. Usually, the maximal invariant test reduces both the dimensions of data and parameter vector.

4.1.4 Wijsman Theorem

Wijsman theorem is well explained in [4]. Here, only the discrete finite group case is considered. Let G be the group of orthogonal transformations defined as

$$G = \left\{ g_i : g_i(\mathbf{x}) = \mathcal{O}_i\mathbf{x}, \mathcal{O}_i^T\mathcal{O}_i = \mathbf{I}, i = 1, 2, \cdots p \right\}$$

where $\mathcal{O}_i$ denotes each elements of orthogonal group. An example of such group is permutation matrix which will be used in section 4.4. Then, the ratio of the maximal invariant densities is given as:

$$\frac{\sum\limits_{i=1}^{p} f_{\mathbf{x}}\left(g_i(\mathbf{x}); H_1\right)}{\sum\limits_{i=1}^{p} f_{\mathbf{x}}\left(g_i(\mathbf{x}); H_0\right)} \tag{4.15}$$

4.2 Invariance Application to General Signal Detection Problem

The general signal detection problem can be written as

$$\begin{aligned} H_0 &: \mathbf{x} = \mu\mathbf{s} + \mathbf{w} \\ H_1 &: \mathbf{x} = \mathbf{w} \end{aligned} \tag{4.16}$$

where $\mathbf{s}$ is the target steering vector which is assumed to be known, μ is the scale factor which controls the target presence and $\mathbf{w} \sim \mathcal{N}(0, \sigma^2\mathbf{I})$.

The optimum Neyman Pearson test is the likelihood ratio test which ensures the highest detection probability for the given false alarm probability. When the all parameters in the probability distributions (for the above problem, μ, σ^2) are known, Neyman-Pearson test is the most powerful test. To realize the Neyman-Pearson test, the conditional pdf's under H_0 should not include any unknown parameter. Then, one can find the threshold which is set to a given P_{fa}.

Uniformly Most Powerful (UMP) tests are monotonically increasing function of the scalar parameter of the LRT itself. This property makes the life easer, because, it can be used as checking whether a test is UMP or not.

When there is an unknown parameter in the null hypothesis pdf, then the test is said to be composite. In that case some suboptimum approaches such as GLRT can be used, furthermore, it is given as asymptotically optimum. Another approach is to use invariance property of the problem in which the dimensions of data and parameter space are reduced by exploiting the symmetries. Then, one can search the uniformly most powerful test within the class of invariant tests, called Uniformly Most Powerful Invariant Test (UMPI).

Another data reduction technique to reduce the dimension of data is to apply the sufficiency principles. Sufficient statistics are helpful in that LRT depends only on sufficient statistic. Sufficient statistics are closely related to the unknown parameters. It is worth noting that sufficient statistics does not reduce the dimension of parameter space by definition. But, invariance principles reduces it as well. This property is another excellent property of invariance approach.

Sufficiency and invariance principles can be applied in either order. But, there is no guarantee that both cases give the same test. General approach is to apply sufficiency principles first, then apply invariance principle in the new reduced domain [38].

In the following sections, we will give the UMPI test for different cases. To obtain UMPI test, different methods can be applied. The classic approach can be summarized as follows:

- Find the group of transformations for which the problem is invariant.

- Find the maximal invariant test for that group.

- Construct the LRT, check to see whether LRT is a monotonically increasing function of some scalar which is UMPI test.

One can also apply the sufficient statistics for the unknown parameters, reduce the data, then apply the above steps in the reduced domain.

4.2.1 $\mu > 0$ unknown, σ^2 known

This case is referred to as one-sided detection problem for which UMP test exists and is same as when μ is known. It is given as $\mathbf{s}^T\mathbf{x}$. In classical detection theory books such as [5, 38, 40], it is shown that only the sign of μ matters to achieve UMP test.

4.2.2 $\mu \neq 0$ unknown, σ^2 known

UMP test exists when the sign of μ is known for gaussian noise case. So, when its sign is not known, any invariant test should be invariant to the sign of μ. The hypothesis testing problem is invariant under sign group defined in (4.2). Let's check whether this claim is true or not. There are two requirements for problem invariance. The first one is that the pdf of transformed random variable should be in the same family with a possible different parameter. The second one is that the parameter space of the problem should not change. Since the operation is linear, the resultant random variable is also Gaussian. The parameter space of the original r.v. for two hypotheses are $H_0 : \theta_0 = \{0\}$ and $H_1 : \theta_1 = \{\mu\}$. Sign group does not affect the variances of the original data. It is clear that $\bar{g}(\theta_0) = \theta_0$. Since μ is not known, $\bar{g}(\theta_1) = \theta_1$ also holds. So the problem is invariant under sign group.

Classical Approach: The pdf of maximal invariant test $\mathbf{y}$ given in (4.3) can be found by the standard method of transformation of random variable. The general formula is given as:

$$f_{\mathbf{y}}(\mathbf{y}) = f_{\mathbf{x}}(m^{-1}\mathbf{y})|J_{m^{-1}}(\mathbf{y})| \tag{4.17}$$

where $\mathbf{x} = m^{-1}(\mathbf{y})$, and $J_{m^{-1}}(\mathbf{y})$ is Jacobian factor.

$$
J_{m^{-1}}(\mathbf{y}) = \det \begin{bmatrix} \dfrac{\partial m_0^{-1}\mathbf{y}}{\partial y[0]} & \dfrac{\partial m_0^{-1}\mathbf{y}}{\partial y[1]} & \cdots \\[2ex] \dfrac{\partial m_1^{-1}\mathbf{y}}{\partial y[0]} & \dfrac{\partial m_1^{-1}\mathbf{y}}{\partial y[1]} & \cdots \\[2ex] \cdots & \cdots & \cdots \end{bmatrix} = \det \begin{bmatrix} \dfrac{\partial x[0]}{\partial y[0]} & \dfrac{\partial x[0]}{\partial y[1]} & \cdots \\[2ex] \dfrac{\partial x[1]}{\partial y[0]} & \dfrac{\partial x[1]}{\partial y[1]} & \cdots \\[2ex] \cdots & \cdots & \cdots \end{bmatrix}
$$

where $x[0] = m_0^{-1}(\mathbf{y})$. After some algebra, the pdf of $\mathbf{y}$ under H_1 hypothesis can be found as the following:

$$
f(\mathbf{y}; H_1) = \frac{1}{(2\pi\sigma^2)^{N/2}} \left\{ \exp\left[-\frac{1}{2\sigma^2} \left(y[N-1]^2 \left(\mathbf{y}_{N-1}^T \mathbf{y}_{N-1} + 1 \right) \right. \right. \right.
$$

$$
\left. - 2\mu y[N-1] \left(\mathbf{y}_{N-1}^T \mathbf{s}_{N-1} + s[N-1] \right) + \mu^2 \mathbf{s}^T \mathbf{s} \right) \right]
$$

$$
+ \exp\left[-\frac{1}{2\sigma^2} \left(y[N-1]^2 \left(\mathbf{y}_{N-1}^T \mathbf{y}_{N-1} + 1 \right) \right. \right.
$$

$$
\left. \left. \left. + 2\mu y[N-1] \left(\mathbf{y}_{N-1}^T \mathbf{s}_{N-1} + s[N-1] \right) + \mu^2 \mathbf{s}^T \mathbf{s} \right) \right] \right\}. \quad (4.18)
$$

where $\mathbf{y}_{N-1} = \begin{bmatrix} y[0] \cdots y[N-2] \end{bmatrix}^T$ and $\mathbf{s}_{N-1} = \begin{bmatrix} s[0] \cdots s[N-2] \end{bmatrix}^T$.

$f(\mathbf{y}; H_0)$ can be found easily by putting $\mu = 0$ to above equation. Cancelling common terms and ignoring non-data dependent terms, LRT can be found as:

$$
\frac{f(\mathbf{y}; H_1)}{p(\mathbf{y}; H_0)} = \exp\left[\frac{1}{2\sigma^2} 2\mu y[N-1] \left(\mathbf{y}_{N-1}^T \mathbf{s}_{N-1} + s[N-1] \right) \right]
$$

$$
+ \exp\left[-\frac{1}{2\sigma^2} 2\mu y[N-1] \left(\mathbf{y}_{N-1}^T \mathbf{s}_{N-1} + s[N-1] \right) \right]. \quad (4.19)
$$

Note that $\exp(a) + \exp(-a)$ is an increasing function of $|a|$ [4]. So, after taking logarithm of test, UMPI test d can be found as:

$$
d = \left| y[N-1] \left(\mathbf{y}_{N-1}^T \mathbf{s}_{N-1} + s[N-1] \right) \right|. \quad (4.20)
$$

Expressing in terms of original data vector $\mathbf{x}$, noting $y[N-1] = |x[N-1]|$ and

$\mathbf{y}_{N-1} = \dfrac{\mathbf{x}_{N-1}}{x[N-1]}$, we can simplify UMPI test as the following:

$$
\begin{aligned}
d &= \left| |x[N-1]| \left(\frac{\mathbf{x}_{N-1}^T}{x[N-1]} \mathbf{s}_{N-1} + s[N-1] \right) \right| \\
&= \left| \left(\mathbf{x}_{N-1}^T \mathbf{s}_{N-1} + s[N-1]x[N-1] \right) \right| \\
&= \left| \mathbf{x}^T \mathbf{s} \right| = \left| \mathbf{s}^T \mathbf{x} \right| = \left| \sum_{i=1}^{N-1} x[i]s[i] \right|.
\end{aligned}
\tag{4.21}
$$

Any one-to-one function of the above test can be considered as UMPI test, so $\left(\mathbf{s}^T \mathbf{x} \right)^2$ is also UMPI test for this problem.

Sufficient Statistic Approach: Sufficient statistic for the unknown parameter μ is $t = \mathbf{s}^T \mathbf{x}$. We apply invariance principle to the new data set t which is one dimensional. The resultant pdf of t under H_1 hypothesis is $\mathcal{N}(\mu \mathbf{s}^T \mathbf{s}, \sigma^2 \mathbf{s}^T \mathbf{s})$ and under H_0 hypothesis is $\mathcal{N}(0, \sigma^2 \mathbf{s}^T \mathbf{s})$. Transformed data is still invariant to sign group. The maximal invariant for sign group is given in (4.3). So $d = |t| = \left| \mathbf{s}^T \mathbf{x} \right|$ is the maximal invariant test. After forming the likelihood ratio test, we check whether this test is UMPI or not by finding the pdf of LRT. It is given in [5] that the test LRT is monotonically increasing function of $d = |t|$, thus making itself a UMPI test.

It is worth noting that the test $d = \left(\mathbf{s}^T \mathbf{x} \right)^2$ under H_0 hypothesis can be completely defined. One can find the threshold for a given P_{fa}. So it possesses CFAR property.

Extension to The Complex Data: In this case, $\mathbf{x}, \mathbf{s}$ are complex random variables. This time; noise appearing in (4.16), $\mathbf{w}$ is complex Gaussian noise having spherical invariance property meaning $\mathbf{w} \sim \mathcal{C}(0, \sigma^2 \mathbf{I})$. Since μ can be negative, it means that target signal $\mathbf{x}$ has unknown phase, only its magnitude is known. $\mathbf{s} = |s| \exp(j\phi_1)$, ϕ_1 is unknown, $r = |s|$ is known.

This case corresponds to non-coherent processing of the return signal. So any unitary transformation of $\mathbf{x}$ does not change hypothesis testing problem. The problem is invariant under the group of rotation transformations given in (4.13). The maximal invariant test for this group given in (4.14) is $||x||^2 = \mathbf{x}^H \mathbf{x}$. The sufficient statistic for unknown parameter μ is $\mathbf{s}^H \mathbf{x}$. As in real case, UMPI test is

$d = ||\mathbf{s}^H \mathbf{x}|| = |\mathbf{s}^H \mathbf{x}|^2$. This detector is inherent to the rotations in the subspace $\mathbf{s}$ and translations in the orthogonal subspace $\mathbf{s}^\perp$. The energy of the data $\mathbf{x}$ in the subspace $\mathbf{s}$ is constant.

4.2.3 $\mu > 0$ unknown, σ^2 unknown

In this case, there are two unknown parameters, namely μ and σ^2. The conditional pdfs under both hypothesis are: $H_1 : \mathcal{N}(\mu\mathbf{s}, \sigma^2\mathbf{I})$ and $H_0 : \mathcal{N}(0, \sigma^2\mathbf{I})$.

The first step is to find the group of transformations for which the problem is invariant. Because of Gaussian random vectors, linear operations ensure that transformed r.v. has Gaussian type. Thus, we can restrict ourself to linear transformations. Considering the unknown variance, we can expect that the operations must include unknown scaling $c\mathbf{x}$. Next, considering the mean of $p(\mathbf{x}, H_1)$; the scale factor must be greater than zero. Otherwise, one can not guarantee unknown $c\mu$ at the output is greater than zero. Finally, we conclude that this problem is invariant to positive scale group of transformations.

Classical Approach: The positive scale group and its maximal invariant test is given in (4.11) and (4.12), respectively. The maximal invariant test is repeated below.

$$\mathbf{y} = m(\mathbf{x}) = \begin{cases} 0 & z = 0 \\ \left[\dfrac{x[0]}{z}, \quad \cdots, \quad \dfrac{x[N-1]}{z} \right]^T & z \neq 0 \end{cases} \tag{4.22}$$

where $z^2 = \sum_{i=1}^{N-1} x_i^2$. To find the pdf of $\mathbf{y}$, we follow the method described in [4], that is, first find the pdf of the following vector. To simplify the notations, we drop the case where $z = 0$.

$$\mathbf{y}_1 = \begin{bmatrix} \dfrac{x[0]}{z} & \dfrac{x[1]}{z} & \cdots & \dfrac{x[N-1]}{z} & z \end{bmatrix} \tag{4.23}$$

After that, we marginalize the pdf of $\mathbf{y}_1$ over z to find the pdf of $\mathbf{y}$, namely

$$f(\mathbf{y}) = \int_{-\infty}^{\infty} f(\mathbf{y}_1) d\mathbf{y}_1.$$

Using the standard formula of transformation of random vectors, $f(\mathbf{y}_1; H_1)$ can

be found as the following:

$$f_{\mathbf{y}_1}(\mathbf{y}; H_1) = \frac{1}{(2\pi\sigma^2)^{N/2}} \exp\left[-\frac{1}{2\sigma^2}(\mathbf{y}z - \mu\mathbf{s})^T(\mathbf{y}z - \mu\mathbf{s})\right]|z|^N$$

$$= \frac{1}{(2\pi\sigma^2)^{N/2}} \exp\left[-\frac{1}{2\sigma^2}(z^2\mathbf{y}^T\mathbf{y} - 2z\mu\mathbf{s}^T\mathbf{y} + \mu^2\mathbf{s}^T\mathbf{s})\right]|z|^N \quad (4.24)$$

where $z = y_1[N]$. Note that $\mathbf{y}$ is the dummy variable in above equation. Integrating the above expression with respect to z, using change of variables $t = z(\mathbf{y}^T\mathbf{y})^{1/2}$, we obtain the following expression:

$$f_{\mathbf{y}}(\mathbf{y}; H_1) = \frac{1}{(2\pi\sigma^2)^{N/2}} \int_{-\infty}^{\infty} \exp\left[-\frac{1}{2\sigma^2}\left(t^2 - 2\mu t \frac{\mathbf{s}^T\mathbf{y}}{(\mathbf{y}^T\mathbf{y})^{1/2}} + \mu^2\mathbf{s}^T\mathbf{s}\right)\right] \frac{|t|^N}{(\mathbf{y}^T\mathbf{y})^{1/2}} dt$$

$$(4.25)$$

Similar expression for $f_{\mathbf{y}}(\mathbf{y}; H_0)$ can be obtained by putting $\mu = 0$ to the above equation.

After forming likelihood ratio, we note that t can not be negative. Thus, the lower limit of integration becomes 0. With this observation in mind LRT is an increasing function of $\frac{\mathbf{s}^T\mathbf{y}}{(\mathbf{y}^T\mathbf{y})^{1/2}}$ which is UMPI test statistic.

Sufficient Statistic Approach: The sufficient statistics for unknown parameters μ and σ^2 are $t_1 = \mathbf{s}^T\mathbf{x}$ and $t_2 = \mathbf{x}^T\mathbf{x}$. Remember that the problem is invariant to group of positive scale transformations in the original data $\mathbf{x}$. After reducing the N-dimensional data to 2-dimensional data $\mathbf{t} = \begin{bmatrix} t_1 & t_2 \end{bmatrix}$, we apply the invariance principle to the reduced set $\mathbf{t}$. Induced transformation g^* on sufficient statistic domain becomes the following:

$$\mathbf{t}' = g^*(\mathbf{t}) = \begin{bmatrix} ct_1 & c^2t_2 \end{bmatrix} \quad (4.26)$$

where $c > 0$ is the scale factor in the original group.

We claim that maximal invariant for this induced transformation g^* is $m(\mathbf{t}) = \frac{t_1}{\sqrt{t_2}}$.

Proof of Invariance Part:

$$m(g^*(\mathbf{t})) = \frac{t_1'}{\sqrt{t_2'}} = \frac{ct_1}{\sqrt{c^2t_2^2}} = \frac{t_1}{\sqrt{t_2}} = m(\mathbf{t}) \quad (4.27)$$

73

Proof of Maximality Part: Let $m(\mathbf{t}) = m(\mathbf{t}^*)$.

$$\frac{t_1}{\sqrt{t_2}} = \frac{t_1^*}{\sqrt{t_2^*}} \Rightarrow t_1^* = t_1 \frac{\sqrt{t_2^*}}{\sqrt{t_2}}$$

$$t_1^* = t_1 c \text{ where } c = \frac{\sqrt{t_2^*}}{\sqrt{t_2}} > 0$$

$$\Rightarrow \sqrt{t_2^*} = \sqrt{t_2} \frac{t_1^*}{t_1}$$

$$\sqrt{t_2^*} = \sqrt{t_2} c \text{ same } c \text{ above}$$

$$t_2^* = c^2 t_2$$

Finally, maximal invariant test is $d = \dfrac{\mathbf{s}^T \mathbf{x}}{\sqrt{\mathbf{x}^T \mathbf{x}}}$.

Induced group on parameter space $\theta = (\mu, \sigma^2)$ is defined as the following:

$$\bar{G} = \left\{ \bar{g} : \bar{g}(\mu, \sigma^2) = (c\mu, c^2 \sigma^2), c > 0 \right\} \tag{4.28}$$

The maximal invariant for the induced group $\bar{g}$ is $v(\theta) = \dfrac{\mu}{\sigma}$. It is invariant since $v(\bar{g}(\theta)) = \dfrac{c\mu}{\sqrt{c^2 \sigma^2}} = \dfrac{\mu}{\sigma} = v(\theta)$, since $c > 0$ is assumed. It is a maximal invariant since if we are given that $v(\theta_1) = v(\theta_2)$, then

$$\frac{\mu_1}{\sigma_1} = \frac{\mu_2}{\sigma_2}$$

$$\Rightarrow \mu_1 = \frac{\sigma_1}{\sigma_2} \mu_2$$

$$\Rightarrow \mu_1 = c\mu_2, \text{ for some } c = \frac{\sigma_1}{\sigma_2} > 0.$$

Similarly,

$$\frac{\mu_1}{\sigma_1} = \frac{\mu_2}{\sigma_2}$$

$$\Rightarrow \sigma_1 = \frac{\mu_1}{\mu_2} \sigma_2$$

$$\Rightarrow \sigma_1 = c\sigma_2, \text{ using the same } c \text{ above}$$

The distribution of maximal invariant test $d = \dfrac{\mathbf{s}^T \mathbf{x}}{\sqrt{\mathbf{x}^T \mathbf{x}}}$ depends only on the maximal invariant for the parameter space $v(\theta) = \dfrac{\mu}{\sigma}$. The hypothesis testing problem is simplified as follows:

$$\begin{cases} H_1 : v(\theta) > 0 \\ H_0 : v(\theta) = 0 \end{cases}$$

It is shown in [9], [5] and [38] that the statistic of d is "Student-t" distributed. It is important to note that under H_0, the test statistic of d is completely characterized even though σ^2 is unknown. Thus, this test has the CFAR property. Scharf and Demeure [9] calls this detector as CFAR Matched Filter.

$$\frac{p(d|H_1)}{p(d|H_0)} \underset{H_0}{\overset{H_1}{\gtrless}} \eta \qquad (4.29)$$

4.2.4 $\mu \neq 0$ unknown, σ^2 unknown

Classical Approach: Since the sign of μ is not known, the problem is invariant to scale group defined in (4.9). Since the scale transformation is linear, the distribution type is preserved because of Gaussian normal r.v. Induced transformation on parameter space can be written as $\bar{g}(\mu, \sigma^2) = (c\mu), c^2\sigma^2$ where $c \neq 0$. It is seen that partitioning of parameter space is also preserved, which means for H_0, $\bar{g}(0, \sigma^2) = (0, \sigma^2)$ (since σ^2 is unknown and for H_1, $\bar{g}(\mu, \sigma^2) = (\mu, \sigma^2)$ since μ and σ^2 are both unknown.

The maximal invariant test is given in (4.10). The difference between positive scale group is the inclusion of positive number $z = \mathbf{s}^T\mathbf{s}$ in the maximal invariant function in positive scale group as opposed to $x[N-1]$ in the scale group.

Same method can be applied to find the pdf of maximal invariant test. The only change is on the limits of integration given in (4.25). This time $z = x[N-1]$ and it can be negative. Thus, LRT is an increasing function of $\left| \frac{\mathbf{s}^T\mathbf{y}}{(\mathbf{y}^T\mathbf{y})^{1/2}} \right|$. Any one-to-one function of this test can be considered also UMPI test. The final test is $\frac{(\mathbf{s}^T\mathbf{y})^2}{(\mathbf{y}^T\mathbf{y})}$. Induced group on parameter space is studied in the next section.

Sufficient Statistic Approach: Hypothesis testing problem is invariant to scale group. Similar steps can be applied as in $\mu > 0$ unknown case. Sufficient statistic is two dimensional vector $\mathbf{t} = \begin{bmatrix} t_1 & t_2 \end{bmatrix}$, where $t_1 = \mathbf{s}^T\mathbf{x}$ and $t_2 = \mathbf{x}^T\mathbf{x}$.

We claim that $m(\mathbf{t}) = \frac{t_1^2}{t_2}$ is maximal invariant test under the induced group of

action on the sufficient statistic domain which are given below.

$$\mathbf{t}' = g^*(\mathbf{t}) = \begin{bmatrix} ct_1 & c^2 t_2 \end{bmatrix} \tag{4.30}$$

where $c \neq 0$ is the scale factor in the original group. $m(\mathbf{x})$ is invariant since $m(g^*(\mathbf{t})) = \dfrac{(ct_1)^2}{c^2 t_2^2} = m(\mathbf{t})$.

Proof for the maximality part: Let $m(\mathbf{t}) = m(\mathbf{t}^*)$.

$$\frac{t_1^2}{t_2} = \frac{t_1^{*2}}{t_2^*} \Rightarrow t_1^{*2} = t_1^2 \frac{t_2^*}{t_2}$$

$$t_1^* = t_1 c \text{ where } c = \pm\sqrt{\frac{t_2^*}{t_2}}$$

$$\Rightarrow t_2^* = t_2 \frac{t_1^{*2}}{t_1^2}$$

$$t_2^* = t_2 c^2 \text{ same } c \text{ above}$$

The induced group on parameter space $\theta = (\mu, \sigma^2)$ is defined as follows:

$$\bar{G} = \left\{ \bar{g} : \bar{g}(\mu, \sigma^2) = (c\mu, c^2\sigma^2), c \neq 0 \right\} \tag{4.31}$$

As in positive scale group, the maximal invariant parameter with respect to the group $\bar{G}$ is found as $v(\theta) = \dfrac{\mu^2}{\sigma^2}$.

4.3 Application of Invariance Principle to LPI Signal Detection Problem: Synchronous Coherent Detectors

Consider a high-rate, random spreading code $c(t)$ as

$$c(t) = \sum_{n=-\infty}^{\infty} c_n p(t - nT_c - \epsilon T_c) \tag{4.32}$$

where $p(t)$ is a unit pulse of duration T_c second, $\{c_n\}_{-\infty}^{\infty}$ is a sequence of i.i.d. random variables with $Pr(c_n = 1) = Pr(c_n = -1) = 0.5$. Furthermore, the chip epoch is modeled by the r.v. ϵ, uniformly distributed over $[0, 1)$. The low-pass equivalent waveform observed by the detector is given as follows (see [41] for further details):

$$\begin{aligned} H_1 &: r(t) = \sqrt{S}c(t) + n_I(t) \\ H_0 &: r(t) = n_I(t) \end{aligned} \tag{4.33}$$

where S is the average signal power and $n_I(t)$ is the in-phase component of noise having variance of $\sigma^2 = N_0/2$ W/Hz. The observation time is T seconds, and assumed to be integer multiple of chip time, i.e, $T = NT_c$ where N is positive integer.

$r(t)$ can be written in terms of orthogonal functions as follows:

$$r(t) = \sum_{i=1}^{\infty} r_i \psi_i(t), \quad 0 \le t \le T. \tag{4.34}$$

where $\psi_i(t) = p(t - iT_c)$. The first N coefficients (r_i) for the functions of $\psi_i(t), i = 1, \ldots, N$ represent the sufficient statistic, while the remaining coefficients $r_i, i > N$ are irrelevant to the hypothesis testing problem.

$$r_i = \int_0^{NT_c} r(t)\psi_i(t)dt = \int_0^{NT_c} r(t)p(t - iT_c)dt = \int_{(i-1)T_c}^{iT_c} r(t)dt \tag{4.35}$$

These coefficients $\{r_i\}_{i=1}^{N}$ are calculated for both hypotheses as follows:

$$H_0 : r_i = \int_{(i-1)T_c}^{iT_c} n_I(t)dt \triangleq w_i$$

$$H_1 : r_i = \int_{(i-1)T_c}^{iT_c} \left(\sqrt{S}c(t) + n_I(t)\right) dt \triangleq \sqrt{S}T_c c_i + w_i. \tag{4.36}$$

Here, $\{r_i\}_{i=1}^{N} \sim \mathcal{N}(0, \frac{N_0 T_c}{2})$ for H_0 and $\mathcal{N}(\sqrt{S}T_c c_i, \frac{N_0 T_c}{2})$ for H_1 where $\mathcal{N}(m, \sigma^2)$ represents Gaussian random variable with mean m and variance σ^2.

After obtaining discrete random variables r_i, several approaches to find the detector can be followed. In order to compare Bayesian and GLRT tests with the test, we give their derivations first.

4.3.1   Bayesian Approach

The vector representation of (4.36) can be written as

$$H_1 : \mathbf{r} = \sqrt{S}T_c \mathbf{c} + \mathbf{w},$$
$$H_0 : \mathbf{r} = \mathbf{w}. \tag{4.37}$$

where $\mathbf{r} = \begin{bmatrix} r_1 & \cdots & r_N \end{bmatrix}^T$ is received vector, $\mathbf{c} = \begin{bmatrix} c_1 & \cdots & c_N \end{bmatrix}^T$ is the unknown code, $\mathbf{w} = \begin{bmatrix} w_1 & \cdots & w_N \end{bmatrix}^T$ is the noise term.

Note that $\{r_i\}_{i=1}^{N}$ are jointly Gaussian and independent random variables. Hence, the pdf of r_i can be found as:

$$f_{r_i}(r_i; H_0) = \frac{1}{\sqrt{\pi N_0 T_c}} \exp\left(-\frac{r_i^2}{N_0 T_c}\right)$$

$$f_{r_i}(r_i|c_i; H_1) = \frac{1}{\sqrt{\pi N_0 T_c}} \exp\left(-\frac{(r_i - \sqrt{S}T_c c_i)^2}{N_0 T_c}\right) \tag{4.38}$$

Since the assumption on codes c_i are random variables with equal probability $Pr(c_i = 1) = Pr(c_i = -1) = 0.5$, the pdf of c_i can be written as:

$$f_{c_i}(c_i; H_1) = 0.5\delta(c_i - 1) + 0.5\delta(c_i + 1) \tag{4.39}$$

Thus, the conditional pdf of r_i for H_1 can found by well-known Bayesian method [42].

$$f_{r_i}(r_i; H_1) = \int_{c_i} f_{r_i}(r_i|c_i; H_1) f_{c_i}(c_i; H_1) dc_i$$

$$= \frac{1}{\sqrt{\pi N_0 T_c}} \exp\left(-\frac{r_i^2 + ST_c^2}{N_0 T_c}\right) \cosh\left(\frac{2}{N_0} r_i \sqrt{S}\right) \tag{4.40}$$

Finally, since each r_i is independent, the LRT becomes the following:

$$\Lambda(\mathbf{r}) = \frac{f_{\mathbf{r}}(\mathbf{r}|H_1)}{f_{\mathbf{r}}(\mathbf{r}|H_0)} = \prod_{i=1}^{N} \frac{f_{r_i}(r_i|H_1)}{f_{r_i}(r_i|H_0)}$$

$$= \exp(-N\gamma_c) \prod_{i=1}^{N} \cosh\left(\frac{2}{N_0} r_i \sqrt{S}\right) \tag{4.41}$$

where $\gamma_c = \dfrac{ST_c}{N_0}$ is the pre-detection SNR of chip. The LLRT of the above test is given as:

$$l_1 = -N\gamma_c + \sum_{j=1}^{N} \ln \cosh\left(\frac{2}{N_0} r_i \sqrt{S}\right) \underset{H_0}{\overset{H_1}{\gtrless}} \zeta_1. \tag{4.42}$$

Since the first term is assumed to be known, equivalent detector is given as

$$l_1 = \sum_{j=1}^{N} \ln \cosh(r_i) \underset{H_0}{\overset{H_1}{\gtrless}} \zeta_1. \tag{4.43}$$

For the low pre-detection SNR values, $\ln \cosh x = \dfrac{x^2}{2}$ hold and the detector (4.42) reduces to the well-known detector, energy detector, commonly called radiometer

as the following:

$$\lambda_1 = \sum_{j=1}^{N} r_j^2 \underset{H_0}{\overset{H_1}{\gtrless}} \eta_1. \tag{4.44}$$

4.3.2 Invariance Approach

In the problem given in (4.37), $\mathbf{c}$ is assumed to be unknown but its elements can take only two values $c_i \in \{1, -1\}$. The group of transformations which leaves the problem invariant after having applied is the following sign group.

$$G = \left\{ g : g(\mathbf{r}) = \begin{bmatrix} a_1 r_1 & \cdots & a_N r_N \end{bmatrix} a_i \in -1, 1 \right\} \tag{4.45}$$

So the group G consists of $2N$ transformations. Note that this group is different than one given in (4.2) in which all the elements of data vector are multiplied by the same constant value, i.e., -1 or 1. Here, each elements of data vector are multiplied by different constants as shown in (4.45). We claim that the maximal invariant test for this sign group is as follows:

$$m(\mathbf{r}) = \begin{bmatrix} |r_1| & |r_2| & \cdots & |r_N| \end{bmatrix}. \tag{4.46}$$

Proof Of Invariance: The requirement for this function to be invariant wrt the transformations in G is given as $m(\mathbf{r}) = m(g(\mathbf{r}))$ for each $g(\mathbf{r})$ given in (4.45). The following equations show that the function given in (4.3) is invariant under the group of transformations G.

$$\begin{aligned} m(\mathbf{r}) &= \begin{bmatrix} |r_1| & \cdots & |r_N| \end{bmatrix} \\ m(g(\mathbf{r})) &= \begin{bmatrix} |a_1 r_1| & \cdots & |a_N r_N| \end{bmatrix} \\ &= \begin{bmatrix} |r_1| & \cdots & |r_N| \end{bmatrix} \\ &= m(\mathbf{r}) \end{aligned} \tag{4.47}$$

Proof Of Maximality: If $m(\mathbf{r}) = m(\mathbf{r}^*)$ then, the maximality of (4.46) requires

$\mathbf{r} = g(\mathbf{r}^*)$ for the the group of transformations given in (4.45).

$$m(\mathbf{r}) = \begin{bmatrix} |r_1| & \cdots & |r_N| \end{bmatrix}$$
$$= \begin{bmatrix} |r_2^*| & \cdots & |r_N^*| \end{bmatrix}$$
$$= m(\mathbf{r}^*) \tag{4.48}$$

Thus, if $|r_i| = |r_i^*|$ then, $r_i = a_i r_i^*$ for $a_i \in \{-1, 1\}$. In other words, r_i and r_i^* are on the same orbit. Next step is to find the pdf of maximal invariant test to look for monotonically increasing function in that for UMPI test.

Classic Method To Find UMPI Test: We will find the pdf of $m(\mathbf{r}) = \begin{bmatrix} |r_1| & \cdots & |r_N| \end{bmatrix}$. Since r_i is independent random variables, so each $m_i = |r_i|$ are independent random variables.

$$f_{m_i}(m_i) = f_{r_i}(m_i) + f_{r_i}(-m_i)$$
$$= \frac{1}{\sqrt{\pi N_0 T_c}} \left[\exp\left(-\frac{(m_i - \sqrt{S}T_c c_i)^2}{N_0 T_c} \right) + \exp\left(-\frac{(-m_i - \sqrt{S}T_c c_i)^2}{N_0 T_c} \right) \right] \tag{4.49}$$

Expanding the term inside the exponential, the following expressions are obtained:

$$f_{m_i}(m_i) = \frac{1}{\sqrt{\pi N_0 T_c}} \left[2 \exp\left(\frac{m_i^2}{N_0 T_c} \right) + 2 \exp\left(\frac{S T_c c_i^2}{N_0} \right) + 2 \cosh\left(\frac{2\sqrt{S} m_i c_i}{N_0} \right) \right] \tag{4.50}$$

The ratio of conditional densities of $\mathbf{m}$ under H_1 and H_0

$$\Lambda_2 = \frac{f(\mathbf{m}; H_1)}{f(\mathbf{m}; H_0)} = \frac{\prod_{i=1}^{N} f_{m_i}(m_i; H_1)}{\prod_{i=1}^{N} f_{m_i}(m_i; H_0)} \tag{4.51}$$

After cancellation of common terms, the following test is obtained

$$\Lambda_2 = 2^{N+1} \exp\left(\frac{S T_c}{N_0} \right) \prod_{i=1}^{N} \cosh\left(\frac{2\sqrt{S} m_i c_i}{N_0} \right) \tag{4.52}$$

Since $m_i = |r_i|$ and $\cosh(\cdot)$ is an even function, the final UMPI test becomes as follows:

$$\Lambda_2 = 2^{N+1} \exp\left(\frac{S T_c}{N_0} \right) \prod_{i=1}^{N} \cosh\left(\frac{2\sqrt{S} r_i}{N_0} \right). \tag{4.53}$$

80

Taking the logarithm of the above test, one can reach the test given in (4.43). When equal a priori probability is assumed for the unknown parameter, the Bayesian approach and invariant detectors turn out to be same.

4.3.3 GLRT Approach

GLRT can be interpreted as maximizing the pdf over group elements or unknown parameter. Namely,

$$
t_{\text{GLRT}} = \frac{\max\limits_{g_i \in G} f\left(g_i(\mathbf{r}); H_1\right)}{\max\limits_{g_i \in G} f\left(g_i(\mathbf{r}); H_0\right)} \tag{4.54}
$$

$$
= \prod_{n=1}^{N} \frac{\max\limits_{g_i' \in G'} f_{r_n}\left(g_i'(r_n); H_1\right)}{\max\limits_{g_i' \in G'} f_{r_n}\left(g_i'(r_n); H_0\right)} \tag{4.55}
$$

where g_i and G are all group elements given in (4.45) and $g_i', (i = 1, 2)$ and $G' = \{-1, 1\}$ are sub group elements acting on each sample r_i. Let denote

$$
t_n \triangleq \frac{\max\limits_{g_i' \in G'} f_{r_n}\left(g_i'(r_n); H_1\right)}{\max\limits_{g_i' \in G'} f_{r_n}\left(g_i'(r_n); H_0\right)}.
$$

Then,

$$
t_n = \frac{\max\limits_{g_i' \in G'} \frac{1}{\sqrt{2\pi}\sigma} \exp\left[-\frac{1}{2\sigma^2}\left(g_i'(r_n) - \mu c_n\right)^2\right]}{\max\limits_{g_i' \in G'} \frac{1}{\sqrt{2\pi}\sigma} \exp\left[-\frac{1}{2\sigma^2}\left(g_i'(r_n)\right)^2\right]}, \tag{4.56}
$$

$$
= \max\limits_{g_i' \in G'} \frac{1}{\sqrt{2\pi}\sigma} \exp\left[\frac{1}{\sigma^2}\left(\mu g_i'(r_n) c_n\right)\right], \tag{4.57}
$$

$$
= \exp\left[\frac{1}{\sigma^2}\mu|r_n|\right]. \tag{4.58}
$$

where $\mu = \sqrt{S}T_c$ and $\sigma^2 = \dfrac{N_0 T_c}{2}$ as given in (4.38). (See [4] for further information.) GLRT test is the product of all t_ns.

$$
\Lambda_3 = \prod_{n=1}^{N} t_n = \prod_{n=1}^{N} \exp\left[\frac{1}{\sigma^2}\mu|r_n|\right] \tag{4.59}
$$

Taking the logarithm of the above expression and ignoring known constants, the following expression is obtained:

$$l_3 = \sum_{n=1}^{N} |r_n|. \tag{4.60}$$

As a conclusion, for this application the invariant test and the Bayesian test with equal prior coincide, but different from the GLRT.

4.3.4   Simulation Results

The performance of the UMPI test given in (4.53) is compared with the GLRT test given in (4.60) and the energy detector given in (4.44). The argument of the UMPI test inside the summation is $\log(\cosh(x))$. For low SNR region, this argument can be approximated as $\dfrac{x^2}{2}$ and results in radiometer. For high SNR region, $\cosh(x)$ can be approximated as $\dfrac{1}{2}\exp(|x|)$ and UMPI detector can be approximated by GLRT detector. In order to differentiate the high and low SNR regions, the signal lengths of 10 and 100 are chosen in simulation. For the case of $N = 10$, the effect of SNR dominates the effect of signal length, thus, when SNR increases, GLRT and UMPI detectors converge and the radiometer detector diverges from UMPI detector.

Figure 4.2 presents the probability of detection as a function of SNR for the probability of false alarms of 0.001, 0.01 and 0.1 when the signal length N is set to 10. It is seen that UMPI outperforms GLRT and the radiometer in all SNR and P_{fa} regions. When SNR > -2dB and $P_{fa} = 0.001$, GLRT and UMPI detectors performs very close to each other while the gap between UMPI and radiometer increases as SNR increases. The performance gap between all three detectors diminishes for low SNR and high P_{fa} regions.

Figure 4.2 shows the powers of UMPI, GLRT and the radiometer detectors when the signal length is set to 100. Since the energy of signal is higher than the previous case of $N = 10$, the performance of all three detectors can be differentiated for the low SNR regions. From Figure 4.2, it is seen that the radiometer performance is in close proximity of UMPI detector. Also, the GLRT

detector performance has worse performance for all regions. For this case, the UMPI detector can well be approximated by the energy detector as seen from the figure.
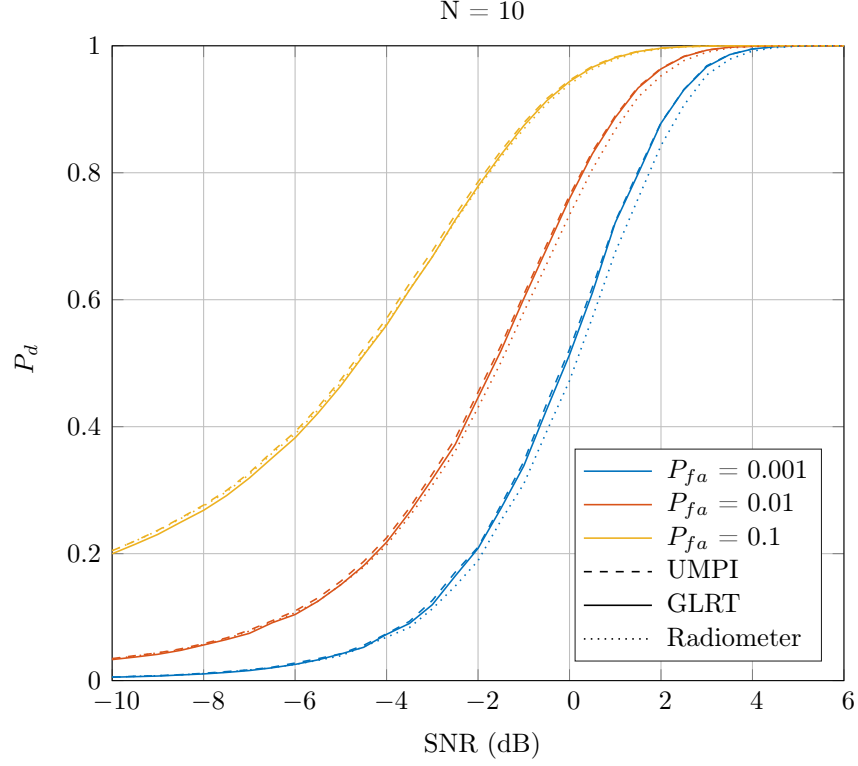
Figure 4.2: Comparison of GLRT, UMPI and radiometer powers for the case of $N = 10$, Ntrial $= 5 \times 10^5$.
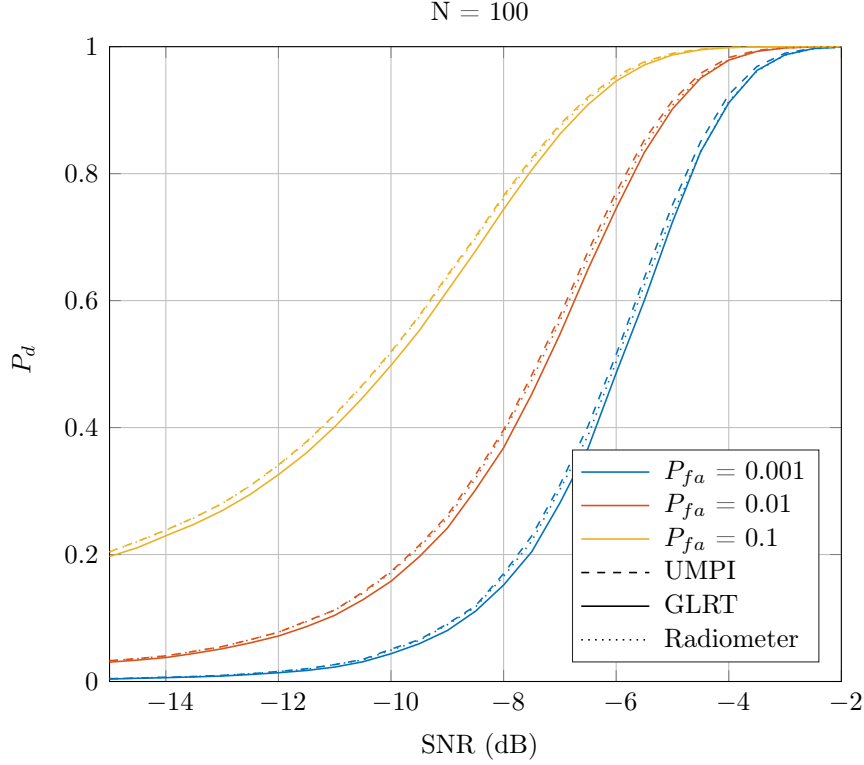
Figure 4.3: Comparison of GLRT, UMPI and radiometer powers for the case of $N = 100$, Ntrial $= 5 \times 10^5$.

4.3.5 Discussion

For the synchronous coherent LPI signal detection problem, it is shown that the UMPI and Bayesian detectors with equal prior turn out to be same, while the GLRT test is different than the UMPI detector. For the low and high SNR regions, UMPI detector can be approximated by the energy detector and the GLRT detector, respectively. Also, the performance gap between all three detectors are not significant.

For the noncoherent LPI signal detection problem case, the invariance principle can be applied and the similar results can be found as in coherent case. Explicitly speaking, the Bayesian and UMPI detectors will be same and the GLRT detector will be in similar form as in coherent case.

4.4 Invariance Application to Detection of Frame Synchronization Words

Let N denote the frame length and assume that the frame is composed of L-digit synchronization word and $(N - L)$-digit random binary data which follows the sync word. The synchronization codeword $\mathbf{c}_L$, which is assumed to be known, and data bits $\mathbf{d}_{N-L}$ are shown as follows [43]:

$$\mathbf{c}_L = \begin{bmatrix} c_0 & c_1 & \cdots & c_{L-1} \end{bmatrix}^T \tag{4.61}$$

$$\mathbf{d}_{N-L} = \begin{bmatrix} d_L & d_{L+1} & \cdots & d_{N-1} \end{bmatrix}^T \tag{4.62}$$

where $Pr(d_i = 1) = Pr(d_i = -1) = 0.5$. Received samples x_n is represented as

$$x(n) = c(n - m) + d(n - m) + w(n), \quad n = 0 \cdots N - 1 \tag{4.63}$$

where m is the starting position of sync word and it is assumed to be unkown. Concatenating $\mathbf{c}$ and $\mathbf{d}$ vectors as $\mathbf{s} = \begin{bmatrix} \mathbf{c} \\ \mathbf{d} \end{bmatrix}$, the received data samples can be written as

$$\mathbf{x} = A\mathbf{P}^m\mathbf{s} + \mathbf{w} \tag{4.64}$$

where $\mathbf{P}^m$ is a cyclic permutation matrix which shifts the samples to the right by m positions and A is known signal amplitude. Then, hypothesis testing problem can be formulated as follows:

$$\begin{aligned} H_1 : \mathbf{x} = A\mathbf{P}^m \begin{bmatrix} \mathbf{c}_L \\ \mathbf{d}_{N-L} \end{bmatrix} + \mathbf{w}, \\ H_0 : \mathbf{x} = A\mathbf{P}^m \begin{bmatrix} \mathbf{d}_L \\ \mathbf{d}_{N-L} \end{bmatrix} + \mathbf{w} \end{aligned} \tag{4.65}$$

Under H_0 hypothesis, each frame assumed to consist of N random data bits and noise. Here, the continuous transmission of data assumed and at the beginning of data bits, synchronization word is located. Receiver window duration is assumed to be less than frame length. Thus, for each look, there can be a sync word followed by data or only data covering whole receive window.

This problem is similar to the detection of signal with unknown location which was considered in [44] and [45]. Below are given the hypothesis testing problem they solved by Wijsman theorem and finding classic maximal test.

$$H_1 : \mathbf{x} = A\mathbf{P}^m\mathbf{s} + \mathbf{w},$$
$$H_0 : \mathbf{x} = \mathbf{w}. \tag{4.66}$$

where $\mathbf{x}$ is the target signal considered.

Here, the assumption of random data bits on both hypothesis and the different length of them should be taken account. As it will be seen later, the permutation of data vector with unknown parameter m can be tackled easily and the group of transformations that leave the problem invariant can be found. But, for the random data bits part, since the length of data bits in both hypothesis are different, no group of transformations take into account of each data bit leaving the hypothesis problem can be found. We use Bayesian approach instead, namely, we will first find the conditional pdf based on given data bit, then we will integrate it with respect to random data bit. This method is not purely invariant, but as it will be shown in subsequent chapter, it will give the similar result as in [44] and [45].

4.4.1   Invariance And Bayesian Approach Combined

The hypothesis testing problem is invariant for the following group:

$$G = \left\{ g : g(\mathbf{x}) = \mathbf{P}^i\mathbf{x}, \quad i = 1, \cdots, N \right\}. \tag{4.67}$$

Here, $\mathbf{P}^i$ is the i-shift permutation matrix.

We assume that random data bits employ known a priori information. For simplicity, we will assume that each random data bit is equally likely.

The conditional pdfs can be found by applying the Bayesian approach. Specifically,

$$f_{\mathbf{x}}\left(g_i(\mathbf{x}); H_1\right) = \sum_{\mathbf{d}'} f_{\mathbf{x}}\left(g_i(\mathbf{x})|\mathbf{d} = \mathbf{d}'; H_1\right) Pr(\mathbf{d} = \mathbf{d}'; H_1) \tag{4.68}$$

where $\mathbf{d}' = \begin{bmatrix} d'_L & d'_{L+1} & \cdots & d'_{N-1} \end{bmatrix}^T$ denotes the values that random vector $\mathbf{d}$ can take. Remember that these values are -1 and 1 with equal probability. So, $Pr(\mathbf{d} = \mathbf{d}'; H_1) = 2^{-(N-L)}$ and $Pr(\mathbf{d} = \mathbf{d}'; H_0) = 2^{-N}$.

(4.15) can be written as

$$\frac{\sum\limits_{i=1}^{N} f_{\mathbf{x}}\left(g_i(\mathbf{x}); H_1\right)}{\sum\limits_{i=1}^{N} f_{\mathbf{x}}\left(g_i(\mathbf{x}); H_0\right)} = 2^L \frac{\sum\limits_{\mathbf{d}'}\sum\limits_{i=1}^{N} f_{\mathbf{x}}\left(g_i(\mathbf{x})|\mathbf{d} = \mathbf{d}'; H_1\right)}{\sum\limits_{\mathbf{d}'}\sum\limits_{i=1}^{N} f_{\mathbf{x}}\left(g_i(\mathbf{x})|\mathbf{d} = \mathbf{d}'; H_0\right)} \tag{4.69}$$

Considering the inner summation of denominator

$$\sum_{i=1}^{N} f_{\mathbf{x}}\left(g_i(\mathbf{x})|\mathbf{d} = \mathbf{d}'; H_1\right) = \sum_{i=1}^{N} \frac{1}{(2\pi\sigma^2)^{N/2}} \exp\left[-\frac{1}{2\sigma^2}\left(g_i(\mathbf{x}) - A\mathbf{s}\right)^T\left(g_i(\mathbf{x}) - A\mathbf{s}\right)\right]$$

$$= K_1 \sum_{i=1}^{N} \exp\left[-\frac{1}{2\sigma^2}\left(\mathbf{x}^T\mathbf{x} - 2A\mathbf{s}^T g_i(\mathbf{x}) + A^2\mathbf{s}^T\mathbf{s}\right)\right]$$

$$\tag{4.70}$$

where $K_1 = \dfrac{1}{(2\pi\sigma^2)^{N/2}}$. Since $\mathbf{x}^T\mathbf{x}$ is common in denominator and numerator and $\mathbf{s}^T\mathbf{s}$ is not data dependent, only the middle term affects the final result,

$$\sum_{i=1}^{N} f_{\mathbf{x}}\left(g_i(\mathbf{x})|\mathbf{d} = \mathbf{d}'; H_1\right) = K_1 K_2 \sum_{i=1}^{N} \exp\left[\frac{1}{\sigma^2}\left(A\mathbf{s}^T g_i(\mathbf{x})\right)\right] \tag{4.71}$$

where K_2 accounts for the terms involving $\mathbf{x}^T\mathbf{x}$ and $\mathbf{s}^T\mathbf{s}$. Note that $g_i x(n) = x(n-i)$, thus

$$\mathbf{s}^T g_i(\mathbf{x}) = \sum_{n=0}^{N-1} s(n)x(n-i).$$

Then,

$$\sum_{i=1}^{N} f_{\mathbf{x}}\left(g_i(\mathbf{x})|\mathbf{d} = \mathbf{d}'; H_1\right) = K_3 \sum_{i=0}^{N-1} \exp\left[\frac{A}{\sigma^2}\sum_{n=0}^{N-1} s(n)x(n-i)\right]$$

$$= K_3 \sum_{i=0}^{N-1} \exp\left[\frac{A}{\sigma^2}\sum_{n=0}^{L-1} c(n)x(n-i) + \sum_{j=L}^{N-1} d'(j)x(j-i)\right]$$

$$= K_3 \sum_{i=0}^{N-1} \exp\left[\frac{A}{\sigma^2}\sum_{n=0}^{L-1} c(n)x(n-i)\right] \prod_{j=L}^{N-1} \exp\left(d'(j)x(j-i)\right)$$

$$\tag{4.72}$$

where $K_3 = K_1 K_2$. Considering the outer summation in (4.68),

$$\sum_{\mathbf{d}'} \sum_{i=1}^{N} f_{\mathbf{X}} \left(g_i(\mathbf{x}) | \mathbf{d} = \mathbf{d}'; H_1 \right) = K_1 K_2 \sum_{i=0}^{N-1} \exp \left[\frac{A}{\sigma^2} \sum_{n=0}^{L-1} c(n) x(n-i) \right]$$

$$\prod_{j=L}^{N-1} \sum_{\mathbf{d}'} \exp \left[d'(j) \left(x(j-i) \right) \right]. \quad (4.73)$$

The final form is obtained as:

$$\sum_{i=1}^{N} f_{\mathbf{X}} \left(g_i(\mathbf{x}); H_1 \right) = K_1 K_2 \sum_{i=0}^{N-1} \exp \left[\frac{A}{\sigma^2} \sum_{n=0}^{L-1} c(n) x(n-i) \right] \prod_{j=L}^{N-1} 2 \cosh \left(x(j-i) \right).$$

$$(4.74)$$

Similarly, $f_{\mathbf{X}} \left(g_i(\mathbf{x}); H_0 \right)$ can be found as:

$$\sum_{i=1}^{N} f_{\mathbf{X}} \left(g_i(\mathbf{x}); H_0 \right) = K_1 K_2 \sum_{i=0}^{N-1} \exp \left[\frac{A}{\sigma^2} \right] \prod_{j=0}^{N-1} 2 \cosh \left(x(j-i) \right). \quad (4.75)$$

The ratio of maximal invariant densities will be

$$t_{\text{invariant}} = \frac{\displaystyle\sum_{i=0}^{N-1} \exp \left[\sum_{n=0}^{L-1} c(n) x(n-i) \right] \prod_{j=L}^{N-1} \cosh \left(x(j-i) \right)}{\displaystyle\sum_{i=0}^{N-1} \prod_{j=0}^{N-1} \cosh \left(x(j-i) \right)}, \quad (4.76)$$

$$= \frac{\displaystyle\sum_{i=0}^{N-1} \exp \left[\sum_{n=0}^{L-1} c(n) x(n-i) \right] \prod_{j=L}^{N-1} \cosh \left(x(j-i) \right)}{\displaystyle N \prod_{j=0}^{N-1} \cosh \left(x(j) \right)}. \quad (4.77)$$

Equivalently, the test given in (4.77) can be expressed as

$$t_{\text{invariant}} = \sum_{i=0}^{N-1} \alpha_i \exp \left[r_{cx}(i) \right] \quad (4.78)$$

where $r_{cx}(i) = \sum_{n=0}^{L-1} c(n) x(n+i)$ is the cross-correlation of the input $x[n]$ with the synchronization code $c[n]$ and $\alpha_i = \prod_{j=0}^{L-1} \left[\cosh \left(x(j-i) \right) \right]^{-1}$ is a weighting factor. The α_i weight can be interpreted as the weight for the synch word starting at the i'th index.

88

4.4.2 GLRT And Bayesian Approach Combined

GLRT can be defined either as a maximization of pdf over group elements or over unknown parameter [4];

$$\frac{\max\limits_{g \in G} f\left(g(\mathbf{x}); \theta_1\right)}{\max\limits_{g \in G} f\left(g(\mathbf{x}); \theta_0\right)} \tag{4.79}$$

where hypotheses H_1 and H_0 correspond to the unknown parameters $\theta_1 \in \Theta_1$ and $\theta_0 \in \Theta_0$ respectively. This interpretation is valid for orthogonal subgroups.

In order to tackle the random data bits, Bayesian approach is used.

Omitting the summation in (4.77) and maximizing with respect to unknown location i, one can find the GLRT test as follows:

$$t_{\text{GLRT}} = \frac{\max\limits_{i \in [0, N-1]} \exp\left[\sum\limits_{n=0}^{L-1} c(n)x(n-i)\right] \prod\limits_{j=L}^{N-1} 2\cosh\left(x(j-i)\right)}{\max\limits_{i \in [0, N-1]} \prod\limits_{j=0}^{N-1} 2\cosh\left(x(j-i)\right)},$$

$$= \max\limits_{i \in [0, N-1]} \exp\left[\sum\limits_{n=0}^{L-1} c(n)x(n-i)\right] \prod\limits_{j=0}^{L-1} \cosh\left(x(j-i)\right). \tag{4.80}$$

Without any loss of generality, we can divide the test given in (4.80) by $\prod\limits_{j=0}^{N-1} \cosh\left(x(j)\right)$. With this modification, t_{GLRT} becomes

$$t_{\text{GLRT}} = \max\limits_{i \in [0, N-1]} \alpha_i \exp\left[r_{cx}(i)\right] \tag{4.81}$$

where the definitions for $r_{cx}(i)$ and α_i coincide with the definitions given for the invariant detector given in (4.78).

Taking the logarithm of (4.81) and simplifying the expression, equivalent test can be written as:

$$\log\left(t_{\text{GLRT}}\right) = \max\limits_{i \in [0, N-1]} \log\left(\alpha_i\right) + r_{cx}(i), \tag{4.82}$$

$$= \max\limits_{i \in [0, N-1]} \log\left(\prod\limits_{j=0}^{L-1} \left[\cosh\left(x(j-i)\right)\right]^{-1}\right) + \sum\limits_{n=0}^{L-1} c(n)x(n+i), \tag{4.83}$$

$$= \max\limits_{i \in [0, N-1]} \sum\limits_{n=0}^{L-1} c(n)x(n+i) - \sum\limits_{j=0}^{L-1} \log\left[\cosh\left(x(j-i)\right)\right]. \tag{4.84}$$

4.4.3 Simulation Results And Discussion

Since the statistics of both detectors given in (4.78) and (4.84) are difficult to obtain analytically, Monte Carlo simulations are used to asses their comparative performance on MATLAB environment.

It should be noted that both detectors have the common goal of discriminating one code from the other. Namely, the problem at hand is to build a detector whose aim is to discriminate two codes of same power. The threshold for this test is found when H_0 is true, i.e., the frame consists of only random data bits. Based on preassigned value for false sync word declaration probability, similar to false alarm probability, a threshold is found for each SNR. This SNR is used to know whether the frame includes the sync word or not.

For the following scenarios, the chosen sync word is represented as hexadecimal equivalent of the code where the values of -1 is represented as false bits (0). If the length of sync word is not multiple of 4, required number of zeros is appended to the left. For example, Barker (7) code (-1, -1, -1, 1, 1, -1, 1) is represented in binary form as 0001101, and its hexadecimal equivalent becomes 0D and one zero is appended to the left side in order to make the length 8.

Table 4.1: Scenario conditions for simulations

Figure No	Frame Length (N)	Name of SW	Hex Value of SW
Figure 4.4	10	Barker (7)	OD
Figure 4.5	15	Barker (13)	OOCA
Figure 4.6	91	Barker (13)	OOCA
Figure 4.7	91	$S20_1$	14B37
Figure 4.8	91	All ones (20)	FFFFF

Figure 4.4 shows the powers of the invariant and GLRT detectors as a function of SNR for different P_{fa} values and chosen sync word is set to Barker (7) and the frame length is chosen as 10. It is seen that for $P_{fa} = 0.001$ and $P_{fa} = 0.01$, P_d does not increase as SNR is increased after some point. This situation can be explained due to the nature of both detectors. Since, the similarity of sync word and equally likely random data bits is tested, when the energy of the sync word

90

is not enough, the highest power value that can be achieved by the structure of this detectors is limited. When the false alarm probability is set to a lower value, the required threshold increases, and since the dissimilarity between two codes is fixed, the power does not approach to 1 as SNR increases.

Also, from Figure 4.4 it can be noted that for higher false alarm probabilities, the performance difference between invariant and GLRT detectors increases compared to lower false alarm rates. For example, for the case of $P_{fa} = 0.4$ and SNR between -5 dB and 5 dB, invariant detector achieves higher detection probabilities.

Figure 4.4: Comparison of GLRT and invariant detector powers for the case of $N = 10$, SW = Barker (7), Ntrial = 10^5.

Figure 4.5 shows the same comparison of both detectors when chosen sync word is Barker (13) and the frame length is 15. Here, it is seen that for $P_{fa} = 0.01$, P_d approaches to 1 as SNR increases. Since the energy of sync word increases as its length is increased from 7 to 13, this behaviour is indeed expected. From this figure, it is also seen that as the frame length gets closer to the length of

sync word, the invariant and GLRT detectors performs very similar. Because, the invariant detectors is build upon the assumption of unknown location of sync word. To put it differently, when the sync word covers the most of the frame, the location of sync word becomes less important compared to the case of long frame.

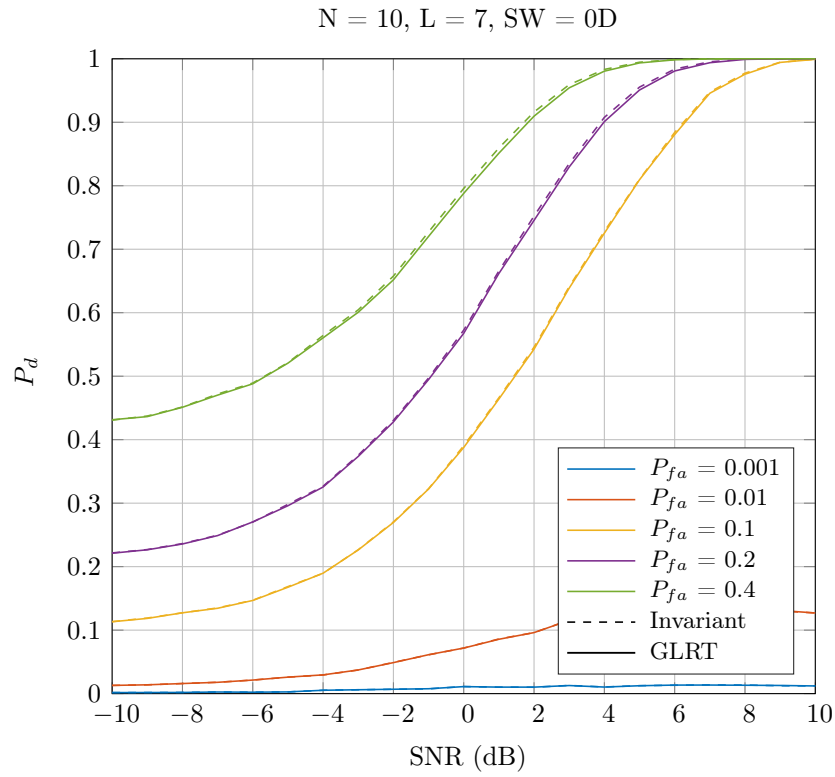

Figure 4.5: Comparison of GLRT and invariant detector powers for the case of $N = 15$, SW = Barker (13), Ntrial = 10^5.

Figure 4.6 presents the same comparison as in Figure 4.5 except the frame length is increased to 91. It is seen that the performance gap between the invariant and GLRT detectors increases as P_{fa} increases. The region where the invariant detector outperforms GLRT is $P_{fa} \in (0.1, 0.4)$ and SNR $\in (-6 \text{ dB}, 0 \text{ dB})$. The performance gap between two detectors diminishes as SNR increases. For the case of $P_{fa} = 0.01$, for SNR is greater than 3 dB, the performance of GLRT detectors is better than the invariant detector by a small amount. This case is attributed to the fact that for the chosen sync word there is an minimum lower bound for the false alarm consideration in order to be in the region where P_d increases as SNR increases. It can be noted that for the case of frame length of

91 and Barker (13) sync word, $P_{fa} = 0.01$ is very close the aforementioned lower bound for the satisfactory operation of both detectors. Remember that when the frame length is set to 15, this situation does not appear (see Figure 4.5).
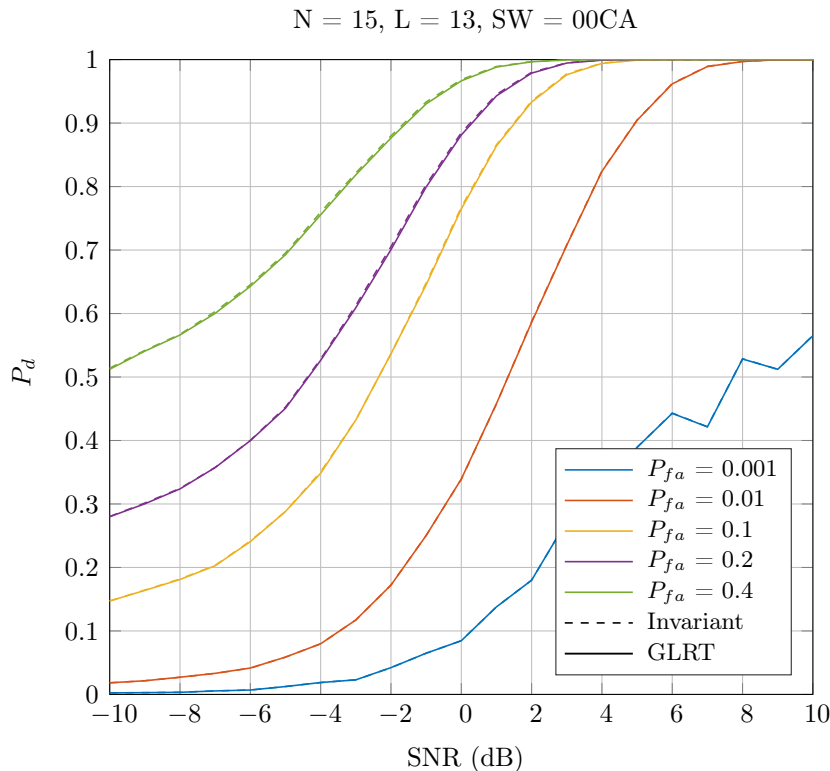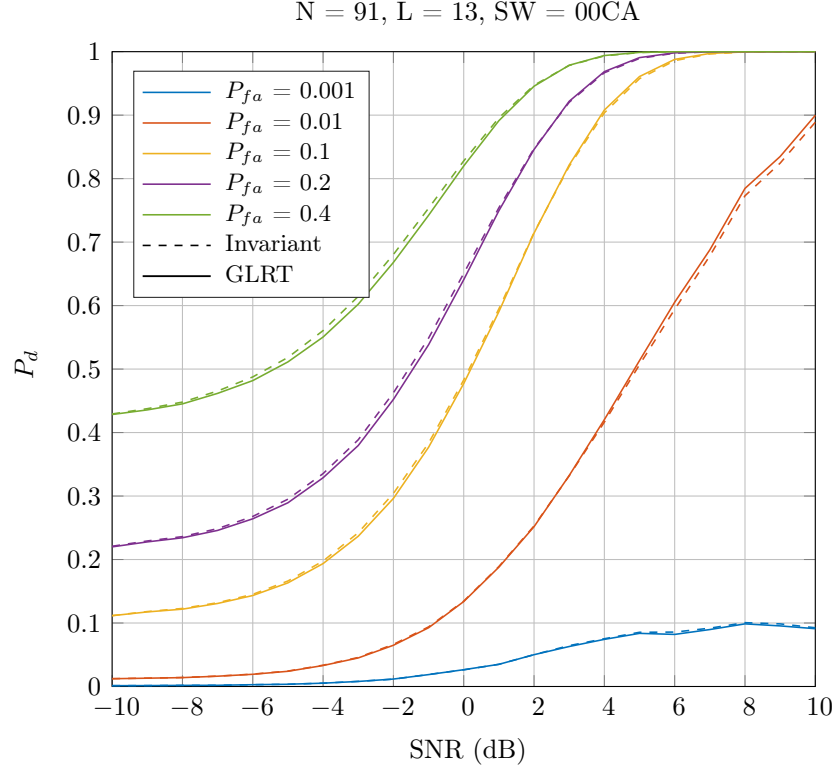

Figure 4.6: Comparison of GLRT and invariant detector powers for the case of $N = 91$, SW = Barker (13), Ntrial = 5×10^5.

Figure 4.7 presents the same comparison when the sync word is chosen as $S20_1$ code (see [46]). It is seen that both detectors operate satisfactorily for the case of $P_{fa} = 0.001$. When P_{fa} is set to 0.001, 0.01 and 0.1 both detectors' performance are almost same, while for higher P_{fa} values the invariant detector's performance has minor improvement.

The previous simulations in which sync words are chosen with the aim of having a better correlation characteristic show that the lengths of frame and sync word and the code of sync word can effect the performances of both detectors as well as the performance gap between them. Figure 4.8 presents the scenario in which sync word is chosen as all 1's meaning having worse autocorrelation properties compared to Barker and the other codes which have the narrow main lobe and low
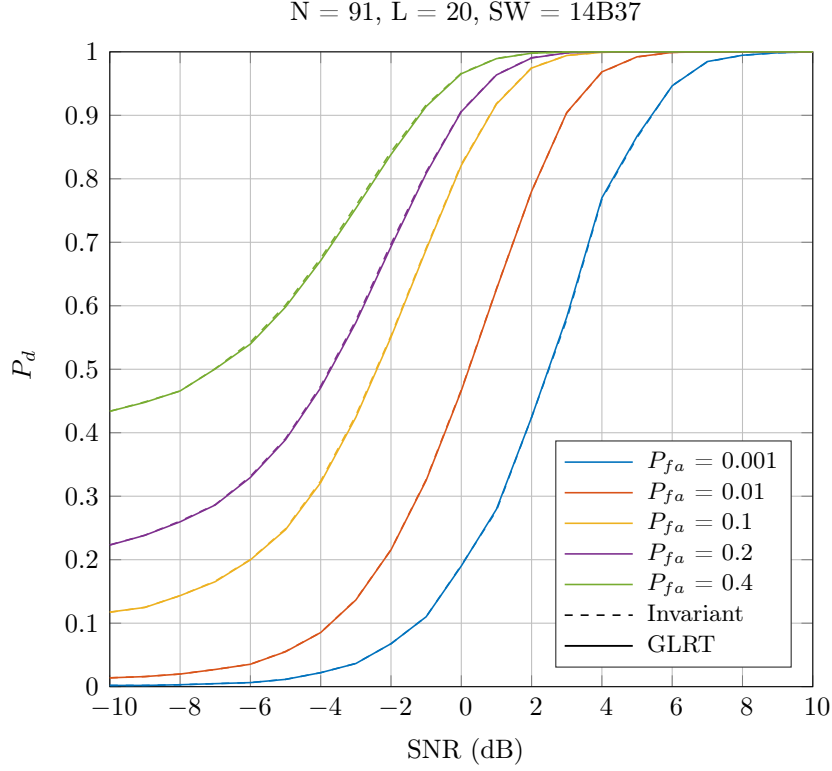
Figure 4.7: Comparison of GLRT and invariant detector powers for the case of $N = 91$, SW $= S20_1$, Ntrial $= 10^5$.

sidelobes. It is seen that the performance gap between both detectors increases and the invariant detector outperforms the GLRT detector. The reason of this behaviour can be attributed to the fact that the autocorrelation of codewords which has narrow main lobes and low sidelobes can cause the better estimate of its maximum, and leading to better GLRT performance. For the case of all 1's codeword, the autocorrelation is triangle and the level of sidelobes is half of its maximum. For the invariant detector, since all the possible locations of sync word is considered and summed up, its performance can be thought of independent of the location of sync word.

Figure 4.9 shows the receiver operating characteristics of both detector for the third scenario described in Table 4.1. The region where the invariant detector outperforms GLRT is of SNR between -3 dB and 3 dB and P_{fa} between 0.2 and 0.6.
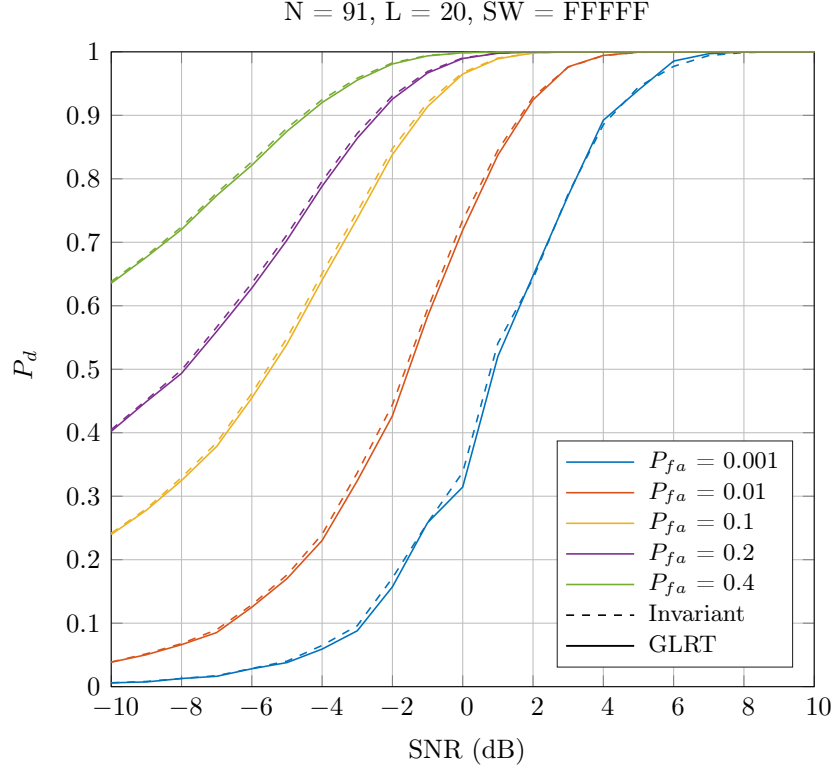
Figure 4.8: Comparison of GLRT and invariant detector powers for the case of $N = 80$, SW = FFFFF, Ntrial = 5×10^5.

4.4.4 Discussion and Further Work

This section shows how to combine invariance principle with Bayesian approach when there is a priori information about unknown data bits. It was shown that the performance of invariant detector is very similar to the performance of GLRT. But, for some regions and for some chosen sync words and frame length, invariant detector can outperform GLRT. To sum it up,

1. When the frame length and the length of sync word is close to each other, the invariant and GLRT detectors' performances approach each other.

2. Depending on the length of sync word, there is an lower limit on P_{fa} for satisfactory operations due to the limited dissimilarity between sync code and equally likely random data bits.

3. The performance difference between the invariant and GLRT detectors
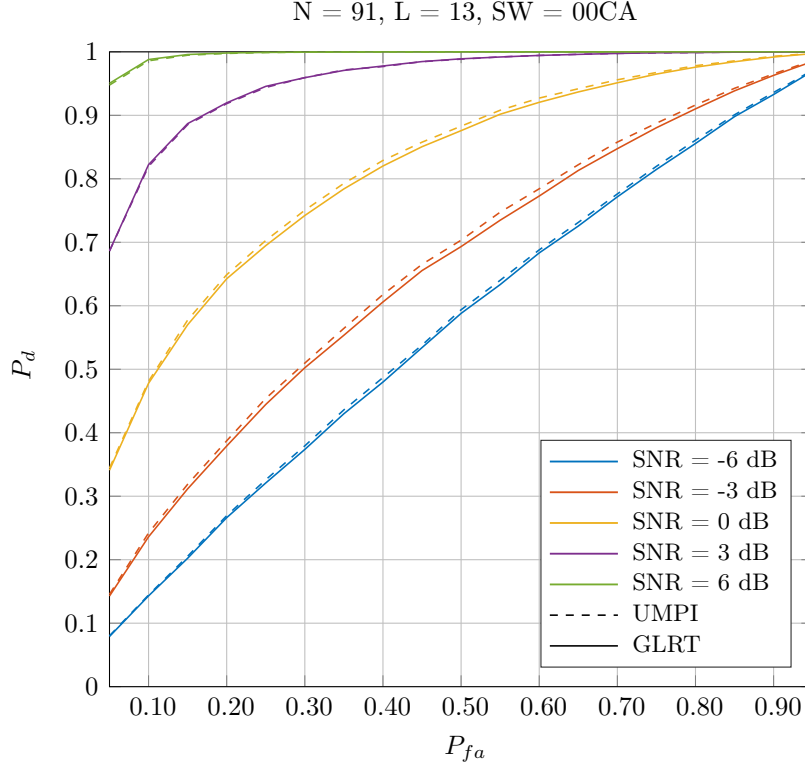
Figure 4.9: Comparison of GLRT and invariant detector ROC curves for the case of $N = 91$, SW = Barker (13), Ntrial = 10^5.

increases, as the desired maximum false alarm probability increases.

4. The performance gap between both detectors increases as the autocorrelation of the sync code has the higher sidelobes as in the code of all ones case.

The detectors built in this section is aimed to detect the presence of synchronization word within the chosen frame. After finding that frame, suitable estimation techniques might be applied, and the location of sync word can be found. One might argue that applying only the estimation of location of sync word approach can be computationally effective. Indeed, in some situation if one wants to fix the false sync declaration probability and aim to increase the probability of detection of frames including sync word at the same time, the methods described in this chapter might be useful. The estimation methods which can be applied afterwards are expected to give more accurate results since the frame of sync word would have been found in advance.

For future work, one can formulate the hypothesis testing problem as testing sync word followed by random data bit against only data bits with the same length as former case. For this problem, one can find pure invariant detector and GLRT detector since the group of transformation leaving the hypothesis testing problem can be found.

CHAPTER 5

CONCLUSIONS AND FUTURE DIRECTIONS

In this dissertation, optimality considerations in multiple hypothesis testing and composite hypothesis testing is studied and some application examples are provided. It is shown that for each problem considered, the definition of optimality is the most crucial point for constructing the relevant detector.

Neyman-Pearson test is the optimal detector in the sense of minimizing the probability of miss detection probability while keeping the probability of false alarm bounded by predetermined upper value. This definition of optimality is suitable for radar target detection problem and well-known concept by many radar receiver designers. In the literature, there is a vast amount of information covering Neyman-Pearson detectors for binary hypothesis testing problem. For multiple hypothesis testing, Neyman-Pearson theory is not well covered due to the complexity of controlling multiple error probabilities. In this work, a literature survey of application of Neyman-Pearson theory to multiple hypothesis testing problem is provided. The results of survey is then used to construct optimum sidelobe blanker for radar receivers. As a future work, these Neyman-Pearson detectors can be applied to adaptive radar detectors, and their performances can be compared.

The Sidelobe blanker (SLB) systems are intended to blank the main channel when there is a jammer in the sidelobe of main antenna. This problem was solved by Maisel and widely used in many radars. Maisel SLB detectors uses two channels to identify the jammer presence. One of them is main channel which has narrow main beam and low sidelobes. The other channel is secondary

channel whose antenna has flat gain and its gain is slightly greater than the sidelobe gain of main antenna. The idea is to divide auxiliary channel signal magnitude by main channel magnitude and see that value is greater than by some threshold. Optimal SLB detectors are derived for each Swerling targets and its performance are compared with classical Maisel SLB detectors. Even though optimum detectors are not realizable, they can be used to assist Maisel SLB design process and show the performance bound for the probability of blanking of jammer and the probability of falsely blanking the target. Several performance figures are provided and design examples of Maisel SLB are given.

As a future work, the new optimum blanking structure can be combined with the second target threshold, and the probability of declaring false target due to jammer and loss of probability of target detection can be analyzed. An example of application fields of optimum SLB detector can be the problem of finding the optimum path for airborne radars. When there are multiple jammer with known location, unmanned airborne vehicle (UAV) equipped with radar, in that case optimum path with respect to minimizing the target blanking probability and desired jammer blanking probability can be found. The fact that SLB detector considered in this dissertation can blank the jammer with low-duty cycle signals is to be remembered. If high-duty cycle signals are desired to be cancelled, in that case sidelobe cancellation systems (SLC) or any beamforming methods suitable needs to be used. Additionally, digital beamforming method can be utilized to form the auxiliary antenna pattern and the gain margin between auxiliary antenna and main beam of main antenna (ω^2) can be increased by decreasing the gain of auxiliary antenna within the region of main lobe.

Next, the invariance principles are studied. It is shown that an alternative to the GLRT detector when there is no a prior information about the unknown parameter can be provided by the invariant detectors. The theoretical framework, group and orbit definitions are provided. The invariant detector can be preferable over the GLRT detector based on the fact that invariant detector is mostly uniformly most powerful (UMPI) within its class called UMPI detector. In addition, the dimension of the unknown parameters can decrease and the resultant detector can be CFAR. Two methods to find the UMPI detectors are provided along with

the combination of sufficient statistics. As an application, general signal detection problem is considered and solved by the classical maximal invariant detector and it's combination with sufficient statistic approach. The other method is Wijsman theorem approach in which one can find the ratio of maximal invariant statistic without knowing the maximal invariant function of group. Only the information of group structure and some common requirements are enough to use Wijsman theorem. Wijsman theorem is applied to the LPI signal detection problem and frame synchronization word detection problems. It is shown that for both examples GLRT detector is different than the invariant detectors. For both problems, the computer simulations are given to asses the performance gap between the invariant and GLRT detector. For the former problem, UMPI detector can be well approximated by the energy detector for low SNR region and GLRT for high SNR region. The performance gap among three detectors are not significant and the invariant detector is the best detector for all P_{fa} and SNR regions. For the latter problem, Depending on the chosen sync word and frame length, invariant and GLRT detectors have probability of detection within close proximity except for the case of relatively high false alarm probability and low SNR region for which the power of the invariant detector is greater than the one of GLRT test.

As a future work, for the problem of detection of frame synchronization word, the invariant detector can be applied to different null hypothesis than the one was considered in this work. Null hypothesis definition may exclude the data vector for the place of sync word and it can contain only noise vector in the place of sync word. Also, the idea can be used to derive more realistic problem of detection of LPI signals where the phase of each bits and/or the variance of noise is unknown. In that case a new group of transformation has to be found and the invariant detector should be derived afterwards.

REFERENCES

[1] Coşkun, O. and Candan, Ç. "Design of Maisel sidelobe blankers with a guarantee on the gap to optimality". In: *IET Radar, Sonar & Navigation* 10 (9 Dec. 2016), 1619–1626(7) (see pp. 3, 121).

[2] Coşkun, O. and Candan, Ç. "On the optimality of Maisel sidelobe blanking system". In: *2015 23nd Signal Processing and Communications Applications Conference (SIU)*. May 2015, pp. 585–591 (see pp. 4, 122).

[3] Coşkun, O. and Candan, Ç. "On the optimality of Maisel sidelobe blanking structure". In: *Radar Conf., 2014 IEEE*. May 2014, pp. 1102–1107 (see pp. 4, 35, 122).

[4] Gabriel, J. *Invariant Hypothesis Testing with Applications in Signal Processing*. University of Rhode Island, 2004 (see pp. 4, 60, 64, 67, 70, 72, 81, 89).

[5] Levy, B. *Principles of Signal Detection and Parameter Estimation*. Springer, 2008 (see pp. 6–9, 11, 17, 60, 61, 69, 71, 75).

[6] Van Trees, H. L. *Detection, Estimation, and Modulation Theory*. 1st ed. Vol. 1. John Wiley & Sons, Inc., 2001 (see pp. 6, 20, 34).

[7] Trees, H. L. V., Bell, K. L., and Tian, Z. *Detection Estimation and Modulation Theory, Part I: Detection, Estimation, and Filtering Theory, 2nd Edition*. Wiley, 2013 (see pp. 8, 11, 17).

[8] Cover, T. M. and Thomas, J. A. *Elements of Information Theory 2nd Edition*. Wiley Series in Telecommunications and Signal Processing. Wiley-Interscience, July 2006 (see p. 9).

[9] Scharf, L. and Demeure, C. *Statistical Signal Processing: Detection, Estimation, and Time Series Analysis*. Addison-Wesley series in electrical and computer engineering. Addison-Wesley Publishing Company, 1991 (see pp. 9, 20, 21, 59, 61, 75).

[10]   Poor, H. V. *An Introduction To Signal Detection And Estimation 2nd Edition.* Springer Texts in Electrical Engineering. Springer-Verlag, 1994 (see p. 9).

[11]   Proakis, J. and Salehi, M. *Digital communications, 5th edition /.* 5th ed. [S.l.] : McGraw-Hill Science, Engineering, Math, 2014. (see pp. 11, 17).

[12]   A.Haroutuniana, E. and M.Hakobyan, P. "On Neyman-Pearson Principle in Multiple Hypotheses Testing". In: *Mathematical Problems of Computer Science* 40 (Oct. 2013), pp. 34–38 (see p. 11).

[13]   Bandiera, F., Farina, A., Orlando, D., and Ricci, G. "Detection Algorithms to Discriminate Between Radar Targets and ECM Signals". In: *IEEE Trans. Signal Process.* 58.12 (2010), pp. 5984–5993 (see p. 13).

[14]   Weinberbger, N. and Merhav, N. "Codeword or Noise?...." In: *IEEE Transactions on Information theory* 60.9 (2014), pp. 68–71 (see pp. 15, 16).

[15]   Shao, J. *Mathematical Statistics.* Springer Texts in Statistics. Springer, 2003 (see p. 19).

[16]   Maisel, L. "Performance of Sidelobe Blanking Systems". In: *IEEE Trans. Aerosp. Electron. Syst.* AES-4.2 (1968), pp. 174–180 (see pp. 23, 24).

[17]   Farina, A. *Antenna-based Signal Processing Techniques For Radar Systems.* English. Artech House Boston, 1992, xvi, 370 p. : (see pp. 24, 25, 39, 54).

[18]   Farina, A. and Gini, F. "Calculation of blanking probability for the sidelobe blanking for two interference statistical models". In: *IEEE Signal Process. Lett.* 5.4 (1998), pp. 98–100 (see pp. 25, 41, 48).

[19]   De Maio, A., Farina, A., and Gini, F. "Performance analysis of the sidelobe blanking system for two fluctuating jammer models". In: *IEEE Trans. Aerosp. Electron. Syst.* 41.3 (2005), pp. 1082–1091 (see p. 25).

[20]   Farina, A. and Gini, F. "Design of SLB systems in the presence of correlated ground clutter". In: *Proc. IEE Radar, Sonar and Navigation* 147.4 (2000), pp. 199–207 (see p. 25).

[21]   Shnidman, D. and Toumodge, S. "Sidelobe blanking with integration and target fluctuation". In: *IEEE Trans. Aerosp. Electron. Syst.* 38.3 (July 2002), pp. 1023–1037 (see p. 25).

[22] Shnidman, D. and Shnidman, N. "Sidelobe Blanking with Expanded Models". In: *IEEE Trans. Aerosp. Electron. Syst.* 47.2 (Apr. 2011), pp. 790–805 (see p. 25).

[23] Cui, G., De Maio, A., Piezzo, M., and Farina, A. "Sidelobe Blanking with Generalized Swerling-Chi Fluctuation Models". In: *IEEE Trans. Aerosp. Electron. Syst.* 49.2 (Apr. 2013), pp. 982–1005 (see p. 25).

[24] Finn, H., Johnson, R. S., and Peebles, P. Z. "Fluctuating Target Detection in Clutter Using Sidelobe Blanking Logic". In: *IEEE Trans. Aerosp. Electron. Syst.* AES-7.1 (1971), pp. 147–159 (see p. 26).

[25] Gradshteyn, I. S. and Ryzhik, I. M. *Table of integrals, series, and products.* 7th ed. Elsevier/Academic Press, Amsterdam, 2007, p. 709 (see pp. 32, 37).

[26] Bello, P. and Nelin, B. D. "Predetection Diversity Combining with Selectively Fading Channels". In: *IEEE Trans. Commun* 10.1 (1962), pp. 32–42 (see pp. 34, 35).

[27] Biyari, K. and Lindsey, W. "Statistical distributions of Hermitian quadratic forms in complex Gaussian variables". In: *IEEE Trans. Inf. Theory* 39.3 (1993), pp. 1076–1082 (see pp. 34, 35).

[28] Fernández-Plazaola, U., Martos-Naya, E., Paris, J. F., and Entrambasaguas, J. T. "Comments on Proakis Analysis of the Characteristic Function of Complex Gaussian Quadratic Forms". In: *Computer Research Repository (CoRR)* abs/1212.0382 (2012) (see pp. 34, 35).

[29] Proakis, J. "On the Probability of Error for Multichannel Reception of Binary Signals". In: *IEEE Trans. Commun. Technol.* 16.1 (1968), pp. 68–71 (see p. 34).

[30] De Maio, A., Farina, A., and Gini, F. "Performance analysis of the sidelobe blanking system for two fluctuating jammer models". In: *IEEE Transactions on Aerospace and Electronic Systems* 41.3 (July 2005), pp. 1082–1091 (see p. 45).

[31] Barton, D. *Radar Technology Encyclopedia.* Artech House, 1997 (see p. 53).

[32] Richards, M. *Fundamentals of Radar Signal Processing.* Professional Engineering. Mcgraw-hill, 2005 (see p. 54).

[33]   O'Donnell, R. M. *IEEE Aerospace and Electronic Systems Society, and IEEE New Hampshire Section Free Video Course in Radar Systems Engineering.* Sept. 2017. URL: http://aess.cs.unh.edu/ (see p. 54).

[34]   MathWorks. *Required SNR using Shnidman's equation.* Sept. 2017. URL: https://www.mathworks.com/help/phased/ref/shnidman.html (see p. 54).

[35]   Bose, S. and Steinhardt, A. "A maximal invariant framework for adaptive detection with structured and unstructured covariance matrices". In: *Signal Processing, IEEE Transactions on* 43.9 (Sept. 1995), pp. 2164–2175 (see pp. 60, 63).

[36]   Bose, S. and Steinhardt, A. "Optimum array detector for a weak signal in unknown noise". In: *Aerospace and Electronic Systems, IEEE Transactions on* 32.3 (July 1996), pp. 911–922 (see p. 60).

[37]   Kraut, S., Scharf, L., and Butler, R. "The adaptive coherence estimator: a uniformly most-powerful-invariant adaptive detection statistic". In: *Signal Processing, IEEE Transactions on* 53.2 (Feb. 2005), pp. 427–438 (see p. 60).

[38]   Cox, D. and Hinkley, D. *Theoretical Statistics.* Taylor & Francis, 1979 (see pp. 60, 68, 69, 75).

[39]   Lehmann, E. and Romano, J. *Testing Statistical Hypotheses.* Springer Texts in Statistics. Springer, 2005 (see pp. 61, 62, 64).

[40]   Kay, S. *Fundamentals of Statistical Signal Processing: Detection theory.* Prentice Hall Signal Processing Series. Prentice-Hall PTR, 1998 (see p. 69).

[41]   Polydoros, A. and Weber, C. "Detection Performance Considerations for Direct-Sequence and Time-Hopping LPI Waveforms". In: *IEEE Journal on Selected Areas in Communications* 3.5 (Sept. 1985), pp. 727–744 (see p. 76).

[42]   Koç, S., Candan, Ç., and Bayramoğlu., F. *Detection of Constant Envelope LPI Signals.* Tech. rep. 2008 (see p. 78).

[43]   Massey, J. "Optimum Frame Synchronization". In: *IEEE Transactions on Communications* 20.2 (Apr. 1972), pp. 115–119 (see p. 85).

[44] Gabriel, J. and Kay, S. "On the relationship between the GLRT and UMPI tests for the detection of signals with unknown parameters". In: *Signal Processing, IEEE Transactions on* 53.11 (Nov. 2005), pp. 4194–4203 (see p. 86).

[45] Nicolls, F. and Jager, G. de. "Uniformly most powerful cyclic permutation invariant detection for discrete-time signals". In: *2001 IEEE International Conference on Acoustics, Speech, and Signal Processing. Proceedings (Cat. No.01CH37221)*. Vol. 5. 2001, 3165–3168 vol.5 (see p. 86).

[46] Shanmugam, S. K., Mongrédien, C., Nielsen, J., and Lachapelle, G. "Design of Short Synchronization Codes for Use in Future GNSS System". In: *International Journal of Navigation and Observation* 2008 (2008) (see p. 93).

[47] Coskun, O. and Uner, M. "Adaptive Censored CFAR Performance in Nonhomogeneous Correlated Clutter". In: *2007 IEEE 15th Signal Processing and Communications Applications*. June 2007, pp. 1–4 (see p. 122).

APPENDIX A

NOTATION CONVENTIONS

Table A.1: Notation Conventions

Notation	Meaning
$\mathbf{x}$	observation data
$\mathcal{X}^N$	N-dimensional sample space
$f(\mathbf{x})$	probability density function (pdf) or probability mass function (pmf)
$f(\mathbf{x}; H_m)$	conditional pdf or pmf when H_m hypothesis is true
$f(\mathbf{x}\|\theta)$	pdf or pmf when the parameter θ is given or $f(\mathbf{x})$ is parameterized by θ
$f(\mathbf{x}\|\theta; H_m)$	conditional pdf or pmf when the parameter θ when H_m hypothesis is true
$\phi(\mathbf{x})$	indicator function for the given decision space
$\phi^*(\mathbf{x})$	indicator function of optimum decision rule (Neyman-Pearson) for the given decision space
$\mathcal{D}_m^*$	decision region of optimum decision rule (Neyman-Pearson) for hypothesis H_m
$\mathcal{D}_m$	decision region of any other decision rule except Neyman-Pearson rule for hypothesis H_m
P_{FA}	probability of false alarm
P_{MD}	probability of miss detection
P_D	probability of correct detection
P_{IE}	probability of inclusive error
P_{EE}	probability of exclusive error
P_b	probability of blanking
P_{tb}	probability of target blanking
$P(H_m\|H_k)$	probability of deciding H_m hypothesis when in fact H_k hypothesis is true
$P(H_m^c\|H_k)$	probability of deciding any hypothesis except H_m when in fact H_k hypothesis is true

APPENDIX B

MATLAB CODES FOR OPTIMUM SIDELOBE BLANKER

B.1   Required JNR vs gain margin

```matlab
function [min_jnr, Pb_attained] = min_jnr_vs_beta(P_tb, Pb_tolerance,
  ↪  Pb_classic_minimum, varargin)
%% function [min_jnr, Pb_attained] = min_jnr_vs_beta(P_tb, Pb_tolerance,
  ↪  Pb_classic_minimum, snr_db, beta_db, omega_db)
%
% This function finds the minimum required JNR (min_jnr) for classical SLB
% system that achieves a minimum $P_b$ (Pb_attained) within a tolerance
  ↪  with
% respect to optimum SLB detector. It plots min_jnr and Pb_attained with
% respect to different antenna gain margins $\beta^2$ (beta_db).
%
% Input Parameters:
% omega_db    : Side lobe gain of main antenna, 1x1 scalar, in dB, default
% value: -30 dB.
% beta_db     : Antenna gain margin between axuilarry antenna and sidelobe
  ↪  of
% main antenna, 1xM vector, in dB, default value: 5:1:10.
% snr_db      : SNR of interest, 1xM vector, in dB, default value: [9 12
  ↪  15].
% P_tb        : Desired probability of target blanking, ex: 0.05, required.
% Pb_tolerance: Tolerance with respect to optimum SLB detector, ex: 0.05.
% Pb_classic_minimum : Desired minimum jammer blanking probability
%
% Sample Run:
% P_tb, Pb_tolerance and Pb_classic_minimum are required to input to run
  ↪  the
% function, snr_db, beta_db and omega_db have default values as defined
% above.
%
% To generate Fig. 8, run >> min_jnr_vs_beta(0.05, 0.05, 0.90);
```

```matlab
25  % To generate Fig. 8 with SNR of [10 15 20] dB
26  % run >> min_jnr_vs_beta(0.05, 0.05, 0.90, [10 15 20]);
27  %
28  % To generate Fig. 8 with P_tb = 0.1, Pb_tolerance = 0.05,
29  % Pb_classic_minimum = 0.85, SNR = [10 15 20], $\beta^2$ = [4:2:20] dB and
30  % $\omega^2$ = -40 dB,
31  % run >> min_jnr_vs_beta(0.1, 0.05, 0.85, [10 15 20], [4:2:20], -40);
32  %
33  % Caution: SNR should be high enough such that requiered $F$ will be less
34  % than chosen $\beta^2$. If $F$ is not less than $\beta^2$, then $P_b$ of
    ↪  0.90 will
35  % not be attained and infinite loop can occur. To avoid this, first find
36  % the minimum SNR that achieves $F << \beta^2$.
37  %
38  % Osman Coskun
39  % Nov. 2015
40  %
41  numvarargs = length(varargin);
42  if numvarargs > 3
43      error('find_min_jnr_wrt_beta:TooManyInputs', ...
44          'requires at most 3 optional inputs');
45  end
46  default_values = {[9 12 15], [5:10], -30};
47  default_values(1:numvarargs) = varargin;
48  [snr_db, beta_db, omega_db] = default_values{:};
49  %initialization
50  Pb_attained = zeros (length(snr_db), length(beta_db));
51  Pb_new = ones (length(snr_db), length(beta_db));
52  min_jnr = Pb_new;
53  aux_legend = cell (size(snr_db));
54  for ii = 1: length (snr_db)
55      [F_db,~] = compute_F_SW1(P_tb, snr_db (ii), omega_db);
56      for jj = 1:length(beta_db)
57          jnr_db = -33;
58          while ~((Pb_new (ii,jj) - Pb_attained (ii,jj) <= Pb_tolerance )&&
            ↪  Pb_attained (ii,jj)>=Pb_classic_minimum)
59              Q = compute_Q_matrix (snr_db (ii), jnr_db, omega_db,
                ↪  beta_db(jj));
60              [a, b] = compute_hypothesis_a_b ('H1', Q, snr_db (ii), jnr_db,
                ↪  omega_db, beta_db(jj));
61              [eta, ~] = compute_threshold (P_tb, a, b);
62              [a, b] = compute_hypothesis_a_b ('H2', Q, snr_db (ii), jnr_db,
                ↪  omega_db, beta_db(jj));
63              Pb_new (ii,jj) = compute_Pb_new (a, b, eta);
64              Pb_attained (ii,jj) = compute_Pb_classic_SW1 (F_db, jnr_db,
                ↪  beta_db(jj));
65              jnr_db = jnr_db + .1;
66          end
67          min_jnr (ii,jj) = jnr_db;
68      end
```

112

```
69      aux_legend(ii) = {['SNR = ' num2str(snr_db (ii)) ' dB' ' $F = $ '
   ↪    sprintf('%1.2f', F_db) ' dB' ]};
70  end
71  %%
72  figure(2)
73  h2= plot(beta_db, Pb_attained);
74  ylabel ('$P_b$ (Maisel)','FontSize', 8,'interpreter', 'latex')
75  xlabel ('$\beta^2$  (dB)','FontSize', 8,'interpreter', 'latex')
76  set (gca(), 'xtick', beta_db, 'FontSize', 8);
77  title (['$\omega^2=$ ' num2str(omega_db) ' dB, ' '$P_{tb}=$ ' num2str(P_tb)
   ↪    ', min.' '$P_{b}=$ ' num2str(Pb_classic_minimum)],'interpreter',
   ↪    'latex');
78  grid on
79  legend(aux_legend, 'Location','northeast','FontSize', 8,'interpreter',
   ↪    'latex');
80  figure(1)
81  h1 = plot(beta_db, min_jnr');
82  set (gca(), 'xtick', beta_db, 'FontSize', 8);
83  grid on
84  ylabel ('Min. JNR','interpreter', 'latex', 'FontSize', 8)
85  xlabel ('$\beta^2$  (dB)','interpreter', 'latex','FontSize', 8)
86  title (['$\omega^2=$ ' num2str(omega_db) ' dB, ' '$P_{tb}=$ ' num2str(P_tb)
   ↪    ', min.' '$P_{b}=$ ' num2str(Pb_classic_minimum)],'interpreter',
   ↪    'latex');
87  marker_style =  ['s', '<', 'o', '+', '>', 'v', ];
88  marker_face_color = ['r', 'b', 'g', 'm'];
89  for jj = 1: length (snr_db)
90      set(h1(jj),'Linestyle', '-', 'Marker', marker_style (jj), 'Linewidth',
   ↪    0.6, ...
91          'MarkerSize',4, 'MarkerFaceColor','w',
   ↪    'MarkerEdgeColor','k','Color',marker_face_color(jj));
92      set(h2(jj),'Linestyle', '-', 'Marker', marker_style (jj), 'Linewidth',
   ↪    0.6, ...
93          'MarkerSize',4, 'MarkerFaceColor',marker_face_color(jj),
   ↪    'MarkerEdgeColor','k','Color',marker_face_color(jj));
94  end
95  legend(aux_legend, 'Location','northeast','FontSize', 8,'interpreter',
   ↪    'latex');
96  % *************
97  % End of main function
98  %%
99  function [F_db,Pb_found] = compute_F_SW1(Pb_desired, jnr_db, beta_db)
100 beta = db2pow(beta_db);        % beta in linear scale
101 jnr = db2pow (jnr_db);
102 tolerance= Pb_desired/1e5;     % Tolerance value for computation of
103 initial = 0.000001;            % Initial value for bisection search
104 final= 200;                    % Final value for bisection search
```

```matlab
105  Pb = @(F) 0.5.*(1-
     ↪  (1./(1+F)).*(jnr.*(F-beta)-F-1)./sqrt((jnr.*(F-beta)+F+1).^2+
     ↪  4.*jnr.*(F+1).*beta) -
     ↪  (F./(1+F)).*(jnr*(F-beta)+F+1)./sqrt((jnr*(F-beta)-F-1).^2+
     ↪  4*jnr*(F+1).*F));
106  initial_Pb = Pb(initial);
107  error = initial_Pb - Pb_desired;
108  while abs(error) > tolerance;
109      F_linear = 0.5*(initial + final);
110      if Pb(F_linear) >= Pb_desired
111          initial = F_linear;
112      else
113          final = F_linear;
114      end
115      error = Pb(F_linear) - Pb_desired;
116  end
117  F_db = 10*log10(F_linear);
118  Pb_found = Pb(F_linear);
119  %*****************
120  function [Q] = compute_Q_matrix (snr_db, jnr_db, omega_db, beta_db)
121  %[Q] = compute_Q_matrix (snr_db, jnr_db, omega_db, beta_db)
122  beta = db2pow(beta_db);        % beta in linear scale
123  omega = db2pow(omega_db);      % omega in linear scale
124  jnr = db2pow (jnr_db);         % JNR in  linear scale
125  snr = db2pow (snr_db);         % SNR in linear scale
126  % Compute covariance matrices
127  C1 = [ (snr +1), sqrt(omega)*snr; sqrt(omega)*snr, (omega*snr +1)];
128  C2 = [ (jnr +1), sqrt(beta)*jnr; sqrt(beta)*jnr, (beta*jnr +1)];
129  Q = inv(C1) - inv(C2);
130  %*****************
131  function [a, b] = compute_hypothesis_a_b (hypothesis, Q, snr_db, jnr_db,
     ↪  omega_db, beta_db)
132  % [a, b] = compute_hypothesis_a_b (hypothesis, Q, snr_db, jnr_db, omega_db,
     ↪  beta_db)
133  beta = db2pow(beta_db);        % beta in linear scale
134  omega = db2pow(omega_db);      % omega in linear scale
135  jnr = db2pow (jnr_db);         % JNR in  linear scale
136  snr = db2pow (snr_db);         % SNR in linear scale
137  % Compute covariance matrices
138  C1 = [ (snr +1), sqrt(omega)*snr; sqrt(omega)*snr, (omega*snr +1)];
139  C2 = [ (jnr +1), sqrt(beta)*jnr; sqrt(beta)*jnr, (beta*jnr +1)];
140  if hypothesis == 'H1'
141      R = C1/2;
142  else
143      R = C2/2;
144  end
145  r = sum(sum(R.*Q))/(-4*det(R)*det(Q));
146  a = sqrt(r^2+1/(-4*det(R)*det(Q))) - r ;
147  b = sqrt(r^2+1/(-4*det(R)*det(Q))) + r ;
148  %*****************
```

```
149  function [eta, threshold] = compute_threshold (P_b, a, b)
150  threshold = b/(a+b);
151  if P_b <= threshold
152      eta = -(log((P_b*(a + b))/b) )/a;
153  else
154      eta = (log(-((a + b)*(P_b - 1))/a) )/b;
155  end
156  %*****************
157  function Pb_temp = compute_Pb_new (a_temp, b, eta_temp)
158  f1 = @(x)(b/(a_temp+b)*exp(-a_temp.*x));
159  f2 = @(x)(a_temp/(a_temp+b))*(1-exp(b.*x))+b/(a_temp+b);
160  Pb_temp = zeros (size(eta_temp));
161  for i = 1: length (eta_temp)
162      if eta_temp(i) >= 0
163          Pb_temp(i) = f1 (eta_temp(i));
164      else
165          Pb_temp(i) = f2 (eta_temp(i));
166      end
167  end
168  %*****************
169  function Pb = compute_Pb_classic_SW1 (F_db, jnr_db, beta_db)
170  beta = db2pow(beta_db);          % beta in linear scale
171  jnr = db2pow (jnr_db);           % JNR in  linear scale
172  F = db2pow (F_db);               % F in linear scale
173  Pb_formula = @(F, jnr, beta) 0.5.*(1-
     ↪  (1./(1+F)).*(jnr.*(F-beta)-F-1)./sqrt((jnr.*(F-beta)+F+1).^2+
     ↪  4.*jnr.*(F+1).*beta) - ...
174  (F./(1+F)).*(jnr*(F-beta)+F+1)./sqrt((jnr*(F-beta)-F-1).^2+
     ↪  4*jnr*(F+1).*F));
175  Pb = Pb_formula (F, jnr, beta);
```

B.2   The probability of blanking jammer vs gain margin

```
1   function Pb = Pb_vs_beta(P_tb, varargin)
2   %% function Pb = Pb_vs_beta(P_tb, jnr_db, snr_db, beta_db, omega_db)
3   %
4   % This function finds and plots the probability of blanking jammer (Pb)
5   % for optimum and Maisel SLB systems with respect to different antenna
6   % gain margins $\beta^2$ (beta_db).
7   %
8   % Input Parameters:
9   % P_tb        : Desired probability of target blanking, ex: 0.05.
10  % snr_db      : SNR of interest, 1xM vector, in dB, default = [9 10 12] dB.
11  % jnr_db      : JNR of interesr, scalar, in dB, default = 5 dB.
12  % beta_db     : Antenna gain margin between axuilarry antenna and sidelobe
     ↪  of
```

115

```matlab
13   % main antenna, 1xM vector, in dB, default = [5:1:10] dB.
14   % omega_db    : Side lobe gain of main antenna, 1x1 scalar, default = -30
     ↪   dB.
15   %
16   % Sample Run:
17   % P_tb is required to input to run the function. jnr_db, snr_db,  beta_db
     ↪   and omega_db
18   % have default values as defined above.
19   %
20   % To generate Fig. 7, run >> Pb_vs_beta(0.05);
21   %
22   % To generate Fig. 7 with P_tb = 0.1, JNR = 8 dB, SNR = [5 10 15],
23   % $\beta^2$ = [2:2:20] dB and $\omega^2$ = -40 dB,
24   % run >> Pb_vs_beta (0.1, 8, [5 10 15], [2:2:20], -40);
25   %
26   % Osman Coskun
27   % Nov. 2015
28   %
29   numvarargs = length(varargin);
30   if numvarargs > 4
31       error('plot_Pb_wrt_beta:TooManyInputs', ...
32           'requires at most 3 optional inputs');
33   end
34   default_values = {5, [9 12 15], [5:10], -30};
35   default_values(1:numvarargs) = varargin;
36   [jnr_db, snr_db, beta_db, omega_db] = default_values{:};
37
38   main_legend = cell (2*length(snr_db),1);
39   Pb = zeros (2*length(snr_db),length(beta_db));
40   for ii = 1: length (snr_db)
41       [F_db,~] = compute_F_SW1(P_tb, snr_db (ii), omega_db);
42       for jj = 1:length(beta_db)
43           Q = compute_Q_matrix (snr_db (ii), jnr_db, omega_db, beta_db(jj));
44           [a, b] = compute_hypothesis_a_b ('H1', Q, snr_db (ii), jnr_db,
               ↪   omega_db, beta_db(jj));
45           [eta, ~] = compute_threshold (P_tb, a, b);
46           [a, b] = compute_hypothesis_a_b ('H2', Q, snr_db (ii), jnr_db,
               ↪   omega_db, beta_db(jj));
47           Pb (2*ii-1,jj) = compute_Pb_new (a, b, eta);
48           Pb (2*ii,jj) = compute_Pb_classic_SW1 (F_db, jnr_db, beta_db(jj));
49       end
50       main_legend  (2*ii-1) = {['Optimum, SNR = ' num2str(snr_db (ii)) '
           ↪   dB']};
51       main_legend (2*ii) = {['Maisel, SNR = ' num2str(snr_db (ii)) ' dB' ' $F
           ↪   = $ ' sprintf('%1.2f', F_db) ' dB']};
52   end
53   % figure(1)
54   %%
55   h1 = plot(beta_db, Pb');
56   y_tick = 0:0.05:1;
```

116

```matlab
57   set (gca(), 'xtick', beta_db, 'FontSize', 8);
58   set(gca(), 'ytick', y_tick, 'FontSize', 8);
59   grid on
60   ylabel ('$P_b$','Interpreter','latex')
61   xlabel ('$\beta^2$  (dB)', 'Interpreter','latex')
62   title ([ '$\omega^2=$ ' num2str(omega_db) ' dB, ' 'JNR = '
     ↪  num2str(jnr_db)...
63       ' dB, ' '$P_{tb}=$ ' num2str(P_tb)],'FontSize', 8, 'interpreter',
         ↪  'latex');
64   marker_style =  ['s', '<', 'o', '+', '>', 'v', ];
65   for jj = 1: length (snr_db)
66       set(h1(2*jj-1),'Linestyle', '-' , 'Marker', marker_style (jj),
         ↪  'Linewidth', 0.5, ...
67           'MarkerEdgeColor','k',...
68           'MarkerFaceColor','w',...
69           'MarkerSize',3, ...
70           'Color', 'Red');
71       set(h1(2*jj),'Linestyle', ':', 'Marker', marker_style (jj),
         ↪  'Linewidth', 0.5, ...
72           'MarkerEdgeColor','k',...
73           'MarkerFaceColor','w',...
74           'MarkerSize',3, ...
75           'Color', 'Blue');
76   end
77   legend(main_legend, 'Location','southeast','FontSize', 8,'interpreter',
     ↪  'latex');
78   set(gca, 'TickLabelInterpreter','latex');
79   % End of main function
80   %%
81   function [F_db,Pb_found] = compute_F_SW1(Pb_desired, jnr_db, beta_db)
82   beta = db2pow(beta_db);       % beta in linear scale
83   jnr = db2pow (jnr_db);
84   tolerance= Pb_desired/1e5;    % Tolerance value for computation of
85   initial = 0.000001;           % ?nitial value for bisection search
86   final= 200;                   % Final value for bisection search
87   Pb = @(F) 0.5.*(1-
     ↪  (1./(1+F)).*(jnr.*(F-beta)-F-1)./sqrt((jnr.*(F-beta)+F+1).^2+
     ↪  4.*jnr.*(F+1).*beta) -
     ↪  (F./(1+F)).*(jnr*(F-beta)+F+1)./sqrt((jnr*(F-beta)-F-1).^2+
     ↪  4*jnr*(F+1).*F));
88   initial_Pb = Pb(initial);
89   error = initial_Pb - Pb_desired;
90   while abs(error) > tolerance;
91       F_linear = 0.5*(initial + final);
92       if Pb(F_linear) >= Pb_desired
93           initial = F_linear;
94       else
95           final = F_linear;
96       end
97       error = Pb(F_linear) - Pb_desired;
```

```matlab
98    end
99    F_db = 10*log10(F_linear);
100   Pb_found = Pb(F_linear);
101   %******************
102   function [Q] = compute_Q_matrix (snr_db, jnr_db, omega_db, beta_db)
103   %[Q] = compute_Q_matrix (snr_db, jnr_db, omega_db, beta_db)
104   beta = db2pow(beta_db);          % beta in linear scale
105   omega = db2pow(omega_db);        % omega in linear scale
106   jnr = db2pow (jnr_db);           % JNR in  linear scale
107   snr = db2pow (snr_db);           % SNR in linear scale
108   % Compute covariance matrices
109   C1 = [ (snr +1), sqrt(omega)*snr; sqrt(omega)*snr, (omega*snr +1)];
110   C2 = [ (jnr +1), sqrt(beta)*jnr; sqrt(beta)*jnr, (beta*jnr +1)];
111   Q = inv(C1) - inv(C2);
112   %******************
113   function [a, b] = compute_hypothesis_a_b (hypothesis, Q, snr_db, jnr_db,
      ↪ omega_db, beta_db)
114   % [a, b] = compute_hypothesis_a_b (hypothesis, Q, snr_db, jnr_db, omega_db,
      ↪ beta_db)
115   beta = db2pow(beta_db);          % beta in linear scale
116   omega = db2pow(omega_db);        % omega in linear scale
117   jnr = db2pow (jnr_db);           % JNR in  linear scale
118   snr = db2pow (snr_db);           % SNR in linear scale
119   % Compute covariance matrices
120   C1 = [ (snr +1), sqrt(omega)*snr; sqrt(omega)*snr, (omega*snr +1)];
121   C2 = [ (jnr +1), sqrt(beta)*jnr; sqrt(beta)*jnr, (beta*jnr +1)];
122   if hypothesis == 'H1'
123       R = C1/2;
124   else
125       R = C2/2;
126   end
127   r = sum(sum(R.*Q))/(-4*det(R)*det(Q));
128   a = sqrt(r^2+1/(-4*det(R)*det(Q))) - r ;
129   b = sqrt(r^2+1/(-4*det(R)*det(Q))) + r ;
130   %******************
131   function [eta, threshold] = compute_threshold (P_b, a, b)
132   threshold = b/(a+b);
133   if P_b <= threshold
134       eta = -(log((P_b*(a + b))/b) )/a;
135   else
136       eta = (log(-((a + b)*(P_b - 1))/a) )/b;
137   end
138   %******************
139   function Pb_temp = compute_Pb_new (a_temp, b, eta_temp)
140   f1 = @(x)(b/(a_temp+b)*exp(-a_temp.*x));
141   f2 = @(x)(a_temp/(a_temp+b))*(1-exp(b.*x))+b/(a_temp+b);
142   Pb_temp = zeros (size(eta_temp));
143   for i = 1: length (eta_temp)
144       if eta_temp(i) >= 0
145           Pb_temp(i) = f1 (eta_temp(i));
```

118

```matlab
146        else
147            Pb_temp(i) = f2 (eta_temp(i));
148        end
149    end
150    %*****************
151    function Pb = compute_Pb_classic_SW1 (F_db, jnr_db, beta_db)
152    beta = db2pow(beta_db);          % beta in linear scale
153    jnr = db2pow (jnr_db);           % JNR in  linear scale
154    F = db2pow (F_db);               % F in linear scale
155    Pb_formula = @(F, jnr, beta) 0.5.*(1-
     ↪ (1./(1+F)).*(jnr.*(F-beta)-F-1)./sqrt((jnr.*(F-beta)+F+1).^2+
     ↪ 4.*jnr.*(F+1).*beta) - ...
156    (F./(1+F)).*(jnr*(F-beta)+F+1)./sqrt((jnr*(F-beta)-F-1).^2+
     ↪ 4*jnr*(F+1).*F));
157    Pb = Pb_formula (F, jnr, beta);
```

CURRICULUM VITAE

PERSONAL INFORMATION

Surname, Name: Coşkun, Osman
Nationality: Turkish (TC)
Date and Place of Birth: 01.02.1982, Erzurum
Marital Status: Married
Phone: 0090 530 342 24 26
EMail: osmanc@gmail.com

EDUCATION

Degree	Institution	Year of Graduation
M.S.	Hacettepe University Graduate School of Science and Engineering	2007
B.S.	Hacettepe University Electrical and Electronic Engineering	2003
High School	Erzurum İbrahim Hakkı Science High School	1998

PROFESSIONAL EXPERIENCE

Year	Place	Enrollment
2003- 2008	3rd Air Supply Maintenance Center, Turkish Air Force	System Engineer
2008- 2014	Electronic Warfare Support Center, Turkish Air Force	EW Reprogramming Officer
2014- 2017	Electronic Warfare Support Center, Turkish Air Force	Head Of EW Systems Reprogramming for Fighter Aircrafts
2017- Current	OCCAR A400M Programme Division, Toulouse/France	Turkey In Service Support Officer

PUBLICATIONS

1. Coşkun, O. and Candan, Ç. "Design of Maisel sidelobe blankers with a guarantee on the gap to optimality". In: *IET Radar, Sonar & Navigation* 10 (9 Dec. 2016), 1619–1626(7)

2. Coşkun, O. and Candan, Ç. "On the optimality of Maisel sidelobe blanking system". In: *2015 23nd Signal Processing and Communications Applications Conference (SIU)*. May 2015, pp. 585–591

3. Coşkun, O. and Candan, Ç. "On the optimality of Maisel sidelobe blanking structure". In: *Radar Conf., 2014 IEEE*. May 2014, pp. 1102–1107

4. Coskun, O. and Uner, M. "Adaptive Censored CFAR Performance in Non-homogeneous Correlated Clutter". In: *2007 IEEE 15th Signal Processing and Communications Applications*. June 2007, pp. 1–4